

An-Najah National University
Faculty of Graduated Studies

Numerical Methods for Solving Volterra Fractional Integral Equations with Applications

By

Safa' Abdel Hakeem Mohammed Hamdan

Supervisor

Prof. Naji Qatanani

**This Thesis is Submitted in Partial Fulfillment of the Requirements for
the Degree of Master of Mathematics, Faculty of Graduate Studies,
An-Najah National University, Nablus, Palestine.**

2018

Numerical Methods for Solving Volterra Fractional Integral Equations with Applications

By


Safa' Abdel Hakeem Mohammed Hamdan

This thesis was successfully defended on 30 /7/2018 and approved by:

Defense Committee Members

Signature

– Prof. Naji Qatanani / Supervisor


.....

– Dr. Saed Mallak / External Examiner


.....

– Dr. Anwar Saleh / Internal Examiner


.....

Dedication

IV

I dedicate this thesis to my beloved homeland, to my parents, to my dear husband Mohammed, to my daughter Eman, to my sisters and my brothers, to my friends, to everyone who supports and encourages me.

Acknowledgement

First of all, I thank my God for all the blessing he bestowed on me and continues to bestow on me.

I would sincerely like to thank and deeply grateful to my supervisor Prof. Dr. Naji Qatanani who without his support, kind supervision, helpful suggestions and valuable remarks, my work would have been more difficult. My thanks also to my external examiner Dr. Saed Mallak and to my internal examiner Dr. Anwar Saleh for their useful and valuable comments. Also, my great thanks are due to my family for their support, encouragement and great efforts for me. Finally, I would also like to acknowledge to all my teachers in An-Najah National University-Mathematical Department.

Numerical Methods for Solving Volterra Fractional Integral Equations with Applications

أقر بأن ما شملت عليه الرسالة هو نتاج جهدي الخاص، باستثناء ما تمت الإشارة إليه حيثما ورد، وأن هذه الرسالة ككل أو أي جزء منها لم يقدم من قبل لنيل أي درجة أو لقب علمي أو بحثي لدى أي مؤسسة علمية أو بحثية.

Declaration

is the ‘ unless otherwise referenced. The work provided in this thesis and has not been submitted elsewhere for any other ‘researcher's own work degrees or qualifications.

اسم الطالبة: **Student's Name:**

التوقيع: **Signature:**

التاريخ: **Date:**

Table of Contents

Dedication	III
Acknowledgement	IV
Declaration	VI
Table of Contents	VI
List of Figures	X
List of Tables	XII
Abstract	XIII
Introduction	1
Chapter One	4
Fractional Integrals and Derivatives	4
1.1 Special Functions	4
Chapter Two.....	16
Analytical and Numerical Methods for Solving Linear Volterra Fractional Integral Equation.....	16
2.1 Theoretical Framework.....	16
2.1.1 Lagrange Interpolation Polynomial 2, 3	16
2.1.2 Composite Trapezoidal Rule 6	17
2.1.3 Convolution.....	18
2.2 The Adomian Decomposition Method (ADM)	19
2.3 The Haar Wavelet Method.....	21
2.4 The Product Integration Method	27
2.5 Fractional Multistep Method.....	31
2.5.1 Review of a Class of Convolution Quadrature Methods and the Basic Notations	31
2.5.1.1 Quadrature Methods of Convolution Form	31
$w\xi$ holomorphic on $\mathbf{B}_{1+\varepsilon} = \{\xi \in \mathbb{C}: \xi < 1 + \varepsilon\}$,	34
2.5.1.2 Starting Weights.....	34

2.5.2 Numerical Solution of Linear Volterra Fractional Integral Equation of the First Kind	37
2.5.2.1 Introductory Remarks and the Basic Algorithm.....	37
2.5.2.2 Uniqueness, Existence and Approximation Properties of the Starting Value	39
Chapter Three.....	41
Numerical Examples and Results	41
3.1 The Numerical Realization of Equation (3.1)Using Adomian Decomposition Method.....	41
3.2 The Numerical Realization of Equation (3.1) Using the Haar Wavelet Method	44
3.3 The Numerical Realization of Equation (3.1) Using the Product Integration Method	49
3.4 The Numerical Realization of Equation (3.2)Using Adomian Decomposition Method.....	56
3.5 The Numerical Realization of Equation 3.2 Using the Haar Wavelet Method	58
3.6 The Numerical Realization of Equation (3.2) Using the Product Integration Method.....	62
3.7 The Numerical Realization of Equation (3.3)Using Adomian Decomposition Method.....	66
3.8 The Numerical Realization of Equation (3.3) Using the Haar Wavelet Method	68
3.9 The Numerical Realization of Equation (3.3) Using the Product Integration Method	71
Chapter Four	77
Applications and Results.....	77
4.1 The Abel's Integral Equation.....	77

4.2 The Numerical Realization of Equation 4.5 Using Adomian Decomposition Method.....	79
4.3 The Numerical Realization of Equation (4.5) Using the Haar Wavelet Method	81
4.4 The Numerical Realization of Equation (4.5) Using the Product Integration Method.....	84
4.5 Linear Volterra Integral Equation.....	89
4.6 The Numerical Realization of Equation 4.10 Using Adomian Decomposition Method.....	90
4.7 The Numerical Realization of Equation 4.10 Using the Haar Wavelet Method	92
4.8 The Numerical Realization of Equation 4.10 Using the Product Integration Method.....	95
Conclusions	98
References	99
Appendix	104
الملخص	ب

List of Figures

Fig1.1: The gamma function.....	4
Fig 2.1: The Haar wavelet.....	22
Fig 2.2: The first eight Haar functions.....	24
Fig. 3.3 (a) A comparison between the exact and numerical solutions in example 3.2 with $N = 32$	59
Fig. 3.3 (c) A comparison between the exact and numerical solutions in example 3.2 with $N = 128$	60
Fig. 3.3 (d) A comparison between the exact and numerical solutions in example 3.2 with $N = 256$	61
Fig. 3.4 (b) A comparison between the exact and numerical solutions in example 3.2 with $N = 64$	63
Fig. 3.4 (c) A comparison between the exact and numerical solutions in example 3.2 with $N = 128$	64
Fig. 3.4 (e) Absolute error between exact and numerical solutions in example 3.2 with $N = 64$	65
Fig. 3.5 (a) A comparison between the exact and numerical solutions in example 3.3 with $N = 32$	69
Fig. 3.5 (b) A comparison between the exact and numerical solutions in example 3.3 with $N = 64$	70
Fig. 3.5 (c) A comparison between the exact and numerical solutions in example 3.3 with $N = 128$	70
Fig. 3.5 (d) A comparison between the exact and numerical solutions in example 3.3 with $N = 256$	71
Fig. 3.5 (e) Absolute error between exact and numerical solutions in example 3.3 with $N = 64$	71
Fig. 3.6 (a) A comparison between the exact and numerical solutions in example 3.3 with $N = 32$	74
Fig. 3.6 (b) A comparison between the exact and numerical solutions in example 3.3 with $N = 64$	75
Fig. 3.6 (c) A comparison between the exact and numerical solutions in example 3.3 with $N = 128$	75

Fig. 3.6 (d) A comparison between the exact and numerical solutions in example 3.3 with $N = 256$.	76
Fig. 3.6 (e) Absolute error between exact and numerical solutions in example 3.3 with $N = 64$.	76
Fig. 4.1 (a) A comparison between the exact and numerical solutions in example 4.1 with $N = 32$.	82
Fig. 4.1 (b) A comparison between the exact and numerical solutions in example 4.1 with $N = 64$.	83
Fig. 4.1 (c) A comparison between the exact and numerical solutions in example 4.1 with $N = 128$.	83
Fig. 4.1 (d) Absolute error between exact and numerical solutions in example 4.1 with $N = 64$.	84
Fig. 4.2 (a) A comparison between the exact and numerical solutions in example 4.1 with $N = 32$.	87
Fig. 4.2 (b) A comparison between the exact and numerical solutions in example 4.1 with $N = 64$.	87
Fig. 4.2 (d) Absolute error between exact and numerical solutions in example 4.1 with $N = 64$.	88
Fig. 4.3 (a) A comparison between the exact and numerical solutions in example 4.2 with $N = 32$.	93
Fig. 4.3 (b) A comparison between the exact and numerical solutions in example 4.2 with $N = 64$.	93
Fig. 4.3 (c) A comparison between the exact and numerical solutions in example 4.2 with $N = 128$.	94
Fig. 4.3 (d) Absolute error between exact and numerical solutions in example 4.2 with $N = 64$.	94
Fig. 4.4 (b) A comparison between the exact and numerical solutions in example 4.2 with $N = 64$.	96

List of Tables

Table 2.1: Index computations for Haar basis function.....	23
Table (3.1): The exact and numerical solutions using the Haar wavelet method with $N = 64$	45
Table (3.2): The exact and numerical solutions using the product integration method with $N = 64$	52
Table (3.3): The exact and numerical solutions using the Haar wavelet method with $N = 64$	58
Table (3.4): The exact and numerical solutions using the product integration method with $N = 64$	62
Table (3.5): The exact and numerical solutions using the Haar wavelet method with $N = 64$	68
Table (3.6): The exact and numerical solutions using the product integration method with $N = 64$	73
Table (4.1): The exact and the numerical solutions using the Haar wavelet method with $N = 64$	81
Table (4.2): The exact and numerical solutions using the product integration method with $N = 64$	86
Table (4.3): The exact and numerical solutions using the Haar wavelet method with $N = 64$	92
Table (4.4): The exact and numerical solutions using the product integration method with $N = 64$	95

XIII
**Numerical Methods for Solving Volterra Fractional Integral Equations
with Applications**

By
Safa' Abdel Hakeem Mohammed Hamdan
Supervisor
Prof. Naji Qatanani

Abstract

In this thesis we focus on the analytical and numerical solutions of the Volterra fractional integral equation of the first and the second kind. This equation has wide range of applications in mathematical physics and chemical reactions including stereology, the heat conduction, crystal growth and electro-chemistry.

After introducing some definitions in fractional integrals and fractional derivatives, we focus our attention mainly on the analytical and numerical methods for solving the linear Volterra fractional integral equation of the first and the second kind. These methods are: The Adomian decomposition method, the Haar wavelet method, the product integration method and fractional multistep method.

The mathematical framework of these numerical methods together with their convergence properties will be presented. These numerical methods will be illustrated by some numerical examples. Comparisons between these methods will be drawn. Numerical results show clearly that the product integration method is one of the most powerful numerical techniques for solving the linear Volterra fractional integral equation of the second kind in comparison with other numerical techniques used in this thesis.

Introduction

The subject of fractional calculus deals with the investigation of integrals and derivatives of any real or complex order, which unifies and extends the notations of fractional order derivatives and n -fold integrals.

Most of the mathematical theories applicable to the study of fractional calculus were developed prior to the turn of the 20th century. Caputo reformulated the more 'classic' definition of the Riemann-Liouville fractional derivative in order to use integer order initial conditions to solve his fractional order differential equations [33]. As recently as 1996, Kolowankar reformulated, the Riemann-Liouville fractional derivative in order to differentiate no-where differentiable fractal functions [20]. After that, the number of researches and studies about the fractional calculus has rapidly increased. This is due to the fact that some physical processes such as anomalous diffusion [8], complex viscoelasticity [27], behavior of mechatronic and biological systems [25], rheology [28] etc, cannot be described by classical models.

There are many contributions from famous mathematicians involved in the theory of the fractional calculus up to the middle of the 20th century, among which; Laplace (1812), Fourier (1822), Abel (1823-1826), Liouville (1832-1837), Riemann (1847), Grunwald (1867-1872), Letnikov (1868-1872), Heaviside (1892-1912), Weyl (1917), Erdélyi (1939-1965) and several others (Gorenflo and Mainardi [12]). The first specialized conference on fractional calculus and its applications was held in 1974 at the University of New Haven, USA.

Integral equations have been a subject of interest for mathematicians as well as physicists and engineers. The development of integral equation has led to the formation of many models of problems in engineering and mathematical

physics such as scattering in quantum mechanics, diffraction problems, conformal mapping, and water waves. Various initial and boundary value problems in physics and engineering can be solved by converting them to an integral equation. These problems include population growth model, biological species living together, heat transformation and heat radiation, electromagnetic and electrostatic problems and many more [39].

The fractional order integral equations have numerous applications in porous media, control, electro-chemistry, electromagnetism fluid structure, coupling and particle mechanics (see e.g. [29, 12, 38]).

The most standard form of the fractional integral equation is the linear Volterra integral equation of the second kind [17]:

$$g(x) = f(x) + \frac{1}{\Gamma(\alpha)} \int_0^x (x-t)^{\alpha-1} k(x,t) g(t) dt, \quad 0 \leq x \leq 1, \quad (1)$$

where the kernel $k(x,t)$ and the right hand side function $f(x)$ are given functions, $\alpha > 0$ is a real number, $\Gamma(\alpha)$ is the gamma function and $g(x)$ is the unknown function that appears under the integral sign.

One common form of the linear Volterra fractional integral equation of the second kind is the Abel's integral equation of the second kind. This equation has the form [39]:

$$g(x) = f(x) + \lambda \int_0^x \frac{g(t)}{(x-t)^B} dt, \quad 0 < B < 1, \quad (2)$$

where $\lambda = \frac{1}{\Gamma(\alpha)}$, $B = 1 - \alpha$.

Many numerical methods for solving equations (1) and (2) have been developed over the past few years, for instance the Haar wavelet method [21], product integration method [4], collocation method [5], fractional

multistep method [24] and backward Euler methods [4]. Some analytical methods, like the Adomian decomposition method, are also available, which produce a series solution, for example; Gorenflo [11] presented some numerical methods based on fractional calculus, e.g., using the Grunwald-Letnikov difference approximation,

$$D^\alpha g \simeq h^{-\alpha} \sum_{r=0}^n (-1)^r \binom{\alpha}{r} g(x - rh). \quad (3)$$

If g is sufficiently smooth and vanishes for $x \leq 0$, then formula (3) has accuracy of order $O(h^2)$, otherwise, it has accuracy of order $O(h)$.

This thesis is organized as follows: In chapter one, we introduce some basic definitions and properties of fractional integrals and fractional derivatives.

In chapter two, we present some analytical and numerical methods for solving linear Volterra fractional integral equation of the first and the second kind, namely; the Adomian decomposition method, the Haar wavelet method, the product integration method and fractional multistep method.

In chapter three, we solve linear Volterra fractional integral equation of the second kind using the aforementioned methods. Finally, chapter four offers numerical solutions and results for Volterra fractional integral equation of the first and the second kind appearing frequently in physics and engineering.

Chapter One

Fractional Integrals and Derivatives

1.1 Special Functions

Definition (1.1) [33]: **Gamma function:** The gamma function denoted by $\Gamma(p)$ is given by the integral:

$$\Gamma(p) = \int_0^{\infty} x^{p-1} e^{-x} dx, \quad \text{Re}(p) > 0. \quad (1.1)$$

The above integral converges only for $\text{Re}(p) > 0$. For $\text{Re}(p) < 0$ we need to consider the analytical continuation of $\Gamma(p)$, that is

$$\Gamma(p) = \frac{1}{p} \Gamma(p + 1).$$

Gamma function is defined for all real numbers except at $x = 0, -1, -2, \dots$

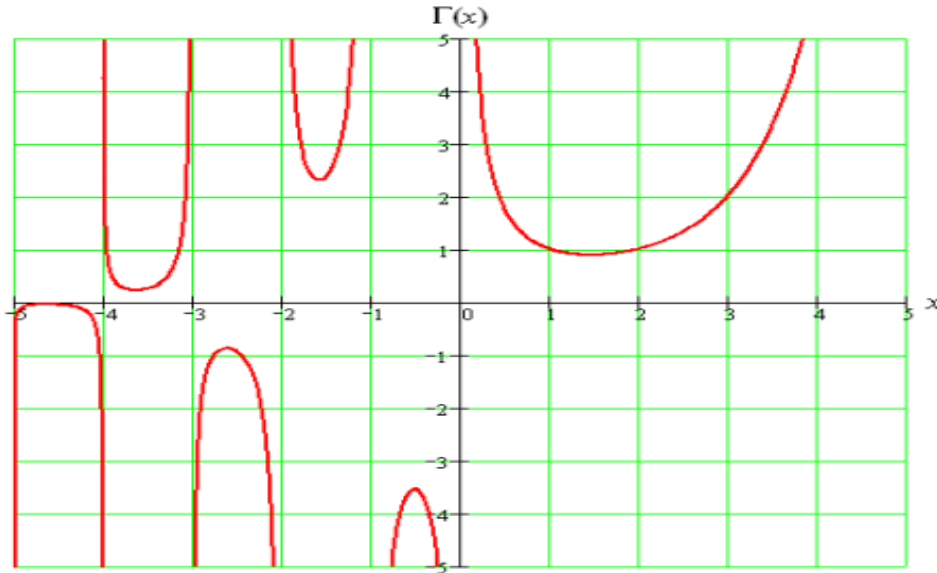


Figure 1.1: The gamma function.

Definition (1.2) [33]: **Beta function:** The beta function denoted by $B(u, v)$ is given by the integral:

$$B(u, v) = \int_0^1 x^{u-1} (1-x)^{v-1} dx. \quad (1.2)$$

This integral converges for $Re(u), Re(v) > 0$.

A key property of the beta function is its relationship to the gamma function;

$$B(u, v) = \frac{\Gamma(u)\Gamma(v)}{\Gamma(u+v)}.$$

1.1 Fractional Integrals

Definition (1.3) [31, 33]: The Riemann-Liouville fractional integral operator of order $\alpha \in \mathbb{R}$, $n-1 < \alpha < n$, $n \in \mathbb{N}$, of the function $g(x)$ is defined by the formula:

$$J^\alpha g(x) = \frac{1}{\Gamma(\alpha)} \int_0^x (x-t)^{\alpha-1} g(t) dt, \quad \alpha, x > 0. \quad (1.3)$$

Theorem (1.1) [33, 36]: **The identity operator:** If we set $\alpha = 0$ in the Riemann-Liouville fractional integral operator of order α (J^α) of the function $g(x)$, then the equation becomes:

$$J^0 g(x) = g(x), \quad (1.4)$$

where $J^0 = I$ (the identity operator).

Theorem (1.2) [31, 33]: **The semi-group property:** Suppose that $\alpha, \beta \geq 0$, the semi-group property of the two operators J^α, J^β is defined by:

$$J^\alpha J^\beta = J^{\alpha+\beta}. \quad (1.5)$$

Theorem (1.3) [33, 36]: **The commutative property:** Suppose that $\alpha, \beta \geq 0$, the commutative property of the two operators J^α, J^β is defined by:

$$J^\alpha J^\beta = J^\beta J^\alpha. \quad (1.6)$$

From (1.5) and (1.6), we conclude that $J^\alpha J^\beta = J^{\alpha+\beta} = J^{\beta+\alpha} = J^\beta J^\alpha$.

Theorem (1.4) [33]: Let $n - 1 < \alpha < n$, $n \in \mathbb{N}$, $\alpha, \lambda \in \mathbb{C}$ and the functions $g(x)$ and $h(x)$ be such that both $J^\alpha g(x)$ and $J^\alpha h(x)$ exists. The fractional integral is a linear operator, i. e.,

$$J^\alpha(\lambda g(x) + h(x)) = \lambda J^\alpha g(x) + J^\alpha h(x). \quad (1.7)$$

Theorem (1.5) [30]: Let $\alpha, x > 0$, $\alpha \in \mathbb{R}$. The Riemann-Liouville fractional integral of the power function satisfies:

$$J^\alpha x^v = \frac{\Gamma(v+1)}{\Gamma(\alpha+v+1)} x^{\alpha+v}, \quad v > -1. \quad (1.8)$$

Proof: The proof follows directly from the definition of the fractional integral equation (1.3), the definition, and the properties of the beta function.

$$J^\alpha x^v = \frac{1}{\Gamma(\alpha)} \int_0^x (x-t)^{\alpha-1} t^v dt$$

$$J^\alpha x^v = \frac{1}{\Gamma(\alpha)} \int_0^x \left(1 - \frac{t}{x}\right)^{\alpha-1} x^{\alpha-1} t^v dt$$

Let $u = \frac{t}{x}$, then:

$$J^\alpha x^v = \frac{1}{\Gamma(\alpha)} \int_0^1 (1-u)^{\alpha-1} x^{\alpha-1} (ux)^v x du$$

$$J^\alpha x^v = \frac{1}{\Gamma(\alpha)} x^{\alpha+v} \int_0^1 (1-u)^{\alpha-1} (u)^v du$$

$$J^\alpha x^v = \frac{x^{\alpha+v}}{\Gamma(\alpha)} B(v+1, \alpha)$$

$$J^\alpha x^v = \frac{x^{\alpha+v}}{\Gamma(\alpha)} \frac{\Gamma(v+1)\Gamma(\alpha)}{\Gamma(\alpha+v+1)}$$

$$J^\alpha x^v = \frac{\Gamma(v+1)}{\Gamma(\alpha+v+1)} x^{\alpha+v}.$$

1.3 Fractional Derivatives

Definition (1.4) [12, 15, 33]: The Riemann-Liouville fractional derivative or the Riemann-Liouville fractional differential operator of order $\alpha > 0$, $x > 0$, $\alpha, x \in \mathbb{R}$, $n \in \mathbb{N}$, of the function $g(x)$ is defined by the formula:

$$D^\alpha g(x) = \begin{cases} \frac{1}{\Gamma(n-\alpha)} \frac{d^n}{dx^n} \int_0^x (x-t)^{n-\alpha-1} g(t) dt, & n-1 < \alpha < n, \\ \frac{d^n}{dx^n} g(x), & \alpha = n. \end{cases} \quad (1.9)$$

Theorem (1.6) [12]: **The identity operator:** If we set $\alpha = 0$ in the Riemann-

Liouville fractional differential operator of order α (D^α) of the function $g(x)$, then the equation becomes:

$$D^0 g(x) = g(x), \quad (1.10)$$

where $D^0 = I$ (the identity operator).

Comment (1.1) [12]: It must be mentioned that the operator (1.9) is the left inverse of the fractional integral operator (1.3), i. e.,

$$D^\alpha J^\alpha = I, \quad (1.11)$$

where $D^\alpha = J^{-\alpha}$.

Lemma (1.1) [15]: If $n - 1 < \alpha \leq n$, $n \in \mathbb{N}$, $g \in C_\mu^m$, and $\mu \geq -1$, then:

$$J^n D^n g(x) = g(x) - \sum_{k=0}^{n-1} g^{(k)}(0^+) \frac{x^k}{k!}, \quad \text{here } x > 0. \quad (1.12)$$

In fact D^α is left inverse to the corresponding inverse operator J^α and not right inverse to the operator J^α .

Lemma (1.2) [12]: Let $\alpha \in \mathbb{R}^+$ and $n \in \mathbb{N}$, where n is the integer satisfying $\alpha < n < \alpha + 1$, then:

$$D^\alpha g(x) = D^n J^{n-\alpha} g(x). \quad (1.13)$$

The Riemann-Liouville fractional derivative is equivalent to n -th order differentiation after $(n - \alpha)$ -fold integration.

Proof. The assumption on n implies that $n \geq [\alpha]$, where $[\alpha]$ denotes the smallest integer greater than or equal to number. Thus,

$$D^n J^{n-\alpha} g(x) = D^{[\alpha]} D^{n-[\alpha]} J^{n-[\alpha]} J^{[\alpha]-\alpha} g(x) = D^{[\alpha]} J^{[\alpha]-\alpha} g(x) = D^\alpha g(x).$$

In view of the semi-group property of fractional integration and the fact that ordinary differentiation is left inverse to integer integration.

Theorem (1.7) [4, 12]: Let $n - 1 < \alpha < n$, $n \in \mathbb{N}$, $\alpha, \lambda \in \mathbb{C}$ and the functions $g(x)$ and $h(x)$ be such that both $D^\alpha g(x)$ and $D^\alpha h(x)$ exists. The fractional derivative is a linear operator, *i. e.*,

$$D^\alpha (\lambda g(x) + h(x)) = \lambda D^\alpha g(x) + D^\alpha h(x). \quad (1.14)$$

Theorem (1.8) [15]: Let $\alpha, x > 0$, $\alpha \in \mathbb{R}$. The Riemann-Liouville fractional derivative of the power function satisfies :

$$D^\alpha x^v = \frac{\Gamma(v+1)}{\Gamma(v+1-\alpha)} x^{v-\alpha}, \quad v > -1. \quad (1.15)$$

Proof: The proof follows straightforwardly from the fact that the fractional differential operator (D^α) is the left inverse of the fractional integral operator (J^α) and the power function of the Riemann-Liouville fractional integral.

$$D^\alpha x^v = D^n [D^{-(n-\alpha)} x^v]$$

$$D^\alpha x^v = D^n [J^{(n-\alpha)} x^v]$$

$$D^\alpha x^v = D^n \left[\frac{\Gamma(v+1)}{\Gamma(v+n-\alpha+1)} x^{v+n-\alpha} \right]$$

$$D^\alpha x^v = \frac{\Gamma(v+1)}{\Gamma(v+n-\alpha+1)} D^n x^{v+n-\alpha}$$

$$D^\alpha x^v = \frac{\Gamma(v+1)}{\Gamma(v+n-\alpha+1)} \times \frac{\Gamma(v+n-\alpha+1)}{\Gamma(v+n-\alpha+1-n)} x^{v+n-\alpha-n}$$

$$D^\alpha x^v = \frac{\Gamma(v+1)}{\Gamma(v+1-\alpha)} x^{v-\alpha}.$$

Lemma (1.3) [33]: The constant function: Let $g(x) = k$, k is constant.

In addition, let the fractional derivative $D^\alpha g \neq 0$ for the constant function g . We have [33]

$$D^\alpha k = \frac{k}{\Gamma(1-\alpha)} x^{-\alpha} \neq 0, \quad (1.16)$$

This is of course $\equiv 0$ for $\alpha \in \mathbb{N}$, where the gamma function is defined for all real numbers except at $x = 0, -1, -2, \dots$

Definition (1.5) [7, 26]: The Caputo fractional derivative or the Caputo fractional differential operator of order $\alpha > 0$, $x > 0$, $\alpha, x \in \mathbb{R}$, $n \in \mathbb{N}$, of the function $g(x)$ is defined by the formula:

$$D_*^\alpha g(x) = \begin{cases} \frac{1}{\Gamma(n-\alpha)} \int_0^x (x-t)^{n-\alpha-1} g^{(n)}(t) dt, & n-1 < \alpha < n \\ \frac{d^n}{dx^n} g(x), & \alpha = n. \end{cases} \quad (1.17)$$

Theorem (1.9) [7, 26]: The identity operator: If we set $\alpha = 0$ in the Caputo fractional differential operator of order α (D_*^α) of the function $g(x)$, then the equation becomes:

$$D_*^0 g(x) = g(x), \quad (1.18)$$

where $D_*^0 = I$ (the identity operator).

Lemma (1.4) [14]: Let $n \in \mathbb{N}$, $\alpha \in \mathbb{R}$, $n - 1 < \alpha < n$, and $g(x)$ be a function such that $D_*^\alpha g(x)$ exist. Then:

$$D_*^\alpha g(x) = J^{n-\alpha} D^n g(x). \quad (1.19)$$

This means that the Caputo fractional operator is equivalent to $(n - \alpha)$ -fold integration after n -th order differentiation.

The Riemann-Liouville fractional derivative is equivalent to n -th order differentiation after $(n - \alpha)$ -fold integration, *i. e.*,

$$D^\alpha g(x) = D^n J^{n-\alpha} g(x). \quad (1.20)$$

From (1.19) and (1.20), we conclude the following lemma.

Lemma (1.5) [12, 33]: Let $g(x)$ be a function for which both $D^\alpha g(x)$ and $D_*^\alpha g(x)$ exists and $n - 1 < \alpha < n$, $n \in \mathbb{N}$. Then in general it holds:

$$D_*^\alpha g(x) \neq D^\alpha g(x). \quad (1.21)$$

The Caputo fractional derivative and the Riemann-Liouville fractional derivative are not equal.

Lemma (1.6)[33]: Non-commutation: Suppose that $n - 1 < \alpha < n$, $\alpha \in \mathbb{R}$, and $n, u \in \mathbb{N}$, and the function $g(x)$ is such that $D_*^\alpha g(x)$ exist. Then in general:

$$D_*^\alpha D^u g(x) = D_*^{\alpha+u} g(x) \neq D^u D_*^\alpha g(x). \quad (1.22)$$

Corollary (1.1)[33]: Suppose that $n - 1 < \alpha < n$, $n \in \mathbb{N}$, $b = \alpha - (n - 1)$, $(0 < b < 1)$, $\alpha, b \in \mathbb{R}$, and the function $g(x)$ is such that $D_*^\alpha g(x)$ exist. Then

$$D_*^\alpha g(x) = D_*^b D^{n-1} g(x). \quad (1.23)$$

Proof: Substitute b for α and $n - 1$ for u in (1.22), then:

$$D_*^b D^{n-1} g(x) = D_*^{b+n-1} g(x) = D_*^{\alpha-(n-1)+(n-1)} g(x) = D_*^\alpha g(x).$$

In general, the Riemann-Liouville operator is also non-commutative and satisfies:

$$D^n D^\alpha g(x) = D^{\alpha+n} g(x) \neq D^\alpha D^n g(x). \quad (1.24)$$

Theorem (1.10) [4, 33]: Let $n - 1 < \alpha < n$, $n \in \mathbb{N}$, $\alpha, \lambda \in \mathbb{C}$ and the functions $g(x)$ and $h(x)$ be such that both $D_*^\alpha g(x)$ and $D_*^\alpha h(x)$ exists. The Caputo fractional derivative is a linear operator, i. e.,

$$D_*^\alpha (\lambda g(x) + h(x)) = \lambda D_*^\alpha g(x) + D_*^\alpha h(x). \quad (1.25)$$

Theorem (1.11) [7, 10]: Let $n - 1 < \alpha < n$, $n \in \mathbb{N}$. The Caputo fractional derivative of the power function satisfies:

$$D_*^\alpha x^v = \begin{cases} \frac{\Gamma(v+1)}{\Gamma(v-\alpha+1)} x^{v-\alpha}, & v > n-1, v \in \mathbb{R}, \\ 0, & v \leq n-1, v \in \mathbb{N}. \end{cases} \quad (1.26)$$

Proof: For the proof, see [10].

Lemma (1.7) [33]: For the Caputo fractional derivative

$$D_*^\alpha k = 0, \quad (1.27)$$

where $k = \text{constant}$.

Proof: As usual $0 < n-1 < \alpha < n$, $n \in \mathbb{N}$, which means $n \geq 1$. Applying the definition of the Caputo derivative and since the n -th derivative $k^{(n)}$, ($n \geq 1$, $n \in \mathbb{N}$) of a constant equals 0. It follows:

$$D_*^\alpha k = \frac{1}{\Gamma(n-\alpha)} \int_0^x k^{(n)}(x-t)^{n-\alpha-1} dt = 0.$$

Lemma (1.8) [33]: **The interpolation property:** Let $n \in \mathbb{N}$, $\alpha \in \mathbb{R}$, and $g(x)$ be a function such that $D_*^\alpha g(x)$ exist. Then the following property for the Caputo operator hold:

$$\begin{aligned} \lim_{\alpha \rightarrow n} D_*^\alpha g(x) &= g^{(n)}(x), \\ \lim_{\alpha \rightarrow n-1} D_*^\alpha g(x) &= g^{(n-1)}(x) - g^{(n-1)}(0). \end{aligned} \quad (1.28)$$

Proof: The proof can be found in [33].

For the Riemann-Liouville fractional differential operator the corresponding interpolation property reads:

$$\lim_{\alpha \rightarrow n} D^\alpha g(x) = g^{(n)}(x), \quad (1.29)$$

$$\lim_{\alpha \rightarrow n-1} D^\alpha g(x) = g^{(n-1)}(x).$$

The following theorem shows the relation between the Caputo fractional derivative and the Riemann-Liouville fractional derivative.

Theorem (1.12) [12]: Let $x > 0$, $n - 1 < \alpha < n$, $n \in \mathbb{N}$, $\alpha \in \mathbb{R}$. Then

$$D_*^\alpha g(x) = D^\alpha g(x) - \sum_{k=0}^{n-1} \frac{x^{k-\alpha}}{\Gamma(k+1-\alpha)} g^{(k)}(0). \quad (1.30)$$

Proof: For the proof, see [12].

Corollary (1.2) [12]: The following relation between the Riemann-Liouville (1.9) and Caputo fractional derivative holds:

$$D_*^\alpha g(x) = D^\alpha \left(g(x) - \sum_{k=0}^{n-1} \frac{x^k}{k!} g^{(k)}(0) \right). \quad (1.31)$$

Proof: For the proof, see [12].

1.4 Linear Volterra Fractional Integral Equation

The most standard form of a linear Volterra fractional integral equation of the first kind is given as [32]

$$f(x) = \frac{1}{\Gamma(\alpha)} \int_0^x (x-t)^{\alpha-1} k(x,t) g(t) dt, \quad 0 \leq x \leq 1, \quad (1.32)$$

where $k(x,t)$ is the kernel function, $\alpha > 0$ is a real number and $g(x)$ is the unknown function that appears under the integral sign.

Moreover, the linear Volterra fractional integral equation of the second kind is given as [17]

$$g(x) = f(x) + \frac{1}{\Gamma(\alpha)} \int_0^x (x-t)^{\alpha-1} k(x,t) g(t) dt, \quad 0 \leq x \leq 1, \quad (1.33)$$

where the kernel $k(x,t)$ and the right hand side function $f(x)$ are given function, $\alpha > 0$ is a real number and $g(x)$ is the unknown function that appears under the integral sign.

This equation is also called the weakly-singular linear Volterra integral equation.

The value $\alpha = 1$ corresponds to the (non fractional) linear Volterra integral equation in the first and the second kind.

Chapter Two

Analytical and Numerical Methods for Solving Linear Volterra Fractional Integral Equation

In this chapter we introduce some important analytical and numerical methods for solving the linear Volterra fractional integral equation of the first and the second kind, namely; the Adomian decomposition method, the Haar wavelet method, the product integration method and fractional multistep method.

2.1 Theoretical Framework

In this chapter, we will use the Lagrange interpolation polynomial and the composite trapezoidal rule in the product integration method. On the other hand, the convolution will be used in the fractional multistep method.

2.1.1 Lagrange Interpolation Polynomial [2, 3]

Given a set of $k + 1$ data points

$$(x_0, y_0), \dots, (x_j, y_j), \dots, (x_k, y_k), \quad (2.1)$$

where no two x_j are the same.

The interpolation polynomial in the Lagrange form is a linear combination [14]:

$$L(x) := \sum_{j=0}^k y_j l_j(x), \quad (2.2)$$

of Lagrange basis polynomials

$$\begin{aligned}
 l_j(x) &:= \prod_{\substack{0 \leq m \leq k \\ m \neq j}} \frac{x - x_m}{x_j - x_m} \\
 &= \frac{(x - x_0)}{(x_j - x_0)} \cdots \frac{(x - x_{j-1})}{(x_j - x_{j-1})} \frac{(x - x_{j+1})}{(x_j - x_{j+1})} \cdots \frac{(x - x_k)}{(x_j - x_k)},
 \end{aligned}$$

where $0 \leq j \leq k$. Note how, given the initial assumption that no two x_j are the same, $x_j - x_m \neq 0$, so this expression is always well-defined. The reason pairs $x_i = x_j$ with $y_i \neq y_j$ are not allowed is that no interpolation function L such that $y_i = L(x_i)$ would exist; a function can only get one value for each argument x_i . On the other hand, if also $y_i = y_j$, then those two points would actually be one single point.

For all $i \neq j$, $l_j(x)$ includes the term $(x - x_i)$ in the numerator, so the whole product will be zero at $x = x_i$:

$$l_{j \neq i}(x_i) = \prod_{m \neq j} \frac{x_i - x_m}{x_j - x_m} = \frac{(x_i - x_0)}{(x_j - x_0)} \cdots \frac{(x_i - x_i)}{(x_j - x_i)} \cdots \frac{(x_i - x_k)}{(x_j - x_k)} = 0. \quad (2.2)$$

On the other hand,

$$l_i(x_i) := \prod_{m \neq i} \frac{x_i - x_m}{x_i - x_m} = 1. \quad (2.3)$$

In other words, all basis polynomials are zero at $x = x_i$, except $l_i(x)$, for which it holds that $l_i(x_i) = 1$, because it lacks that $(x - x_i)$ term.

2.1.2 Composite Trapezoidal Rule [6]

The trapezoidal rule works by approximating the area under the graph of the function $g(x)$ as a trapezoidal and calculating its area.

Suppose that the interval $[a, b]$ is subdivided into N subintervals $[x_k, x_{k+1}]$ of width $h = (b - a)/N$ by using the equally spaced nodes $x_k = a + kh$, for $k = 0, 1, \dots, N$.

The composite trapezoidal rule for N subintervals can be expressed in any of three equivalent ways:

$$\int_a^b g(x)dx \approx \frac{h}{2} \sum_{k=1}^N (g(x_{k-1}) + g(x_k)), \quad (2.4)$$

or

$$\begin{aligned} \int_a^b g(x)dx \\ \approx \frac{h}{2} (g_0 + 2g_1 + 2g_2 + \dots + 2g_{N-2} + 2g_{N-1} + g_N), \end{aligned} \quad (2.5)$$

or

$$\int_a^b g(x)dx \approx \frac{h}{2} \left[g(a) + g(b) + 2 \sum_{k=1}^{N-1} g(x_k) \right]. \quad (2.6)$$

The error of the composite trapezoidal rule is the difference between the value of the integral and the numerical result:

$$\text{error} = \int_a^b g(x)dx - \frac{h}{2} \left[g(a) + g(b) + 2 \sum_{k=1}^{N-1} g(x_k) \right].$$

There exists a number ξ between a and b , such that

$$\text{error} = - \frac{(b - a)^3}{12N^2} g''(\xi).$$

2.1.3 Convolution

Definition (2.1) [33]: The convolution of two arbitrary continuous functions $h, g: [0, d] \rightarrow \mathbb{R}$ is given by:

$$(h * g)(x) = \int_0^x h(x-t)g(t)dt, \quad 0 \leq x \leq d, \quad (2.7)$$

where $h(x-t)$ is a difference kernel, $h * g: [0, d] \rightarrow \mathbb{R}$, and $d > 0$ is a real number.

The convolution of two arbitrary continuous functions is commutative. That is:

$$h * g = \int_0^x h(x-t)g(t)dt = \int_0^x g(x-t)h(t)dt = g * h. \quad (2.8)$$

2.2 The Adomian Decomposition Method (ADM)

The Adomian decomposition method (ADM) was developed from the 1970s to the 1990s by George Adomian [1]. This method can be used to solve the linear and the non-linear Volterra fractional integral equation. In this section we will use the ADM to solve the linear Volterra fractional integral equation in the second kind which has the general form:

$$g(x) = f(x) + \frac{1}{\Gamma(\alpha)} \int_0^x (x-t)^{\alpha-1} k(x,t) g(t)dt, \quad (2.9)$$

This method involves decomposing the unknown function $g(x)$ of any equation into a sum of an infinite number of components defined by the decomposition series:

$$g(x) = \sum_{n=0}^{\infty} g_n(x), \quad (2.10)$$

or equivalently

$$g(x) = g_0(x) + g_1(x) + g_2(x) + \dots, \quad (2.11)$$

we substitute (2.10) into the linear Volterra fractional integral equation of the second kind (2.9), to obtain

$$\begin{aligned} \sum_{n=0}^{\infty} g_n(x) &= f(x) \\ &+ \frac{1}{\Gamma(\alpha)} \int_0^x (x-t)^{\alpha-1} k(x,t) \left(\sum_{n=0}^{\infty} g_n(t) \right) dt, \end{aligned} \quad (2.12)$$

or equivalently

$$\begin{aligned} g_0(x) + g_1(x) + g_2(x) + \dots &= f(x) + \frac{1}{\Gamma(\alpha)} \int_0^x (x-t)^{\alpha-1} k(x,t) [g_0(t) + \\ g_1(t) + g_2(t) + \dots] dt. \end{aligned} \quad (2.13)$$

Usually the zeroth component $g_0(x)$ is identified by all terms that are not included under the integral sign. The other components $g_{k+1}(x)$, $\forall k \geq 0$ of the unknown function $g(x)$ are determined by the recurrence relation:

$$\begin{aligned} g_0(x) &= f(x), \\ g_{k+1}(x) &= \frac{1}{\Gamma(\alpha)} \int_0^x (x-t)^{\alpha-1} k(x,t) g_k(t) dt, \quad \forall k \geq 0, \end{aligned} \quad (2.14)$$

or equivalently

$$g_0(x) = f(x),$$

$$g_1(x) = \frac{1}{\Gamma(\alpha)} \int_0^x (x - t)^{\alpha-1} k(x, t) g_0(t) dt,$$

$$g_2(x) = \frac{1}{\Gamma(\alpha)} \int_0^x (x - t)^{\alpha-1} k(x, t) g_1(t) dt,$$

and so on for other components. The components $g_0(x)$, $g_1(x)$, $g_2(x)$, ... are completely obtained. As a result, the solution $g(x)$ of the linear Volterra fractional integral equation of the second kind (2.9) is easily determined by a series form by using the series (2.11).

2.3 The Haar Wavelet Method

In this section, we will clarify some basic definitions for the Haar wavelet method [21], then we will solve linear Volterra fractional integral equations of the second kind by using Haar wavelet method with collocation method.

The Haar wavelets are usually defined for the interval $x \in [0, 1]$. In this section we want to define the method mentioned above in more general case $x \in [A, B]$.

First, we want to define the quantity $M = 2^I$, (I is the maximal level of resolution). Then we will divide the interval $[A, B]$ into $2M$ subintervals of equal length; each subinterval has the length $\Delta z = (B - A)/(2M)$. After that, two parameters are introduced: the dilation parameter i for which $i = 0, 1, \dots, I$ and the translation parameter $c = 0, 1, \dots, m - 1$ (here the notation $m = 2^i$ is introduced). The wavelet number j is identified as $j = m + c + 1$, ($m > c$ and $m \neq c$).

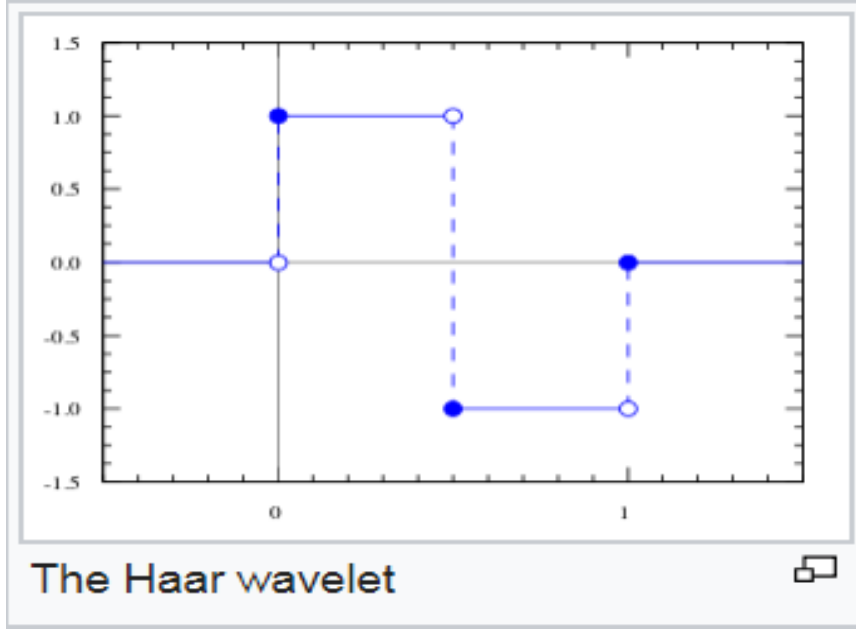


Figure 2.1: The Haar wavelet.

Figure 2.1 indicates that the Haar wavelet has good time localization but poor frequency localization. Most of applications of wavelet exploit their ability to approximate functions as efficiently as possible, which means as few coefficients as possible.

The j -th Haar wavelet is defined as:

$$h_j(x) = \begin{cases} 1 & \text{for } x \in [\tau_1, \tau_2), \\ -1 & \text{for } x \in [\tau_2, \tau_3), \\ 0 & \text{otherwise,} \end{cases} \quad (2.15)$$

where

$$\tau_1 = A + 2c \mu \Delta z,$$

$$\tau_2 = A + (2c + 1) \mu \Delta z,$$

$$\tau_3 = A + 2(c + 1) \mu \Delta z,$$

$$\mu = M/m.$$

For $j = 1$ and $x \in [0, 1]$, the function $h_1(x)$ is the scaling function or the father wavelet for the family of the Haar wavelets which is defined as

$$h_1(x) = \begin{cases} 1 & x \in [0, 1) \\ 0 & \text{otherwise} \end{cases} \quad (2.16)$$

For $j = 2$ and $x \in [0, 1]$, the function $h_2(x)$ is the mother wavelet for the family of the Haar wavelet which is defined as

$$h_2(x) = \begin{cases} 1 & 0 \leq x < \frac{1}{2} \\ -1 & \frac{1}{2} \leq x < 1 \\ 0 & \text{otherwise} \end{cases} \quad (2.17)$$

For $j = 3$ and $x \in [0, 1]$, the function $h_3(x)$ is defined as

$$h_3(x) = \begin{cases} 1 & 0 \leq x < \frac{1}{4} \\ -1 & \frac{1}{4} \leq x < \frac{2}{4} \\ 0 & \text{otherwise} \end{cases} \quad (2.18)$$

For $j = 4$ and $x \in [0, 1]$, the function $h_4(x)$ is defined as

$$h_4(x) = \begin{cases} 1 & \frac{2}{4} \leq x < \frac{3}{4} \\ -1 & \frac{3}{4} \leq x < \frac{4}{4} \\ 0 & \text{otherwise} \end{cases} \quad (2.19)$$

Table 2.1: Index computations for Haar basis function

i	0	1	1	2	2	2	2
c	0	0	1	0	1	2	3
$j = 2^i + c + 1$	2	3	4	5	6	7	8

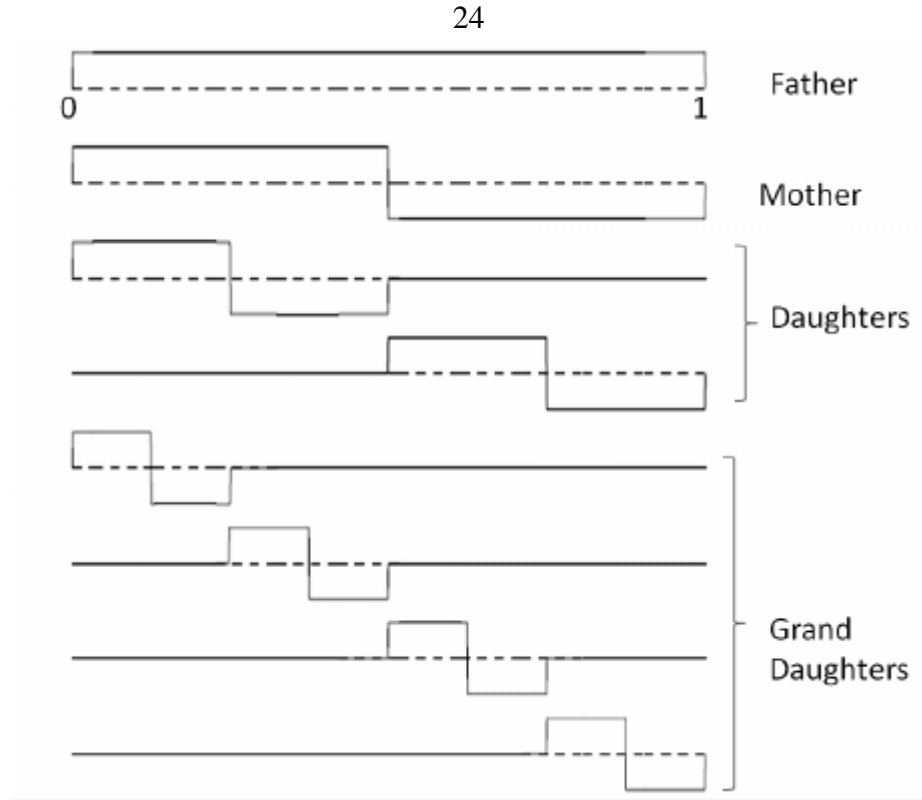


Figure 2.2: The first eight Haar functions

The orthogonal set of Haar wavelets from $h_1(x)$ to $h_8(x)$ is shown in figure 2.2, which contains a family of single square wavelets. The first basis $h_1(x)$ is called scaling function, which is equal to one for whole unit time interval. The second basis $h_2(x)$ is the fundamental square wave is called mother wavelet. The others, $h_3(x)$ to $h_8(x)$ are generated from $h_2(x)$ via two operations: dilation and translation.

The expansion of a given function $g(x)$ into the Haar wavelet series is

$$g(x) = \sum_{j=1}^{2M} b_j h_j(x), \quad x \in [A, B], \quad (2.20)$$

here b_j are the wavelet coefficients.

There are many methods for calculating b_j . In this section we apply the collocation method to calculate it.

The collocation points are defining as

$$x_k = A + (k - 0.5) \Delta z, \quad k = 1, 2, \dots, 2M. \quad (2.21)$$

Set (2.21) into (2.20) gives the discrete version, *i. e.*,

$$g(x_k) = \sum_{j=1}^{2M} b_j h_j(x_k). \quad (2.22)$$

It is convenient to put this result into the matrix form

$$g = bH, \quad (2.23)$$

where g and b are $2M$ -dimensional row vector and the Haar coefficients $H(j, k) = h_j(x_k)$ is the element of a $2M \times 2M$ matrix.

Now we want to apply the Haar wavelet method into linear Volterra fractional integral equation of the second kind which has the general form [17]:

$$g(x) = f(x) + \frac{1}{\Gamma(\alpha)} \int_0^x (x-t)^{\alpha-1} k(x, t) g(t) dt, \quad 0 \leq x \leq 1. \quad (2.24)$$

Replacing (2.22) into (2.24) and satisfying this equation in the collocation points, we obtain

$$g(x_k) = f(x_k) + \frac{1}{\Gamma(\alpha)} \int_0^{x_k} (x_k - t)^{\alpha-1} k(x_k, t) g(t) dt, \quad (2.25)$$

$$\sum_{j=1}^{2M} b_j h_j(x_k) = f(x_k) + \frac{1}{\Gamma(\alpha)} \int_0^{x_k} (x_k - t)^{\alpha-1} k(x_k, t) \sum_{j=1}^{2M} b_j h_j(t) dt,$$

$$\sum_{j=1}^{2M} b_j h_j(x_k) - \frac{1}{\Gamma(\alpha)} \int_0^{x_k} (x_k - t)^{\alpha-1} k(x_k, t) \sum_{j=1}^{2M} b_j h_j(t) dt = f(x_k),$$

$$\sum_{j=1}^{2M} b_j \left[h_j(x_k) - \frac{1}{\Gamma(\alpha)} \int_0^{x_k} (x_k - t)^{\alpha-1} k(x_k, t) h_j(t) dt \right] = f(x_k),$$

assume that

$$u_j(x_k) = \frac{1}{\Gamma(\alpha)} \int_0^{x_k} (x_k - t)^{\alpha-1} k(x_k, t) h_j(t) dt, \quad (2.26)$$

we obtain

$$\sum_{j=1}^{2M} b_j [h_j(x_k) - u_j(x_k)] = f(x_k), \quad k = 1, 2, \dots, 2M. \quad (2.27)$$

The matrix form of (2.27) is

$$b [H - U] = F, \quad (2.28)$$

where $U(j, k) = u_j(x_k)$, $F(k) = f(x_k)$.

The solution of (2.28) is

$$b = F([H - U])^{-1}. \quad (2.29)$$

The function $g(x)$ can be calculated by (2.22). Considered as (2.15) the equation (2.26) can be rewritten in the following form

$$(i) \quad U(j, k) = 0 \quad \text{for } x_k < \tau_1.$$

$$(ii) \quad U(j, k) = \frac{1}{\Gamma(\alpha)} \int_{\tau_1}^{x_k} (x_k - t)^{\alpha-1} k(x_k, t) dt, \quad \text{for } x_k \in [\tau_1, \tau_2].$$

$$(iii) \quad U(j, k) = \frac{1}{\Gamma(\alpha)} \left[\int_{\tau_1}^{\tau_2} (x_k - t)^{\alpha-1} k(x_k, t) dt - \int_{\tau_2}^{x_k} (x_k - t)^{\alpha-1} k(x_k, t) dt \right] \text{ for } x_k \in [\tau_2, \tau_3]. \quad (2.30)$$

$$(iv) \quad U(j, k) = \frac{1}{\Gamma(\alpha)} \left[\int_{\tau_1}^{\tau_2} (x_k - t)^{\alpha-1} k(x_k, t) dt - \int_{\tau_2}^{\tau_3} (x_k - t)^{\alpha-1} k(x_k, t) dt \right], \quad \text{for } x_k \geq \tau_3.$$

The integral in (2.30) can be calculated by some numerical techniques; but for simpler forms of $k(x_k, t)$ analytical integration is possible.

2.4 The Product Integration Method

In this section, we will introduce the product integration method that can be used to solve linear Volterra fractional integral equation of the second kind.

To use the product integration method as a numerical technique [9], we consider the linear Volterra integral equation of the second kind which has the general form:

$$g(x) = f(x) + \lambda \int_a^x k(x, t) g(t) dt, \quad a \leq x \leq b, \quad (2.31)$$

where $k(x, t)$ is the kernel (and is known), λ is a constant parameter and

$g(x)$ is unknown function to be determined.

We often factor out the singularity $k(x, t)$ in by writing:

$$k(x, t) = p(x, t) G(x, t), \quad (2.32)$$

where $G(x, t)$ is well-behaved function and $p(x, t)$ is badly-behaved function.

The product integration method may be used to solve linear Volterra fractional integral equation of the second kind of the form:

$$g(x) = f(x) + \lambda \int_a^x p(x, t) G(x, t) g(t) dt, \quad a \leq x \leq b. \quad (2.33)$$

First, we decompose the interval $[a, b]$ into N subintervals $\{h_i\}$ where:

$$h_i = x_{i+1} - x_i, \quad i = 0, 1, 2, \dots, N-1,$$

and

$$(2.34)$$

$$a = x_0 < x_1 < \dots < x_N = b.$$

If we use the N -point quadrature rule and collocate (2.33) at the nodes $\{x_i\}_{i=1}^N \cup \{0\}$, we get

$$g(x_i) = f(x_i) + \lambda \int_a^{x_i} p(x_i, t) G(x_i, t) g(t) dt, \quad i = 0, 1, \dots, N. \quad (2.35)$$

By a suited Lagrange interpolation polynomial. Equation (2.35) can be written as:

$$g(x_i) = f(x_i) + \lambda \sum_{j=0}^i w_{ij} G(x_i, t_j) g(t_j), \quad (2.36)$$

where $t_i = x_i = a + ih$ for $i = 0, 1, \dots, N$, with $h = (b - a)/N$ and w_{ij} are the weights which can be determined directly.

We approximate the integral terms by a product integration using composite trapezoidal rule, where $x = x_i$

$$\int_a^{x_i} p(x_i, t) G(x_i, t) g(t) dt \approx \sum_{j=0}^i w_{ij} G(x_i, t_j) g(t_j), \text{ for } i = 1, \dots, N. \quad (2.37)$$

It follows that

$$\begin{aligned} \int_a^{x_i} p(x_i, t) G(x_i, t) g(t) dt \\ = \sum_{j=0}^{i-1} \int_{t_j}^{t_{j+1}} p(x_i, t) G(x_i, t) g(t) dt \end{aligned} \quad (2.38)$$

$$\begin{aligned} \approx \sum_{j=0}^{i-1} \int_{t_j}^{t_{j+1}} p(x_i, t) \left[\frac{(t_{j+1} - t)}{h_j} G(x_i, t_j) g(t_j) \right. \\ \left. + \frac{(t - t_j)}{h_j} G(x_i, t_{j+1}) g(t_{j+1}) \right] dt \\ = \sum_{j=0}^i w_{ij} G(x_i, t_j) g(t_j), \end{aligned} \quad (2.39)$$

where

$$w_{i0} = \int_{t_0}^{t_1} p(x_i, t) \frac{(t_1 - t)}{h_0} dt, \quad \text{for } j = 0, \quad (2.40)$$

$$w_{ij} = \int_{t_j}^{t_{j+1}} p(x_i, t) \frac{(t_{j+1} - t)}{h_j} dt + \int_{t_{j-1}}^{t_j} p(x_i, t) \frac{(t - t_{j-1})}{h_{j-1}} dt,$$

$$\text{for } j = 1, \dots, i-1, \quad (2.41)$$

$$w_{ii} = \int_{t_{i-1}}^{t_i} p(x_i, t) \frac{(t - t_{i-1})}{h_{i-1}} dt, \quad \text{for } i = j. \quad (2.42)$$

The approximation solution to equation (2.35) is determined recursively using:

$$\hat{g}_n(x_i) = f(x_i) + \lambda \sum_{j=0}^i w_{ij} G(x_i, t_j) \hat{g}_n(t_j), \quad (2.43)$$

for $i = 1, 2, \dots, N$, with

$$\hat{g}_n(x_0) = f(a). \quad (2.44)$$

The resulting estimate of $g(x) = \hat{g}_n(x_n)$.

Hence, the equation (2.35) yields a system of linear algebraic equations:

$$B\hat{G}_n = F, \quad (2.45) \quad \hat{G}_n =$$

$$B^{-1}F, \quad (2.46)$$

where the matrix $B = (b_{ij})$, $0 \leq i \leq N$, $0 \leq j \leq i - 1$ with:

$$\begin{cases} b_{00} = 1, \\ b_{ij} = 0, & \forall j \leq i + 1 \\ b_{0j} = 0, & \forall j \geq 1 \\ b_{ij} = 0, & \forall j > i \\ b_{i0} = -\lambda w_{i0} G(x_i, x_0), & j = 0 \\ b_{ii} = 1 - \lambda w_{ii} G(x_i, x_i), & i = j \\ b_{ij} = -\lambda w_{ij} G(x_i, x_j), & j = 0, \dots, i - 1 \end{cases} \quad (2.47)$$

$$B = \begin{bmatrix} 1 & 0 & 0 & \cdots & 0 \\ b_{10} & b_{11} & 0 & \cdots & 0 \\ b_{20} & b_{21} & b_{22} & \cdots & 0 \\ \vdots & & & \ddots & \vdots \\ b_{N,0} & b_{N,1} & \cdots & \cdots & b_{N,N} \end{bmatrix}$$

$$F = [f(x_0) = f(a), f(x_1), \dots, f(x_N) = f(b)]^T, \quad (2.48)$$

$$\hat{G}_n = [\hat{g}_n(x_0) = \hat{g}_n(a), \hat{g}_n(x_1), \dots, \hat{g}_n(x_N)]^T, \quad (2.49)$$

where B is lower triangle matrix $(N + 1) * (N + 1)$ square matrix and $(1 - \lambda w_{ii} G(x_i, x_i)) \neq 0$ for any i , we can clearly solve this set of equations, by direct forward substitution.

2.5 Fractional Multistep Method

In this section, we will introduce the fractional multistep method that can be used to solve linear Volterra fractional integral equation of the first kind.

2.5.1 Review of a Class of Convolution Quadrature Methods and the Basic Notations

2.5.1.1 Quadrature Methods of Convolution Form

Consider the linear Volterra fractional integral equation of the first kind having the general form [32]:

$$f(x) = \mathcal{V}_\alpha g(x) = \frac{1}{\Gamma(\alpha)} \int_0^x (x-t)^{-(1-\alpha)} k(x,t) g(t) dt, \quad 0 \leq x \leq d \quad (2.50)$$

with $0 < \alpha < 1$, some real number $d > 0$ and with smooth kernel function $k: [0, d] \times [0, d] \rightarrow \mathbb{R}$.

First, we consider in (2.50) the special case $k \equiv 1$, this case called the Abel integral equation of the first kind:

$$f(x) = (\mathcal{V}_\alpha g)(x) = \frac{1}{\Gamma(\alpha)} \int_0^x (x-t)^{-(1-\alpha)} g(t) dt, \quad 0 \leq x \leq d, \quad (2.51)$$

where $g: [0, d] \rightarrow \mathbb{R}$ is a continuous function.

The convolution quadrature method of equation (2.51) at a point $0 \leq x \leq d$ is then given by:

$$(\Omega_h g)(x) = h^\alpha \sum_{j=0}^m w_{m-j} g(jh), \quad \text{for } h = x/m, \quad m = 1, 2, \dots \quad (2.52)$$

Here w_0, w_1, \dots denotes an infinite sequence of real coefficients which is assumed to be independent of the considered point x and the step size h .

The error of the convolution quadrature method (2.52) at a point $0 \leq x \leq d$ is then given by:

$$(E_h g)(x) = (\Omega_h g)(x) - (\mathcal{V}_\alpha g)(x) \quad \text{for } h = x/m, \quad m = 1, 2, \dots \quad (2.53)$$

Definition (2.1) [32]: The convolution quadrature method (2.52) for the numerical integration of (2.51) is called convergent of $q \geq 1$, if

$$(E_h t^p)(1) = \mathcal{O}(h^{p+1}) \quad \text{as } h = 1/m \rightarrow 0 \quad (p = 0, 1, \dots, q-1). \quad (2.54)$$

Note the error for equation (2.54) is satisfied only at the point $x = 1$. For a given smooth function $g : [0, d] \rightarrow \mathbb{R}$ we consider the error $(E_h g)(x)$ of the convolution quadrature method (2.52). We can write the error as the following form:

$$(E_h g)(x) = \sum_{r=0}^{q-1} \frac{g^{(r)}(0)}{r!} (E_h t^r)(x) + (E_h R_q)(x) \quad \text{for } h = x/m, \quad (2.55)$$

for $m = 1, 2, \dots$, with the remainder $R_q(t) = \frac{1}{(q-1)!} \int_0^t (t-z)^{q-1} g^{(q)}(z) dz$. Now we take arbitrary step sizes h and points x to extend the definition of the convolution quadrature method (2.52) as follows,

$$(\Omega_h g)(x) = h^\alpha \sum_{j=0}^{\lfloor x/h \rfloor} w_j g(x - jh) \quad \text{for } h > 0, \quad (2.56)$$

where $\lfloor z \rfloor$ denotes the largest integral $\leq z$. The error $(E_h g)(x)$ in (2.53) for arbitrary step sizes h and points x can be extended definition by using the definition (2.56) of the considered quadrature method there holds,

$$(E_h(g * v))(x) = ((E_h g) * v)(x) \quad \text{for } h > 0, \quad 0 \leq x \leq d, \quad (2.57)$$

for continuous functions $g, v : [0, d] \rightarrow \mathbb{R}$. Additionally for integers $p = 0, 1, \dots$ we have

$$(E_h t^p)(x) = x^{\alpha+p} (E_{h/x} t^p)(1) \quad \text{for } h > 0, \quad x > 0. \quad (2.58)$$

Both equations (2.57) and (2.58) are similar properties for the Abel integral equation and the quadrature method, respectively.

We need some properties of the weights w_0, w_1, w_2, \dots considered in the convolution quadrature method (2.52), these weights are considered as the coefficients of a power series,

$$w(\xi) = \sum_{m=0}^{\infty} w_m \xi^m, \quad (2.59)$$

which is called the generating function of the quadrature method (2.52). We suppose that this power series converges for $|\xi| < 1$, and we restrict the considerations to those generating functions $w(\xi)$ which can be represented as follows,

$$w(\xi) = (1 - \xi)^{-\alpha} \tilde{w}(\xi), \quad (2.60)$$

$\tilde{w}(\xi)$ holomorphic on $\mathbf{B}_{1+\varepsilon} = \{ \xi \in \mathbb{C} : |\xi| < 1 + \varepsilon \}$,

$$\tilde{w}(\xi) \neq 0 \quad \text{for } \xi \in \mathbf{B}_{1+\varepsilon}, \quad (2.61)$$

with some real number $\varepsilon > 0$. The representation (2.60 – 2.61) has implications on the decay of the coefficients w_m ,

$$w_m = bm^{-(1-\alpha)} + \mathcal{O}(m^{-(2-\alpha)}), \quad \text{as } m \rightarrow \infty, \quad (2.62)$$

with some real constant $b \neq 0$. In fact, (2.62) is a stability property.

2.5.1.2 Starting Weights

Now the convolution quadrature method $(\mathcal{Q}_h g)(x)$ given by (2.52) is considered as uniformly distributed grid points $x = mh$ for $m = 1, 2, \dots, N$, the integer N and the step size h are related as follows,

$$h = d/N. \quad (2.63)$$

We assume that the convolution quadrature method $(\Omega_h g)(x)$ has convergence order q , the modification convolution quadrature method is then given by [32]:

$$(\tilde{\Omega}_h g)(x) = \overbrace{h^\alpha \sum_{j=0}^m w_{m-j} g(jh)}^{=(\Omega_h g)(x)} + h^\alpha \sum_{j=0}^{q-1} w_{m,j} g(jh), \quad (2.64)$$

as approximations to fractional integral $(\mathcal{V}_\alpha g)(x)$ for $x = mh$, $m = 1, \dots, N$, respectively. $w_{m,j}$ are correction weights for the starting values to be specified for $j = 0, 1, \dots, q-1$.

In the modified quadrature method (2.64), a reasonable approach is to select starting weights such that (2.64) is exact at $x = mh$, for each $m = 1, 2, \dots, N$ for all polynomials of degree $\leq q-1$, i. e.,

$$(\tilde{\Omega}_h t^p)(x) = (\mathcal{V}_\alpha t^p)(x) \quad \text{for } p = 0, 1, \dots, q-1. \quad (2.65)$$

This means

$$\sum_{j=0}^{q-1} w_{m,j} j^p = \frac{\Gamma(p+1)}{\Gamma(\alpha+p+1)} m^{\alpha+p} - \sum_{j=0}^m w_{m-j} j^p, \quad (2.66)$$

which is a linear system of q equations for the unknowns $w_{m,j}$, with a Vandermonde matrix which does not depend on m . The right-hand side of the identity in (2.66) is holds the estimate

$$w_{m,j} = \mathcal{O}(m^{-(1-\alpha)}) \quad \text{as } m \rightarrow \infty \quad \text{for } j = 0, 1, \dots, q-1. \quad (2.67)$$

Note the considered approach for choose the starting weights in (2.65) cannot be applied in the point $x = 0$. In that case one obtains $(\tilde{\Omega}_h t^p)(0) = 0$ for

$p = 0, \dots, q - 1$ which cannot be used in the numerical solution of the integral equations of the first kind.

The error of the modified quadrature method at a point $0 \leq x \leq d$ is then given by:

$$(\tilde{E}_h g)(x) = (\tilde{\Omega}_h g)(x) - (\mathcal{V}_\alpha g)(x) \quad \text{for } h = x/m, \quad m = 1, 2, \quad (2.68)$$

For fixed step size h this error can be written as

$$(\tilde{E}_h g)(x) = (E_h R_q)(x) + h^\alpha \sum_{j=0}^{q-1} w_{m,j} R_q(jh). \quad (2.69)$$

The error of the modified quadrature method can be written in another form, *i.e.*,

$$(\tilde{E}_h g)(x) = c_q h^{q+\alpha} \sum_{j=0}^m w_{m-j} g^{(q)}(jh) + \mathcal{O}(h^{q+\alpha}), \quad \text{for } x = mh, \quad (2.70)$$

and $m = 0, 1, 2, \dots, N$, for $h \rightarrow 0$ uniformly with respect to x , with some real constant c_q .

2.5.2 Numerical Solution of Linear Volterra Fractional Integral Equation of the First Kind

2.5.2.1 Introductory Remarks and the Basic Algorithm

First, we suppose that the values of the right-hand side of equation (2.50) are given at uniformly distributed grid points

$$x_m = mh, \quad \text{for } m = 1, 2, \dots, N, \quad (2.71)$$

respectively. The modified stating weights as in (2.64) are used to approximations $g_m \approx g(x_m)$ for $m = 1, \dots, N$. This implies that the starting value $g_0 = g(0)$, approximations g_1, \dots, g_N have be determined such that the identities

$$h^\alpha \sum_{j=0}^m w_{m-j} k(x_m, x_j) g_j + h^\alpha \sum_{j=0}^{q-1} w_{m,j} k(x_m, x_j) g_j = f(x_m), \quad (2.72)$$

are satisfied for $m = 1, \dots, N$. Note that the assumption $k \equiv 1$ is now omitted. The procedure for determining these approximations is as follows:

- (a) First determine a starting value $g_0 = g(0)$.
- (b) Then solve (2.72) for $m = 1, 2, \dots, q - 1$. This leads to a linear system of $q - 1$ equations for the $q - 1$ unknowns g_1, g_1, \dots, g_{q-1} .
- (c) The identities (2.72) then are used successively for $m = q, q + 1, \dots, N$ to determine the approximations g_q, g_{q+1}, \dots, g_N .

Assumption (2.1) [32]:

- a) The convolution quadrature method (2.52) is convergent of order $q \geq 1$,
- b) the corresponding generating function $w(\xi)$ considered in (2.59) can be represented as in (2.60 – 2.61),
- c) the starting weights are determined according to the conditions in (2.65),
- d) the kernel function k in the integral operator (2.50) has continuous partial derivatives g_q to the order $q + 1$ on $[0, d] \times [0, d]$, and the solution g of the integral (2.50) is $(q + 1)$ -times continuously differentiable on the interval $[0, d]$,
- e) $k(x, x) = 1$ holds for each $0 \leq x \leq d$.

We introduce notations for the error of the scheme (2.72)

$$e_m := g(x_m) - g_m \quad \text{for } m = 0, 1, \dots, N. \quad (2.73)$$

If the conditions in **Assumption (2.1)** are satisfied, then there holds

$$\begin{aligned} & h^\alpha \sum_{j=0}^m w_{m-j} k(x_m, x_j) e_j + h^\alpha \sum_{j=0}^{q-1} w_{m,j} k(x_m, x_j) e_j \\ &= c_q h^{q+\alpha} \sum_{j=0}^m w_{m-j} \varphi(x_j) + \mathcal{O}(h^{q+\alpha}), \quad \text{for } m = 1, \dots, N, \end{aligned} \quad (2.74)$$

uniformly with respect to m , with the function $\varphi(x) = \frac{d^q}{dt^q} \{k(x, t)g(t)\}_{|t=x}$ for $0 \leq x \leq d$.

2.5.2.2 Uniqueness, Existence and Approximation Properties of the Starting Value

We now consider uniqueness, existence and approximation properties of the starting value g_1, \dots, g_{q-1} . First, we consider the linear system of equations

$$h^\alpha \sum_{j=0}^{q-1} \underbrace{(w_{m-j} + w_{m,j})}_{=: \bar{w}_{m,j}} k(x_m, x_j) g_j = f(x_m), \quad m = 1, \dots, q-1, \quad (2.75)$$

with the notation $w_m = 0$ for $m < 0$. The linear system of equation (2.75) can be written in the form:

$$h^\alpha \begin{bmatrix} \bar{w}_{1,1} k_{1,1} & 0 & \cdots & 0 \\ \bar{w}_{2,1} k_{2,1} & \bar{w}_{2,2} k_{2,2} & \cdots & 0 \\ \vdots & & \ddots & \vdots \\ \bar{w}_{q-1,1} k_{q-1,1} & \bar{w}_{q-1,2} k_{q-1,2} & \cdots & \bar{w}_{q-1,q-1} k_{q-1,q-1} \end{bmatrix} \begin{pmatrix} g_1 \\ g_2 \\ \vdots \\ g_{q-1} \end{pmatrix} \quad (2.76)$$

$$= \begin{pmatrix} f(x_1) \\ f(x_2) \\ \vdots \\ f(x_{q-1}) \end{pmatrix} - h^\alpha \begin{pmatrix} \bar{w}_{1,0} k_{1,0} \\ \bar{w}_{2,0} k_{2,0} \\ \vdots \\ \bar{w}_{q-1,0} k_{q-1,0} \end{pmatrix} g_0$$

with the notation:

$$k_{m,j} = k(x_m, x_j), \quad \text{for } 0 \leq m \leq q-1.$$

Now we offer the approximation properties of the considered starting values g_1, g_2, \dots, g_{q-1} .

Proposition (2.1) [32]: Assume that **Assumption (2.1)** be satisfied, let g_0 be a starting value with $g_0 - g(x_0) = \mathcal{O}(h^q)$ as $h \rightarrow 0$, and let the other starting values g_1, \dots, g_{q-1} be determined by (2.72) for $m = 1, \dots, q - 1$. Then there holds

$$\max_{m=1,2,\dots,q-1} |g_m - g(x_m)| = \mathcal{O}(h^q), \quad \text{as } h \rightarrow 0. \quad (2.77)$$

Proof: The proof can be found in [24].

2.5.2.3 The Approximation Properties of the Values g_q, \dots, g_N

Now we offer the main result on the convergence order of the approximations obtained by the scheme (2.72). We consider the reciprocal

$$\frac{1}{w(\xi)} = \sum_{m=0}^{\infty} w_m^{(-1)} \xi^m,$$

of the generating function $w(\xi) = \sum_{m=0}^{\infty} w_m \xi^m$, and the coefficients of the reciprocal function $1/w(\xi)$ satisfy

$$w_m^{(-1)} = \mathcal{O}(m^{-\alpha-1}), \quad \text{as } m \rightarrow \infty. \quad (2.78)$$

Theorem(2.1) [24]: Let the conditions of **Proposition (2.1)** be satisfied. Then the approximations g_q, g_{q+1}, \dots, g_N (determined by (2.72) for $m = q, \dots, N$, respectively) can be estimated as follows,

$$\max_{m=q,q+1,\dots,N} |g_m - g(x_m)| = \mathcal{O}(h^q), \quad \text{as } h \rightarrow 0.$$

Proof: The proof can be found in [24].

Chapter Three

Numerical Examples and Results

In this chapter we try to implement the aforementioned numerical methods in chapter two to solve some numerical examples. This will be carried out using proper algorithms and Matlab software. Comparison between the exact and the approximate solutions will be tabulated and graphically illustrated.

Example 3.1

Consider the linear Volterra fractional integral equation of the second kind:

$$g(x) = x^{\frac{1}{2}} - \frac{3}{4}\sqrt{\pi} x^2 + \frac{8}{3\sqrt{\pi}}x^{\frac{3}{2}} - 1 + \frac{1}{\sqrt{\pi}} \int_0^x (x-t)^{-\frac{1}{2}} 2t g(t) dt. \quad (3.1)$$

The exact solution of equation (3.1) [21] is:

$$g(x) = x^{\frac{1}{2}} - 1.$$

3.1 The Numerical Realization of Equation (3.1) Using Adomian Decomposition Method.

We notice that $f(x) = x^{\frac{1}{2}} - \frac{3}{4}\sqrt{\pi} x^2 + \frac{8}{3\sqrt{\pi}}x^{\frac{3}{2}} - 1$, $\lambda = \frac{1}{\sqrt{\pi}}$ and $k(x, t) = 2t$. The solution $g(x)$ is supposed to have a series form given in (2.10). Substituting the decomposition series (2.10) into both sides of equation (3.1) gives

$$\sum_{n=0}^{\infty} g_n(x) = x^{\frac{1}{2}} - \frac{3}{4}\sqrt{\pi} x^2 + \frac{8}{3\sqrt{\pi}} x^{\frac{3}{2}} - 1 + \frac{1}{\sqrt{\pi}} \int_0^x (x-t)^{-\frac{1}{2}} 2t \sum_{n=0}^{\infty} g_n(t) dt,$$

or equivalently

$$\begin{aligned} g_0(x) + g_1(x) + \dots \\ = x^{\frac{1}{2}} - \frac{3}{4}\sqrt{\pi} x^2 + \frac{8}{3\sqrt{\pi}} x^{\frac{3}{2}} - 1 + \frac{1}{\sqrt{\pi}} \int_0^x (x-t)^{-\frac{1}{2}} 2t [g_0(t) \\ + g_1(t) + \dots] dt. \end{aligned}$$

We identify the zeroth component $g_0(x)$ by all terms that are not included under the integral sign. There for, we obtain the following recurrence relation:

$$\begin{aligned} g_0(x) &= x^{\frac{1}{2}} - \frac{3}{4}\sqrt{\pi} x^2 + \frac{8}{3\sqrt{\pi}} x^{\frac{3}{2}} - 1, \\ g_{k+1}(x) &= \frac{1}{\sqrt{\pi}} \int_0^x (x-t)^{-\frac{1}{2}} 2t g_k(t) dt, \quad \forall k \geq 0, \end{aligned}$$

thus, we obtain

$$\begin{aligned} g_0(x) &= x^{\frac{1}{2}} - \frac{3}{4}\sqrt{\pi} x^2 + \frac{8}{3\sqrt{\pi}} x^{\frac{3}{2}} - 1, \\ g_1(x) &= \frac{1}{\sqrt{\pi}} \int_0^x (x-t)^{-\frac{1}{2}} 2t g_0(t) dt, \\ g_1(x) &= \frac{1}{\sqrt{\pi}} \int_0^x (x-t)^{-\frac{1}{2}} 2t \left[t^{\frac{1}{2}} - \frac{3}{4}\sqrt{\pi} t^2 + \frac{8}{3\sqrt{\pi}} t^{\frac{3}{2}} - 1 \right] dt, \end{aligned}$$

$$g_1(x) = \frac{3}{4}\sqrt{\pi} x^2 - \frac{48}{35}x^{\frac{7}{2}} + \frac{5}{3}x^3 - \frac{8}{3\sqrt{\pi}}x^{\frac{3}{2}},$$

$$g_2(x)$$

$$= \frac{1}{\sqrt{\pi}} \int_0^x (x-t)^{-\frac{1}{2}} 2t g_1(t) dt,$$

$$g_2(x)$$

$$= \frac{1}{\sqrt{\pi}} \int_0^x (x-t)^{-\frac{1}{2}} 2t \left[\frac{3}{4}\sqrt{\pi} t^2 - \frac{48}{35}t^{\frac{7}{2}} + \frac{5}{3}t^3 - \frac{8}{3\sqrt{\pi}}t^{\frac{3}{2}} \right] dt,$$

$$g_2(x) = \frac{48}{35}x^{\frac{7}{2}} - \frac{27}{40}\sqrt{\pi} x^5 + \frac{512}{189\sqrt{\pi}}x^{\frac{9}{2}} - \frac{5}{3}x^3,$$

and so on. Using (2.11) gives the series solution:

$$g(x) = g_0(x) + g_1(x) + g_2(x) + \dots,$$

$$\begin{aligned} g(x) &= x^{\frac{1}{2}} - \frac{3}{4}\sqrt{\pi} x^2 + \frac{8}{3\sqrt{\pi}}x^{\frac{3}{2}} - 1 + \frac{3}{4}\sqrt{\pi} x^2 - \frac{48}{35}x^{\frac{7}{2}} + \frac{5}{3}x^3 - \frac{8}{3\sqrt{\pi}}x^{\frac{3}{2}} \\ &\quad + \frac{48}{35}x^{\frac{7}{2}} - \frac{27}{40}\sqrt{\pi} x^5 + \frac{512}{189\sqrt{\pi}}x^{\frac{9}{2}} - \frac{5}{3}x^3 + \dots \end{aligned}$$

We can easily notice the appearance of identical terms with opposite signs. This phenomenon of such terms is called noise terms phenomenon.

Canceling the identical terms with opposite terms gives the exact solution:

$$g(x) = x^{\frac{1}{2}} - 1.$$

3.2 The Numerical Realization of Equation (3.1) Using the Haar Wavelet Method

Algorithm (3.1)

This algorithm can be illustrated as follows:

1. Input: 1) A, B : $[A, B]$ is the interval for the solution function.

2) I : The maximal level of resolution.

3) i : The dilation parameter.

4) c : The translation parameter.

5) $f(x)$: The function of the integral equation.

6) $k(x, t)$: The kernel function.

7) $h_1(x)$: The scaling function.

8) λ : Is a constant parameter.

2. Calculate: 1) The quantity $M = 2^I$.

2) $N = 2M$.

3) The length of each subintervals $\Delta z = \frac{B-A}{N}$.

4) $m = 2^i$.

5) The wavelet number $j = m + c + 1$.

3. Calculate: The collocation points $x_k = A + (k - 0.5) \Delta z$.

4. Calculate: $h_j(x_k), u_j(x_k)$ and $f(x_k)$.

5. Calculate: 1) The matrix $[H - U]$.

2) Calculate $b = F ([H - U]^{-1})$.

6. The solution of the linear system

$$g = b H.$$

For more details see [17, 21].

This linear system has a dimension $N \times 1$. For equation (3.1) the dimension of the system is 64×1 .

We use algorithm (3.1) to solve equation (3.1). Table (3.1) displays the exact and the numerical results using the Haar wavelet method for equation (3.1) with $\Delta z = 0.0156$.

Table (3.1): The exact and numerical solutions using the Haar wavelet method with $N = 64$.

x_k	Exact solution $g(x) = x^{\frac{1}{2}} - 1$	Numerical solution $g_h(x)$	Error = $ g - g_h $
0.0078	-0.9116116523	-0.9116009499	1.0702e-05
0.1172	-0.6576734015	-0.6576324164	4.0985e-05
0.2266	-0.5240141808	-0.5239489931	6.5188e-05
0.3359	-0.4203988440	-0.4203067536	9.2090e-05
0.4453	-0.3326826092	-0.3325562333	1.2638e-04
0.5547	-0.2552265445	-0.2550525941	1.7395e-04
0.6641	-0.1850996993	-0.1848551078	2.4459e-04
0.7734	-0.1205470450	-0.1201906958	3.5635e-04
0.8828	-0.0604189763	-0.0598738640	5.4511e-04
0.9922	-0.0039139093	-0.0030264584	8.8745e-04

The maximum error with $N = 32$ is $2.36779\text{e-}03$, the maximum error with $N = 64$ is $8.8745\text{e-}04$, the maximum error with $N = 128$ is $3.2582\text{e-}04$ and the maximum error with $N = 256$ is $1.1804\text{e-}04$.

The exact and numerical results of $g(x)$ with $N = 32$, $N = 64$,

$N = 128$, and $N = 256$, are shown in Fig. 3.1 (a), Fig. 3.1 (b), Fig. 3.1 (c), and Fig. 3.1 (d), respectively, and the resulted error with $N = 64$ is shown in Fig. 3.1 (e).

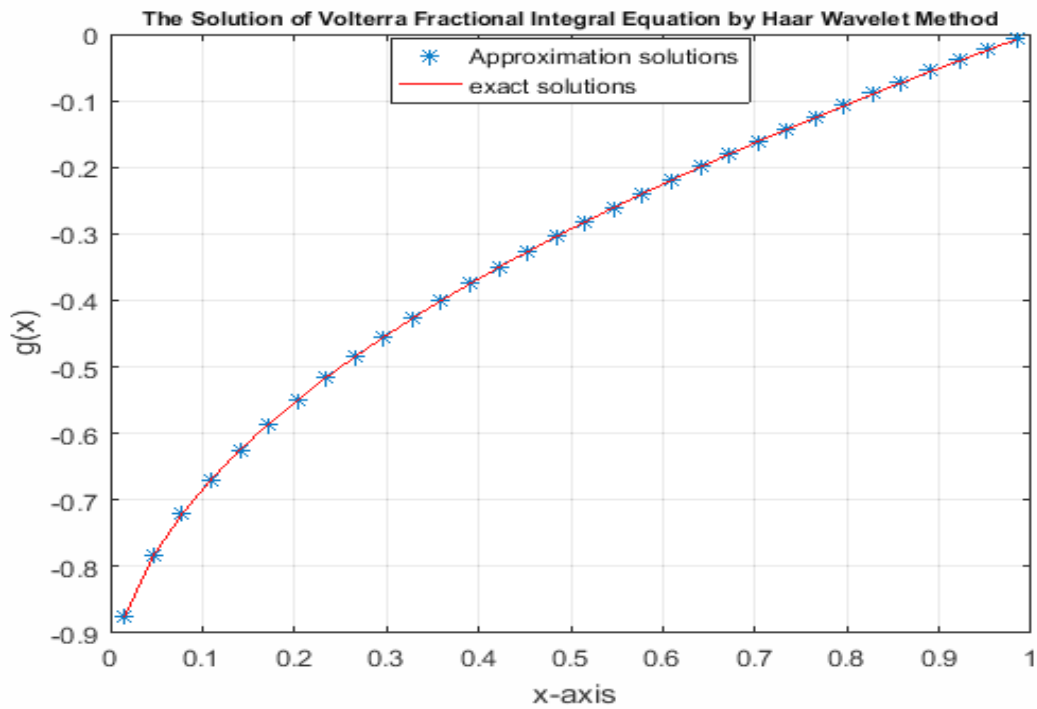


Fig. 3.1 (a) A comparison between the exact and numerical solutions in example 3.1 with $N = 32$.

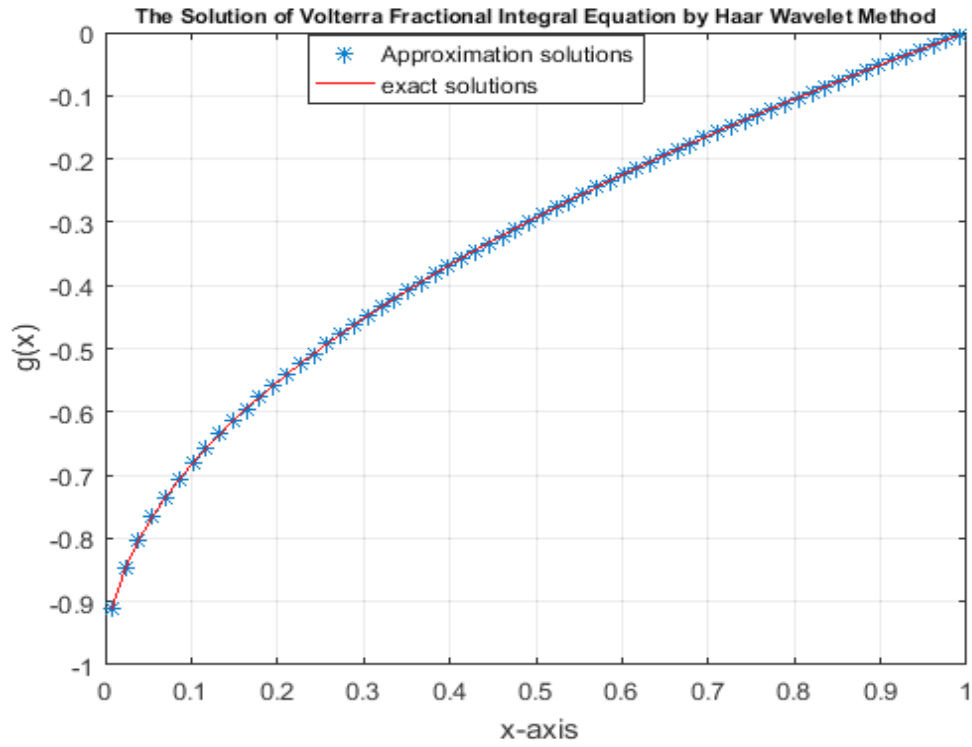


Fig. 3.1 (b) A comparison between the exact and numerical solutions in example 3.1 with $N = 64$.

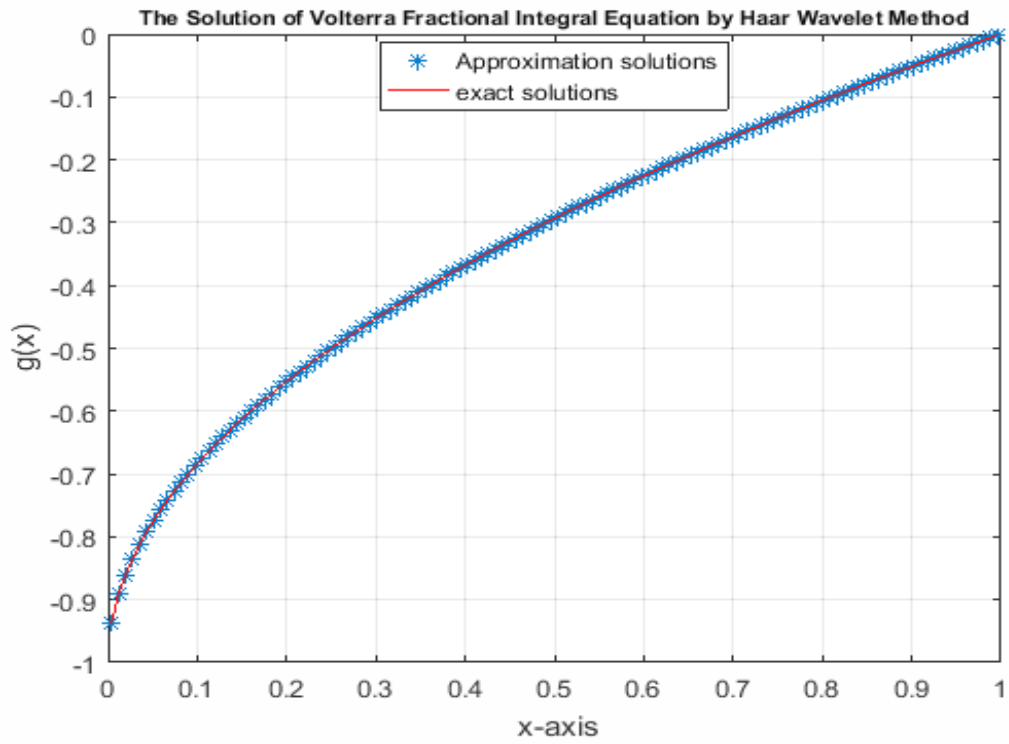


Fig. 3.1 (c) A comparison between the exact and numerical solutions in example 3.1 with $N = 128$.

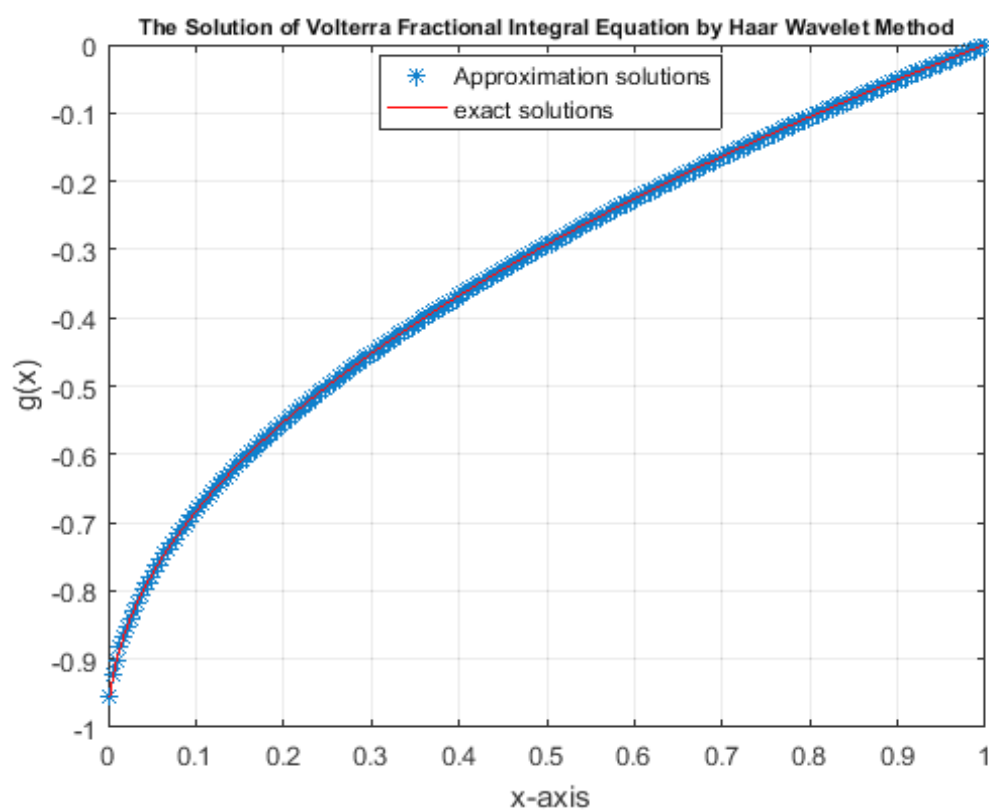


Fig. 3.1 (d) A comparison between the exact and numerical solutions in example 3.1 with $N = 256$.

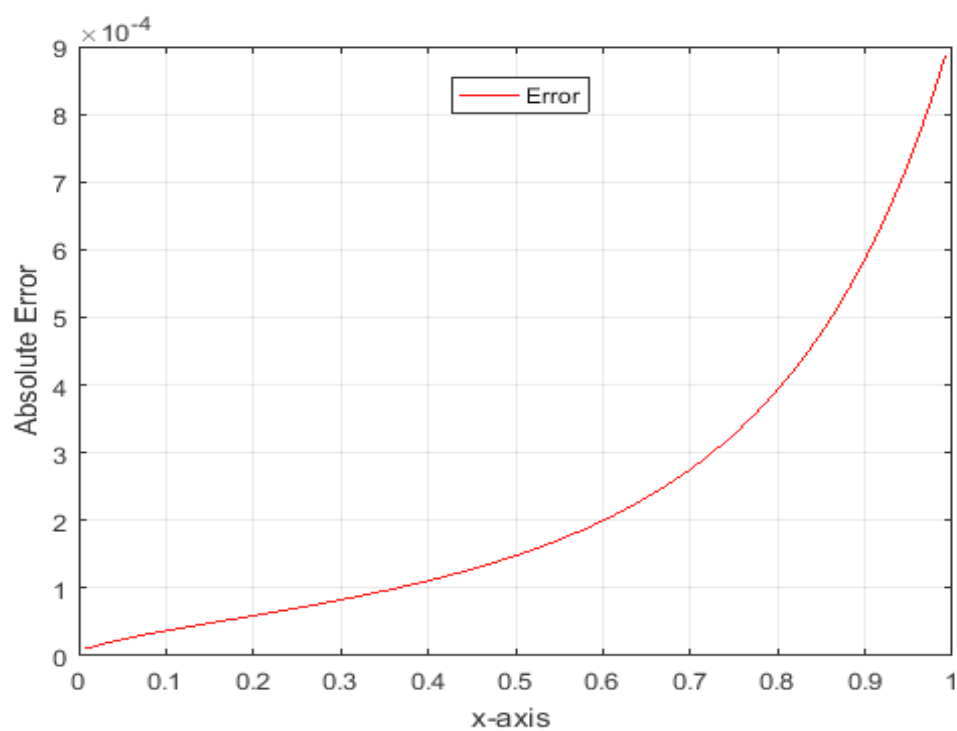


Fig. 3.1 (e) Absolute error between exact and numerical solutions in example 3.1 with $N = 64$.

3.3 The Numerical Realization of Equation (3.1) Using the Product Integration Method

The following algorithm is apply to find an approximation solution of equation (3.1) by using the product integration method.

Algorithm (3.2)

1. Input: 1) a, b : $[a, b]$ is the interval for the solution function.

2) N : The number of subdivisions of $[a, b]$.

3) $f(x)$: The function of the integral equation.

4) $G(x, t)$, $p(x, t)$: The kernel functions.

5) λ : Is a constant parameter.

6) Set $x_0 = a$ and $x_N = b$.

2. Calculate: 1) $h = \frac{b-a}{N}$.

2) $t_i = x_i = a + ih$.

3) $h_i = x_{i+1} - x_i$.

3. Calculate w_{i0} , w_{ij} and w_{ii}

$$w_{i0} = \int_{t_0}^{t_1} p(x_i, t) \frac{(t_1 - t)}{h_0} dt, \quad \text{for } j = 0,$$

$$w_{ij} = \int_{t_j}^{t_{j+1}} p(x_i, t) \frac{t_{j+1} - t}{h_j} dt + \int_{t_{j-1}}^{t_j} p(x_i, t) \frac{t - t_{j-1}}{h_{j-1}} dt, j = 1, \dots, i-1,$$

$$w_{ii} = \int_{t_{i-1}}^{t_i} p(x_i, t) \frac{(t - t_{i-1})}{h_{i-1}} dt, \quad \text{for } i = j.$$

4. Solve the recurrence relation:

$$\begin{aligned} \hat{g}_n(x_0) &= f(x_0) = f(a), \\ \hat{g}_n(x_i) &= f(x_i) + \lambda \sum_{j=0}^i w_{ij} G(x_i, t_j) \hat{g}_n(t_j), \quad \text{for } i \\ &= 1, 2, \dots, N, \end{aligned}$$

or we can also solve the linear system of algebraic equations:

$$\hat{G}_n = B^{-1}F.$$

For more details see [9].

We use algorithm (3.2) to solve equation (3.1). According to that, we get the following results:

W Function

If $p(x_i, t) = (x_i - t)^{-\frac{1}{2}}$, then the equations becomes:

$$w_{i0} = \frac{1}{h_0} \int_{t_0}^{t_1} p(x_i, t)(t_1 - t) dt, \quad \text{for } j = 0,$$

$$w_{i0} = \frac{1}{h} \int_0^h (x_i - t)^{-\frac{1}{2}} (h - t) dt,$$

$$w_{i0} = \frac{1}{h} \int_0^h (ih - t)^{-\frac{1}{2}} (h - t) dt,$$

$$w_{i0} = \frac{2}{3} h^{\frac{1}{2}} \left[3i^{\frac{1}{2}} + 2 \left[(i-1)^{\frac{3}{2}} - (i)^{\frac{3}{2}} \right] \right].$$

$$w_{ij} = \int_{t_j}^{t_{j+1}} p(x_i, t) \frac{t_{j+1} - t}{h_j} dt + \int_{t_{j-1}}^{t_j} p(x_i, t) \frac{t - t_{j-1}}{h_{j-1}} dt, j = 1, \dots, i-1$$

$$w_{ij} = \int_{jh}^{(j+1)h} (x_i - t)^{-\frac{1}{2}} \frac{(j+1)h - t}{h} dt \\ + \int_{(j-1)h}^{jh} (x_i - t)^{-\frac{1}{2}} \frac{t - (j-1)h}{h} dt$$

$$w_{ij} = \int_{jh}^{(j+1)h} (ih - t)^{-\frac{1}{2}} \frac{(j+1)h - t}{h} dt \\ + \int_{(j-1)h}^{jh} (ih - t)^{-\frac{1}{2}} \frac{t - (j-1)h}{h} dt$$

$$w_{ij} = \frac{4}{3} h^{\frac{1}{2}} \left[(i-j-1)^{\frac{3}{2}} + (i-j+1)^{\frac{3}{2}} - 2(i-j)^{\frac{3}{2}} \right].$$

$$w_{ii} = \frac{1}{h_{i-1}} \int_{t_{i-1}}^{t_i} p(x_i, t) (t - t_{i-1}) dt, \quad \text{for } i = j,$$

$$w_{ii} = \frac{1}{h} \int_{(i-1)h}^{ih} (x_i - t)^{-\frac{1}{2}} (t - (i-1)h) dt,$$

$$w_{ii} = \frac{1}{h} \int_{(i-1)h}^{ih} (ih - t)^{-\frac{1}{2}} (t - (i-1)h) dt,$$

$$w_{ii} = \frac{4}{3} h^{\frac{1}{2}}.$$

From above equations we obtain the linear system of algebraic equations:

$$G_n = B^{-1}F.$$

This linear system has a dimension $(N + 1) \times 1$. For equation (3.1) the dimension of the system is 65×1 .

Table (3.2) displays the exact and the numerical results using the product integration method for equation (3.1) with $h = 0.0156$.

Table (3.2): The exact and numerical solutions using the product integration method with $N = 64$.

x_i	Exact solution $g(x) = x^{\frac{1}{2}} - 1$	Numerical solution $g_h(x)$	Error = $ g - g_h $
0	-1	-1	0
0.125	-0.6464466094	-0.6463939905	5.2619e-05
0.250	-0.5000000000	-0.4999385093	6.1491e-05
0.375	-0.3876275643	-0.3875532017	7.4363e-05
0.500	-0.2928932188	-0.2927990146	9.4204e-05
0.625	-0.2094305849	-0.2093044528	1.2613e-04
0.750	-0.1339745962	-0.1337942129	1.8038e-04
0.875	-0.0645856533	-0.0643065527	2.7910e-04
1	0	4.7435e-04	4.7435e-04

The maximum error with $N = 32$ is $1.871827e-03$, the maximum error with $N = 64$ is $4.7435e-04$, the maximum error with $N = 128$ is $1.1997e-04$ and the maximum error with $N = 256$ is $3.0256e-05$.

The exact and numerical results of $g(x)$ with $N = 32$, $N = 64$, $N = 128$, and $N = 256$, are shown in Fig. 3.2 (a), Fig. 3.2 (b), Fig. 3.2 (c), and Fig. 3.2 (d), respectively, and the resulted error with $N = 64$ is shown in Fig. 3.2 (e).

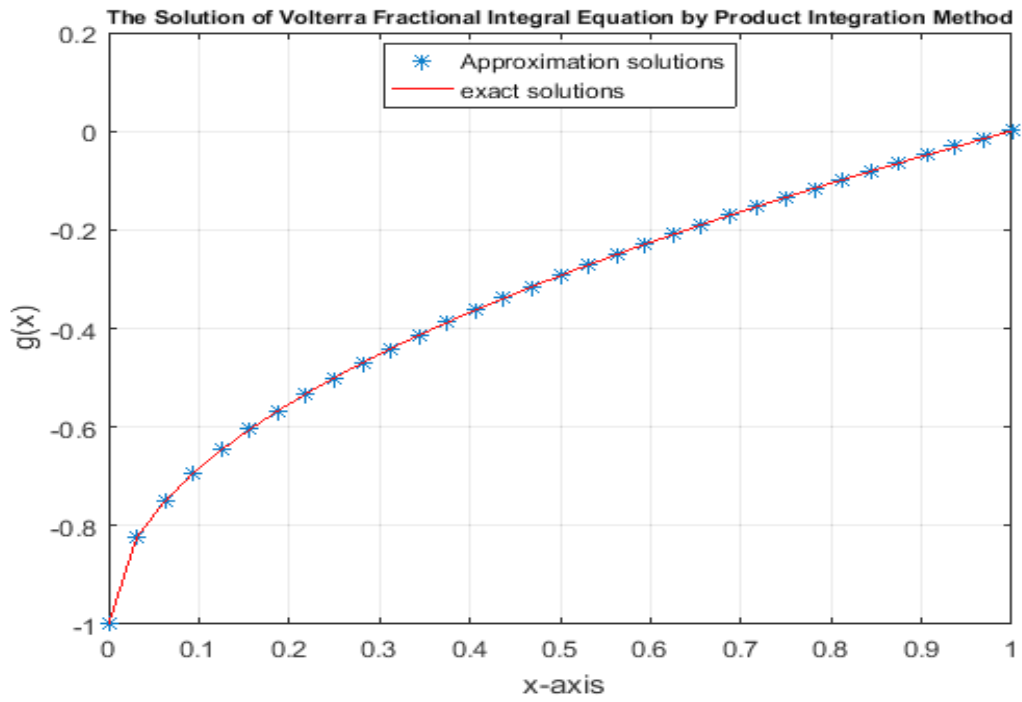


Fig. 3.2 (a) A comparison between the exact and numerical solutions in example 3.1 with $N = 32$.

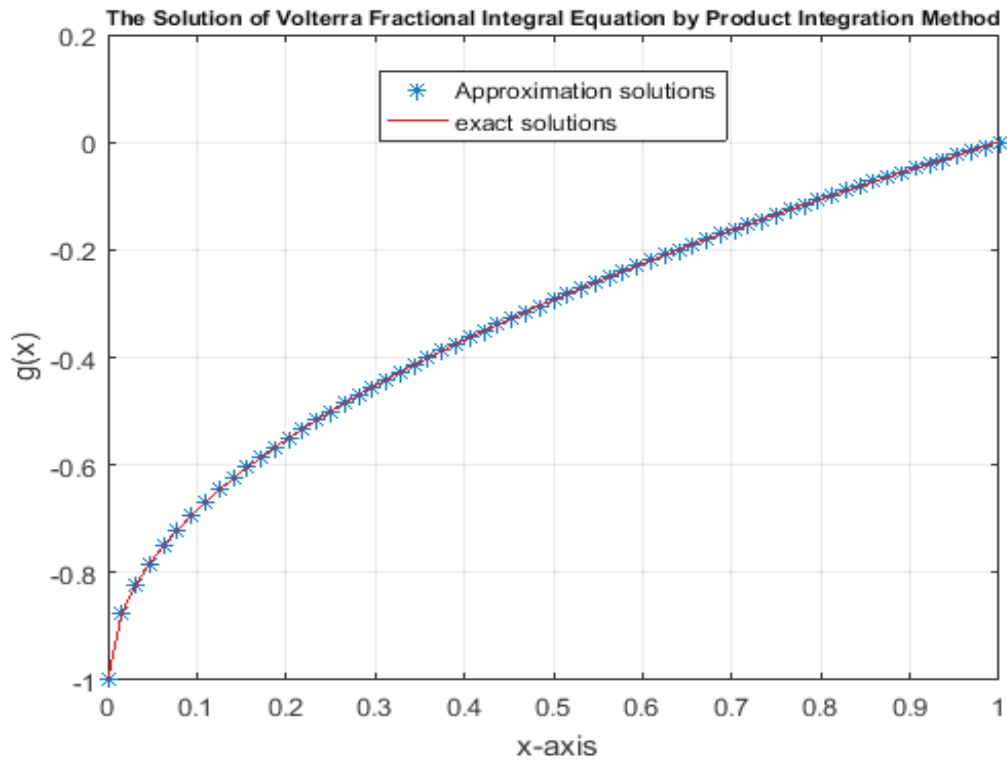


Fig. 3.2 (b) A comparison between the exact and numerical solutions in example 3.1 with $N = 64$.

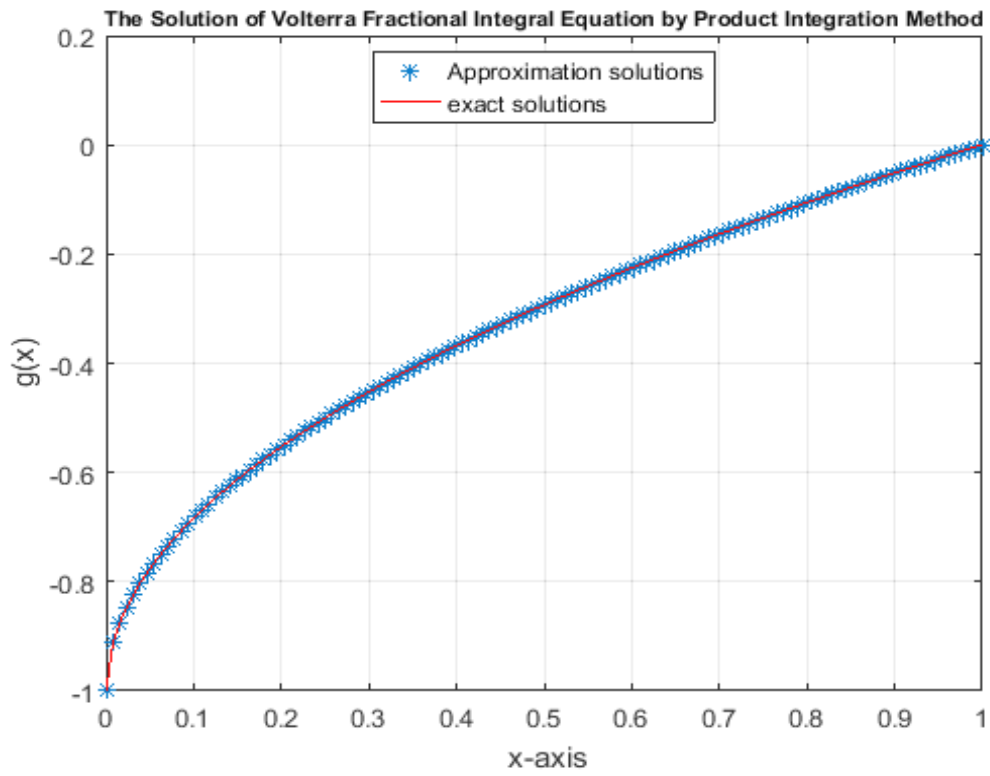


Fig. 3.2 (c) A comparison between the exact and numerical solutions in example 3.1 with $N = 128$.

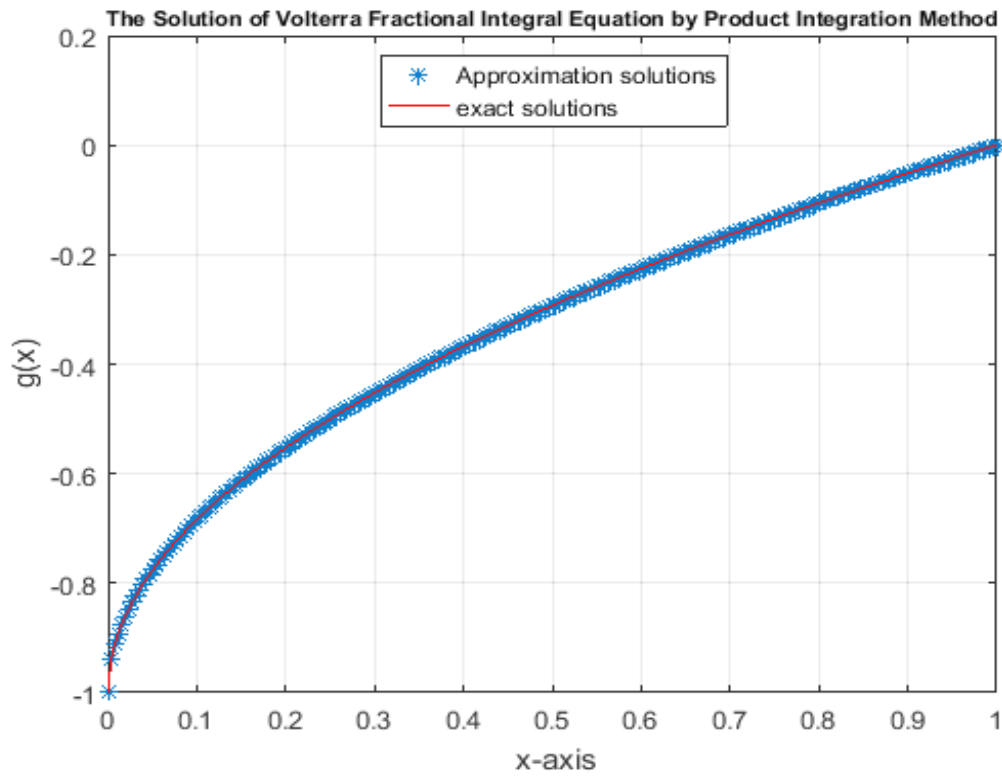


Fig. 3.2 (d) A comparison between the exact and numerical solutions in example 3.1 with $N = 256$.

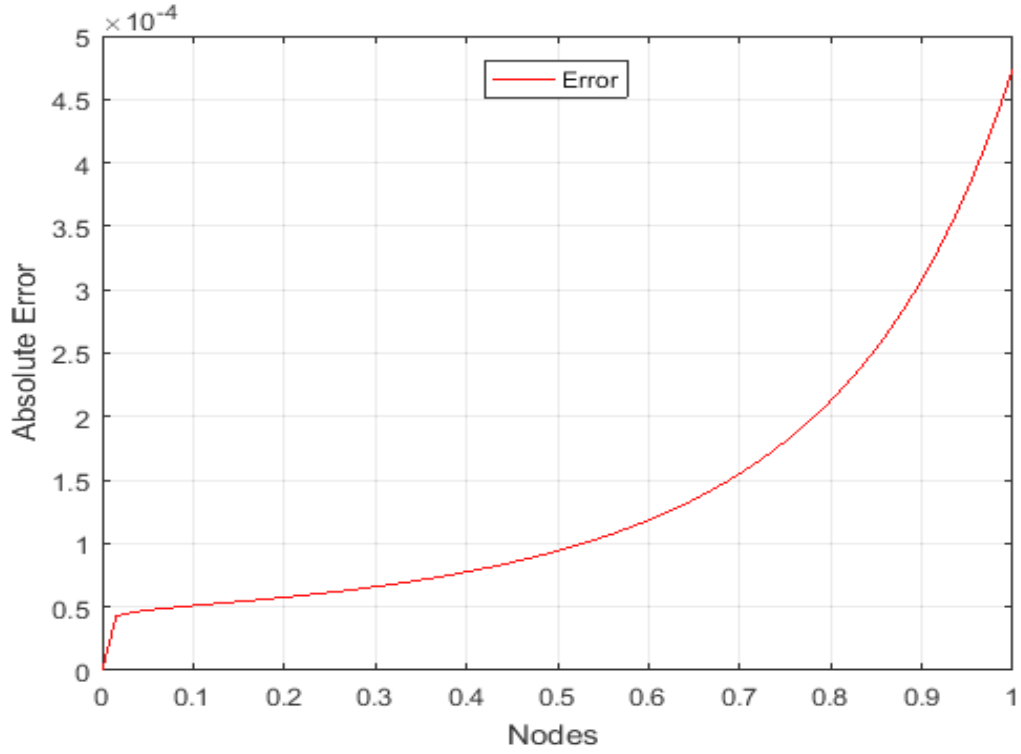


Fig. 3.2 (e) Absolute error between exact and numerical solutions in example 3.1 with $N = 64$.

Example 3.2

Consider the linear Volterra fractional integral equation of the second kind:

$$g(x) = 2x^{\frac{3}{2}} - \frac{x}{2} - \frac{5\sqrt{\pi}}{8} x^{\frac{7}{2}} + \frac{8}{15\sqrt{\pi}} x^3 + \frac{1}{\sqrt{\pi}} \int_0^x (x-t)^{-\frac{1}{2}} x^{\frac{1}{2}} t g(t) dt. \quad (3.2)$$

The exact solution of equation (3.2) [9] is:

$$g(x) = 2x^{\frac{3}{2}} - \frac{x}{2}.$$

Now, we apply all numerical methods mentioned in chapter two to solve (3.2).

3.4 The Numerical Realization of Equation (3.2) Using Adomian Decomposition Method

We notice that $f(x) = 2x^{\frac{3}{2}} - \frac{x}{2} - \frac{5\sqrt{\pi}}{8}x^{\frac{7}{2}} + \frac{8}{15\sqrt{\pi}}x^3$, $\lambda = \frac{1}{\sqrt{\pi}}$ and $k(x, t) = x^{\frac{1}{2}}t$.

The solution $g(x)$ is supposed to have a series form given in (2.10). Substituting the decomposition series (2.10) into both sides of equation (3.2) gives

$$\begin{aligned} \sum_{n=0}^{\infty} g_n(x) &= 2x^{\frac{3}{2}} - \frac{x}{2} - \frac{5\sqrt{\pi}}{8}x^{\frac{7}{2}} + \frac{8x^3}{15\sqrt{\pi}} \\ &\quad + \frac{1}{\sqrt{\pi}} \int_0^x (x-t)^{-\frac{1}{2}} x^{\frac{1}{2}} t \sum_{n=0}^{\infty} g_n(t) dt \end{aligned}$$

or equivalently

$$\begin{aligned} g_0(x) + g_1(x) + \dots \\ = 2x^{\frac{3}{2}} - \frac{x}{2} - \frac{5\sqrt{\pi}}{8}x^{\frac{7}{2}} + \frac{8x^3}{15\sqrt{\pi}} + \frac{1}{\sqrt{\pi}} \int_0^x (x-t)^{-\frac{1}{2}} x^{\frac{1}{2}} t [\\ g_0(t) + g_1(t) + \dots] dt. \end{aligned}$$

We identify the zeroth component $g_0(x)$ by all terms that are not included under the integral sign. There for, we obtain the following recurrence relation:

$$\begin{aligned} g_0(x) &= 2x^{\frac{3}{2}} - \frac{x}{2} - \frac{5\sqrt{\pi}}{8}x^{\frac{7}{2}} + \frac{8}{15\sqrt{\pi}}x^3, \\ g_{k+1}(x) &= \frac{1}{\sqrt{\pi}} \int_0^x (x-t)^{-\frac{1}{2}} x^{\frac{1}{2}} t g_k(t) dt, \quad \forall k \geq 0, \end{aligned}$$

thus, we obtain

$$g_0(x) = 2x^{\frac{3}{2}} - \frac{x}{2} - \frac{5\sqrt{\pi}}{8}x^{\frac{7}{2}} + \frac{8}{15\sqrt{\pi}}x^3,$$

$$g_1(x) = \frac{1}{\sqrt{\pi}} \int_0^x (x-t)^{-\frac{1}{2}} x^{\frac{1}{2}} t g_0(t) dt,$$

$$g_1(x) = \frac{1}{\sqrt{\pi}} \int_0^x (x-t)^{-\frac{1}{2}} x^{\frac{1}{2}} t \left[2t^{\frac{3}{2}} - \frac{t}{2} - \frac{5\sqrt{\pi}}{8}t^{\frac{7}{2}} + \frac{8}{15\sqrt{\pi}}t^3 \right] dt,$$

$$g_1(x) = \frac{5\sqrt{\pi}}{8}x^{\frac{7}{2}} - \frac{8}{15\sqrt{\pi}}x^3 - \frac{315\pi}{2048}x^{\frac{11}{2}} + \frac{2048}{4725\pi}x^5,$$

$$g_2(x) = \frac{1}{\sqrt{\pi}} \int_0^x (x-t)^{-\frac{1}{2}} x^{\frac{1}{2}} t g_1(t) dt,$$

$$g_2(x) = \frac{1}{\sqrt{\pi}} \int_0^x (x-t)^{-\frac{1}{2}} x^{\frac{1}{2}} t \left[\frac{5\sqrt{\pi}t^{\frac{7}{2}}}{8} - \frac{8t^3}{15\sqrt{\pi}} - \frac{315\pi t^{\frac{11}{2}}}{2048} + \frac{2048t^5}{4725\pi} \right] dt,$$

$$g_2(x) = \frac{315\pi}{2048}x^{\frac{11}{2}} - \frac{2048}{4725\pi}x^5 - \frac{135135\pi^{\frac{3}{2}}}{1048576}x^{\frac{15}{2}} + \frac{20971520}{70945875\pi^{\frac{3}{2}}}x^7,$$

and so on. Using (2.11) gives the series solution:

$$g(x) = g_0(x) + g_1(x) + g_2(x) + \cdots,$$

$$g(x) = 2x^{\frac{3}{2}} - \frac{x}{2} - \frac{5\sqrt{\pi}}{8}x^{\frac{7}{2}} + \frac{8}{15\sqrt{\pi}}x^3 + \frac{5\sqrt{\pi}}{8}x^{\frac{7}{2}} - \frac{8}{15\sqrt{\pi}}x^3 - \frac{315\pi}{2048}x^{\frac{11}{2}} + \frac{2048}{4725\pi}x^5 + \frac{315\pi}{2048}x^{\frac{11}{2}} - \frac{2048}{4725\pi}x^5$$

$$-\frac{135135 \pi^{\frac{3}{2}}}{1048576} x^{\frac{15}{2}} + \frac{20971520}{70945875 \pi^{\frac{3}{2}}} x^7 + \dots$$

We can easily notice the appearance of identical terms with opposite signs.

This phenomenon of such terms is called noise terms phenomenon.

Canceling the identical terms with opposite terms gives the exact solution:

$$g(x) = 2x^{\frac{3}{2}} - \frac{x}{2}.$$

3.5 The Numerical Realization of Equation (3.2) Using the Haar Wavelet Method

Using algorithm (3.1) for equation (3.2). Table (3.3) displays the exact and the numerical results using the Haar wavelet method for equation (3.2) with $\Delta z = 0.0156$.

Table (3.3): The exact and numerical solutions using the Haar wavelet method with $N = 64$.

x_k	Exact solution $g(x) = 2x^{\frac{3}{2}} - \frac{1}{2}x$	Numerical solution $g_h(x)$	Error = $ g - g_h $
0.0078	-0.0025251820	-0.0025252012	1.9151e-08
0.1172	0.02163904650	0.02164230903	3.2625e-06
0.2266	0.10239982428	0.10241481435	1.4990e-05
0.3359	0.22145077666	0.22148741651	3.6640e-05
0.4453	0.37167330113	0.37174356233	7.0261e-05
0.5547	0.54888930218	0.54900834042	1.1904e-04
0.6641	0.75025821180	0.75044613143	1.8792e-04
0.7734	0.97368503971	0.97396969675	2.8466e-04
0.8828	1.21754149948	1.21796312374	4.2163e-04
0.9922	1.48051458614	1.48113375569	6.1917e-04

The maximum error with $N = 32$ is $1.728318\text{e-}03$, the maximum error with $N = 64$ is $6.1917\text{e-}04$, the maximum error with $N = 128$ is $2.1962\text{e-}04$ and the maximum error with $N = 256$ is $7.7580\text{e-}05$.

The exact and numerical results of $g(x)$ with $N = 32$, $N = 64$, $N = 128$, and $N = 256$, are shown in Fig. 3.3 (a), Fig. 3.3 (b), Fig. 3.3 (c), and Fig. 3.3 (d), respectively, and the resulted error with $N = 64$ is shown in Fig. 3.3 (e).

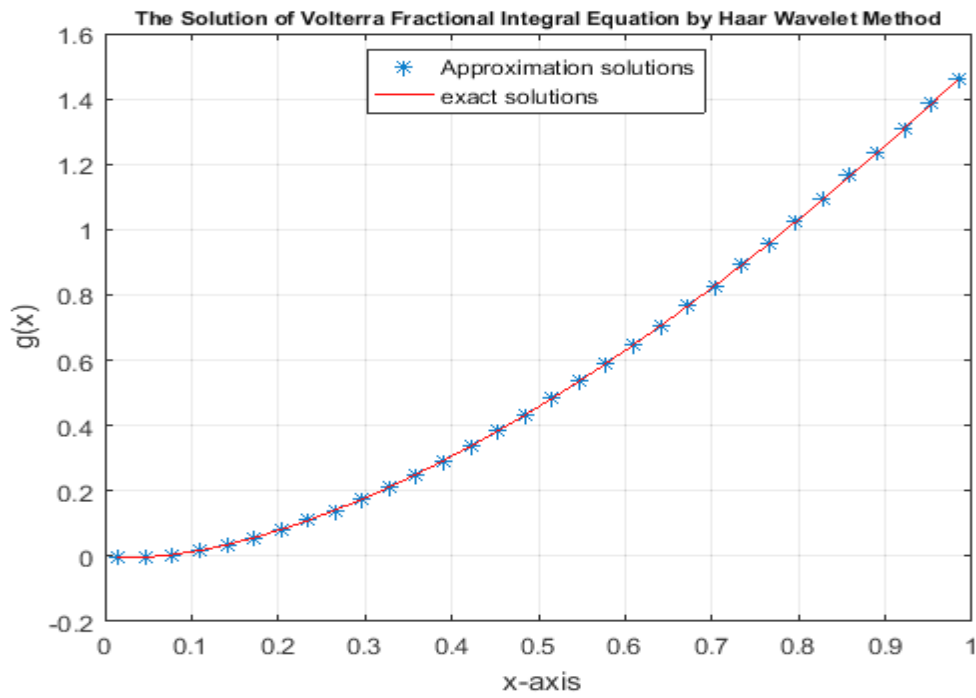


Fig. 3.3 (a) A comparison between the exact and numerical solutions in example 3.2 with $N = 32$.

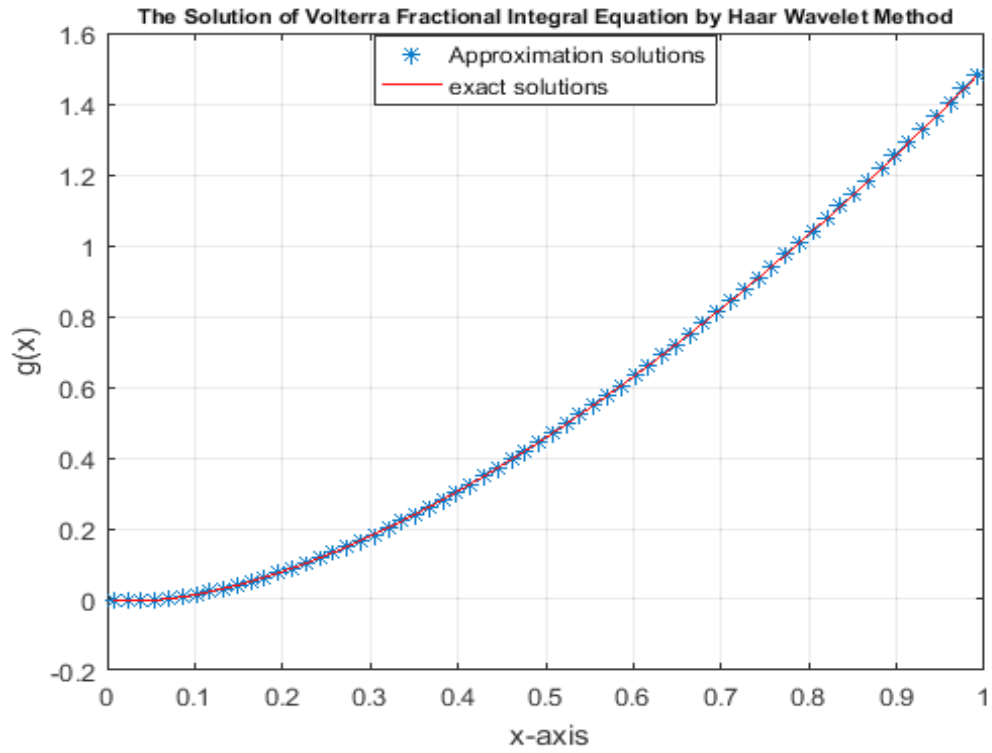


Fig. 3.3 (b) A comparison between the exact and numerical solutions in example 3.2 with $N = 64$.

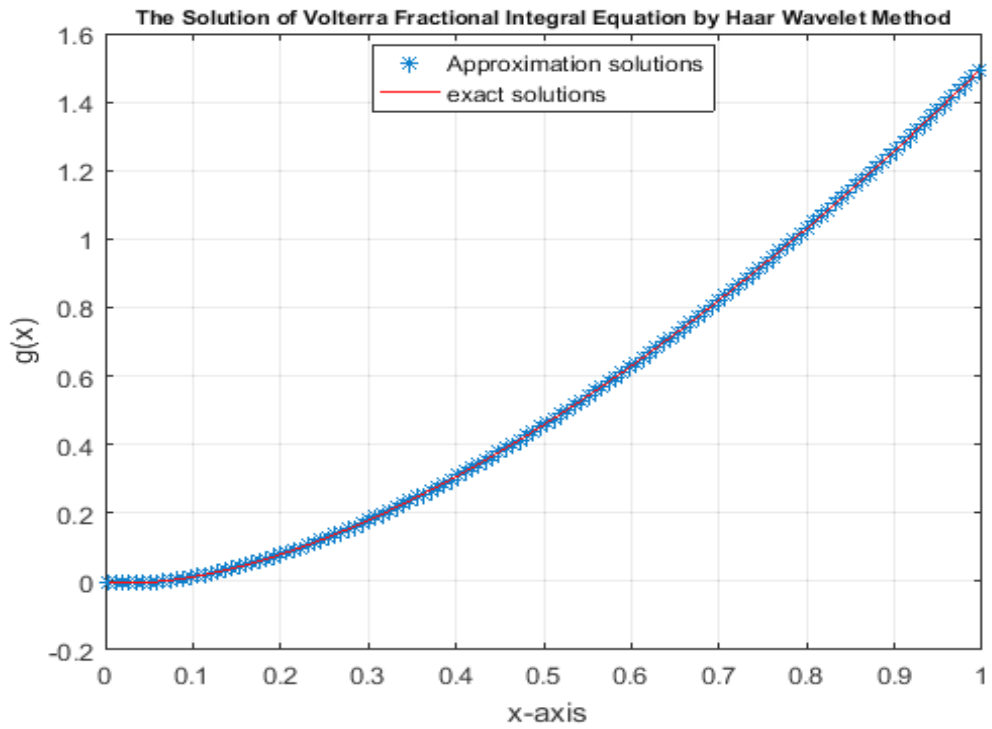


Fig. 3.3 (c) A comparison between the exact and numerical solutions in example 3.2 with $N = 128$.

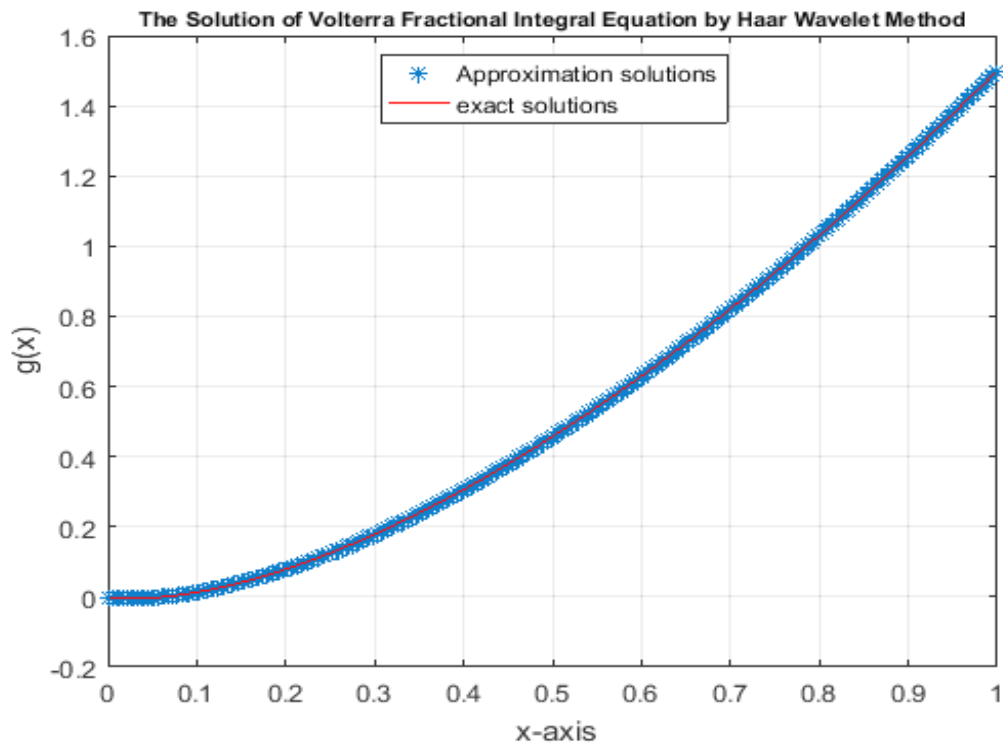


Fig. 3.3 (d) A comparison between the exact and numerical solutions in example 3.2 with $N = 256$.

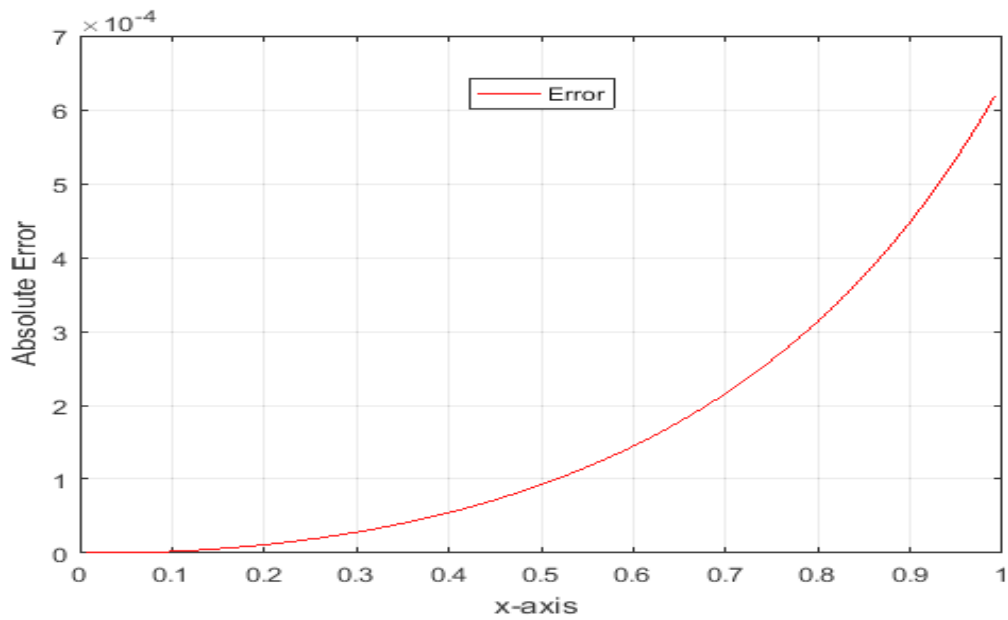


Fig. 3.3 (e) Absolute error between exact and numerical solutions in example 3.2 with $N = 64$.

3.6 The Numerical Realization of Equation (3.2) Using the Product Integration Method

Using algorithm (3.2) for equation (3.2). Table (3.4) displays the exact and the numerical results using the product integration method for equation (3.2) with $h = 0.0156$.

Table (3.4): The exact and numerical solutions using the product integration method with $N = 64$.

x_i	Exact solution $g(x) = 2x^{\frac{3}{2}} - \frac{1}{2}x$	Numerical solution $g_h(x)$	Error = $ g - g_h $
0	0	0	0
0.125	0.02588834764	0.02589112774	2.7801e-06
0.250	0.12500000000	0.12501070272	1.0703e-05
0.375	0.27177932677	0.27180216287	2.2836e-05
0.500	0.45710678118	0.45714650388	3.9723e-05
0.625	0.67571176880	0.67577456999	6.2801e-05
0.750	0.92403810567	0.92413277868	9.4673e-05
0.875	1.19947510671	1.19961494314	1.3984e-04
1	1.50000000000	1.50020621277	2.0621e-04

The maximum error with $N = 32$ is 8.1266e-04, the maximum error with $N = 64$ is 2.0621e-04, the maximum error with $N = 128$ is 5.2106e-05 and the maximum error with $N = 256$ is 1.3125e-05.

The exact and numerical results of $g(x)$ with $N = 32$, $N = 64$, $N = 128$, and $N = 256$, are shown in Fig. 3.4 (a), Fig. 3.4 (b), Fig. 3.4 (c), and Fig. 3.4 (d), respectively, and the resulted error with $N = 64$ is shown in Fig. 3.4 (e).

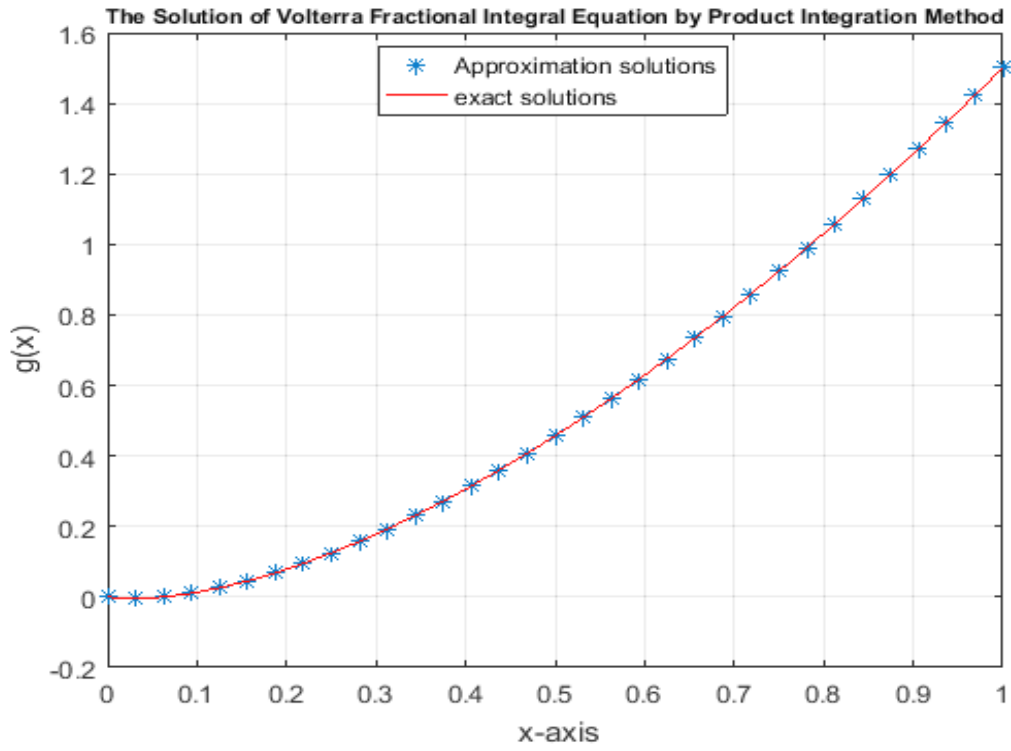


Fig.

3.4 (a) A comparison between the exact and numerical solutions in example 3.2 with

$$N = 32.$$

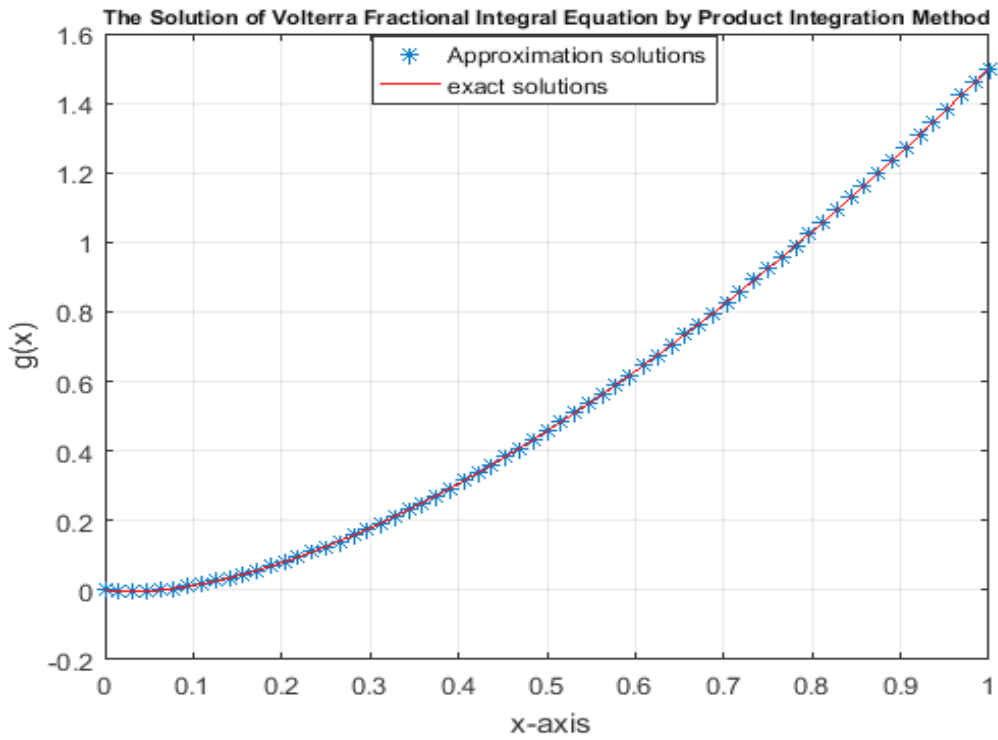


Fig. 3.4 (b) A comparison between the exact and numerical solutions in example 3.2 with $N = 64$.

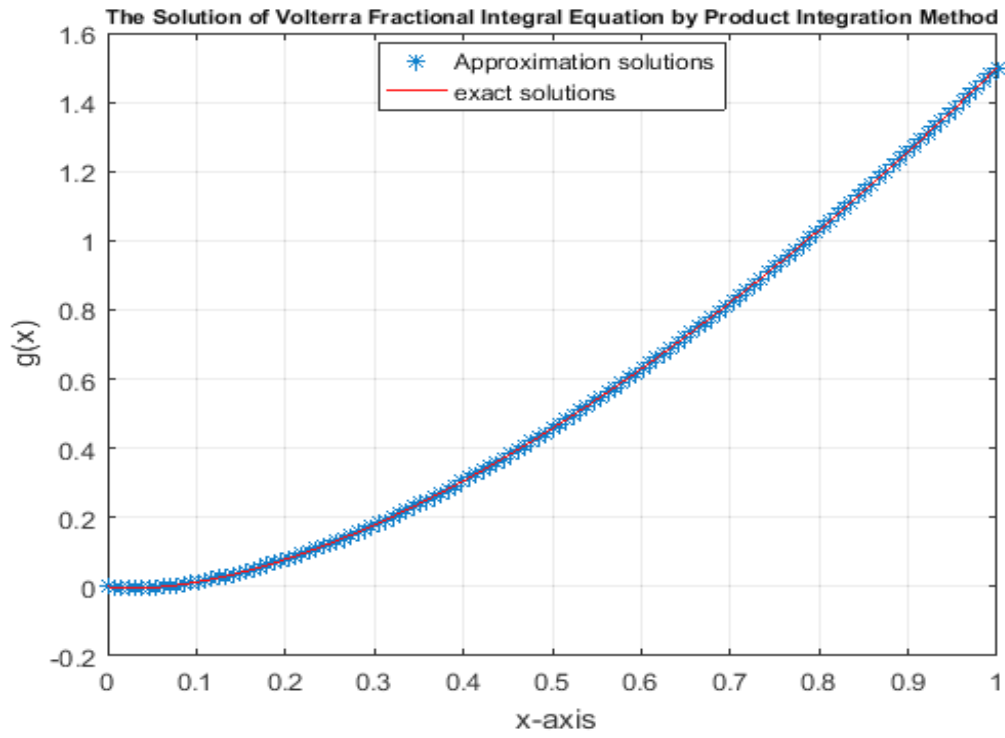


Fig. 3.4 (c) A comparison between the exact and numerical solutions in example 3.2 with $N = 128$.

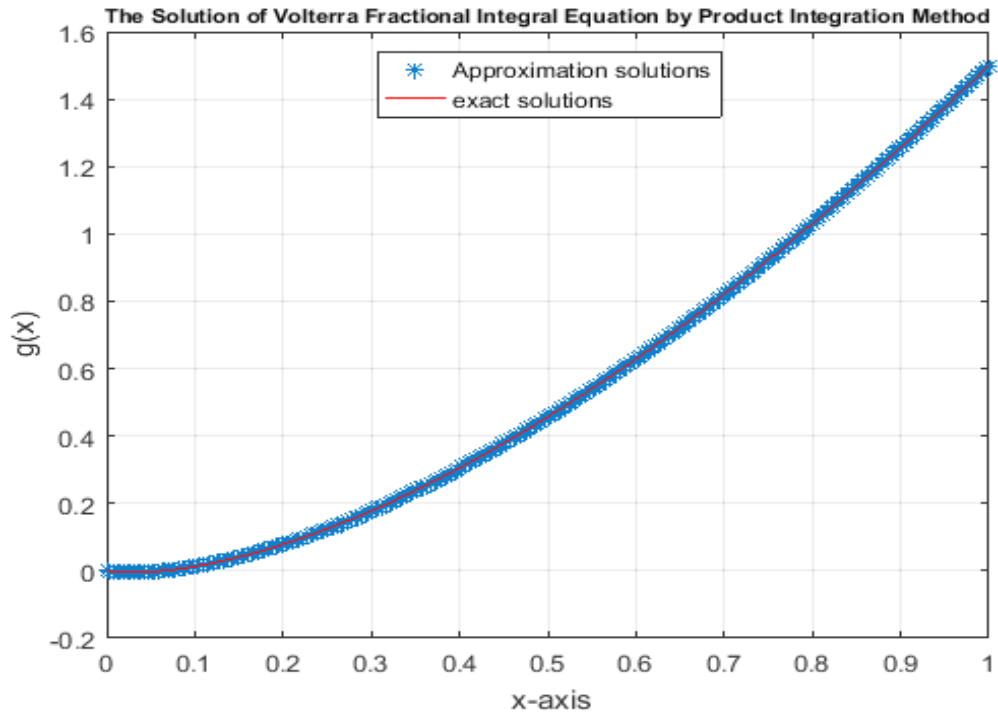


Fig. 3.4 (d) A comparison between the exact and numerical solutions in example 3.2 with $N = 256$.

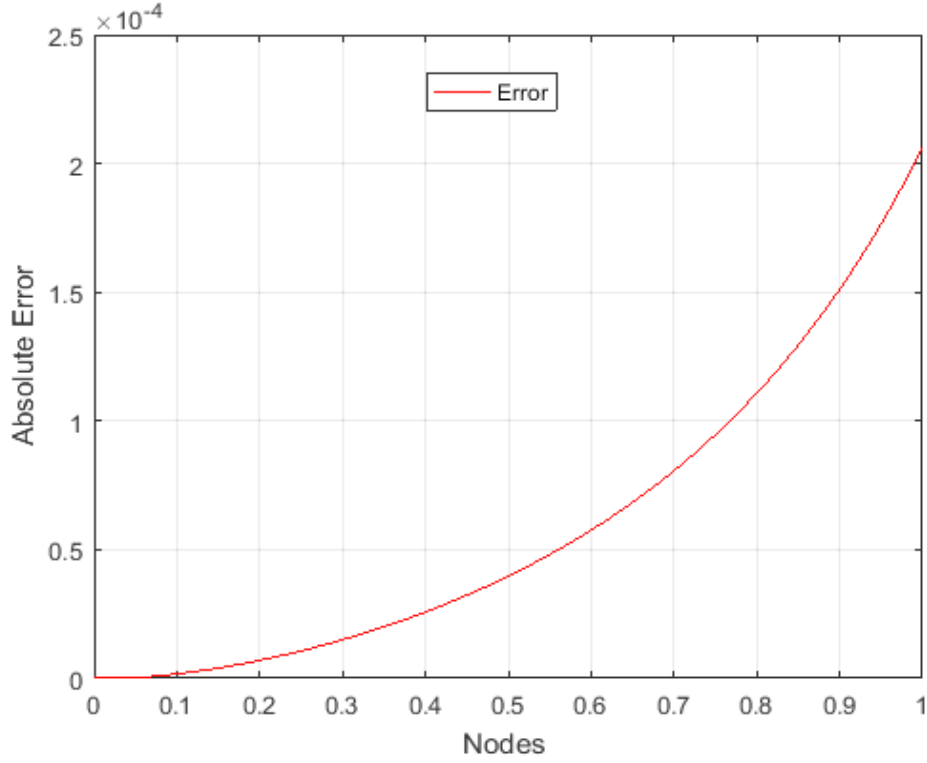


Fig. 3.4 (e) Absolute error between exact and numerical solutions in example 3.2 with $N = 64$.

Example 3.3

Consider the linear Volterra fractional integral equation of the second kind:

$$g(x) = x - \frac{1}{3} - 0.2615x^{\frac{9}{4}} + 0.0981x^{\frac{5}{4}} + \frac{1}{\Gamma(\frac{1}{4})} \int_0^x (x-t)^{-\frac{3}{4}} \frac{t}{3} g(t) dt \quad (3.3)$$

The exact solution of equation (3.3) [17] is:

$$g(x) = x - \frac{1}{3}.$$

Now, we apply all numerical methods mentioned in chapter two to solve (3.3).

3.7 The Numerical Realization of Equation (3.3) Using Adomian Decomposition Method

We notice that $f(x) = x - \frac{1}{3} - 0.2615 x^{\frac{9}{4}} + 0.0981 x^{\frac{5}{4}}$, $k(x, t) = \frac{t}{3}$ and $\lambda = \frac{1}{\Gamma(\frac{1}{4})}$. The solution $g(x)$ is supposed to have a series form given in (2.10). Substituting the decomposition series (2.10) into both sides of equation (3.3) gives

$$\sum_{n=0}^{\infty} g_n(x) = x - \frac{1}{3} - 0.2615 x^{\frac{9}{4}} + 0.0981 x^{\frac{5}{4}} + \lambda \int_0^x (x-t)^{-\frac{3}{4}} \frac{t}{3} \sum_{n=0}^{\infty} g_n(t) dt,$$

or equivalently

$$\begin{aligned} g_0(x) + g_1(x) + \dots \\ = x - \frac{1}{3} - 0.2615 x^{\frac{9}{4}} + 0.0981 x^{\frac{5}{4}} + \lambda \int_0^x (x-t)^{-\frac{3}{4}} \frac{t}{3} [\\ g_0(t) + g_1(t) + \dots] dt. \end{aligned}$$

We identify the zeroth component $g_0(x)$ by all terms that are not included under the integral sign. There for, we obtain the following recurrence relation:

$$\begin{aligned} g_0(x) &= x - \frac{1}{3} - 0.2615 x^{\frac{9}{4}} + 0.0981 x^{\frac{5}{4}}, \\ g_{k+1}(x) &= \lambda \int_0^x (x-t)^{-\frac{3}{4}} \frac{t}{3} g_k(t) dt, \quad \forall k \geq 0, \end{aligned}$$

thus, we obtain

$$g_0(x) = x - \frac{1}{3} - 0.2615 x^{\frac{9}{4}} + 0.0981 x^{\frac{5}{4}},$$

$$g_1(x) = \lambda \int_0^x (x-t)^{-\frac{3}{4}} \frac{t}{3} g_0(t) dt,$$

$$g_1(x) = \lambda \int_0^x (x-t)^{-\frac{3}{4}} \frac{t}{3} \left[t - \frac{1}{3} - 0.2615t^{\frac{9}{4}} + 0.0981t^{\frac{5}{4}} \right] dt,$$

$$g_1(x) = 0.2615x^{\frac{9}{4}} - 0.0981x^{\frac{5}{4}} - 0.0621x^{\frac{7}{2}} + 0.0251x^{\frac{5}{2}},$$

$$g_2(x) = \lambda \int_0^x (x-t)^{-\frac{3}{4}} \frac{t}{3} g_1(t) dt,$$

$$g_2(x) = \lambda \int_0^x (x-t)^{-\frac{3}{4}} \frac{t}{3} \left[0.2615t^{\frac{9}{4}} - 0.0981t^{\frac{5}{4}} - 0.0621t^{\frac{7}{2}} + 0.0251t^{\frac{5}{2}} \right] dt$$

$$g_2(x) = 0.0621x^{\frac{7}{2}} - 0.0251x^{\frac{5}{2}} - 0.0138x^{\frac{19}{4}} + 0.00586x^{\frac{15}{4}},$$

and so on. Using (2.11) gives the series solution:

$$g(x) = g_0(x) + g_1(x) + g_2(x) + \dots,$$

$$\begin{aligned} g(x) = & x - \frac{1}{3} - 0.2615x^{\frac{9}{4}} + 0.0981x^{\frac{5}{4}} + 0.2615x^{\frac{9}{4}} - 0.0981x^{\frac{5}{4}} \\ & - 0.0621x^{\frac{7}{2}} + 0.0251x^{\frac{5}{2}} + 0.0621x^{\frac{7}{2}} - 0.0251x^{\frac{5}{2}} \\ & - 0.0138x^{\frac{19}{4}} + 0.00586x^{\frac{15}{4}} + \dots \end{aligned}$$

We can easily notice the appearance of identical terms with opposite signs.

This phenomenon of such terms is called noise terms phenomenon.

Canceling the identical terms with opposite terms gives the exact solution:

$$g(x) = x - \frac{1}{3}.$$

3.8 The Numerical Realization of Equation (3.3) Using the Haar Wavelet Method

Using algorithm (3.1) for equation (3.3). Table (3.5) displays the exact and the numerical results using the Haar wavelet method for equation (3.3) with $\Delta z = 0.0156$.

Table (3.5): The exact and numerical solutions using the Haar wavelet method with $N = 64$.

x_k	Exact solution $g(x) = x - \frac{1}{3}$	Numerical solution $g_h(x)$	Error = $ g - g_h $
0.0078	-0.3255208333	-0.3255201452	6.8810e-07
0.1172	-0.2161458333	-0.2161308905	1.4943e-05
0.2266	-0.1067708333	-0.1067403308	3.0502e-05
0.3359	0.00260416666	0.00265124972	4.7083e-05
0.4453	0.11197916666	0.11204451523	6.5349e-05
0.5547	0.22135416666	0.22143832174	8.4155e-05
0.6641	0.33072916666	0.33083364476	1.0448e-04
0.7734	0.44010416666	0.44023172549	1.2756e-04
0.8828	0.54947916666	0.54963034573	1.5118e-04
0.9922	0.65885416666	0.65903078260	1.7662e-04

The maximum error with $N = 32$ is 3.6119e-04, the maximum error with $N = 64$ is 1.7662e-04, the maximum error with $N = 128$ is 9.8105e-05 and the maximum error with $N = 256$ is 6.4861e-05.

The exact and numerical results of $g(x)$ with $N = 32$, $N = 64$, $N = 128$ and $N = 256$ are shown in Fig. 3.5 (a), Fig. 3.5 (b), Fig. 3.5 (c), and Fig. 3.5 (d), respectively, and the resulted error with $N = 64$ is shown in Fig. 3.5 (e).

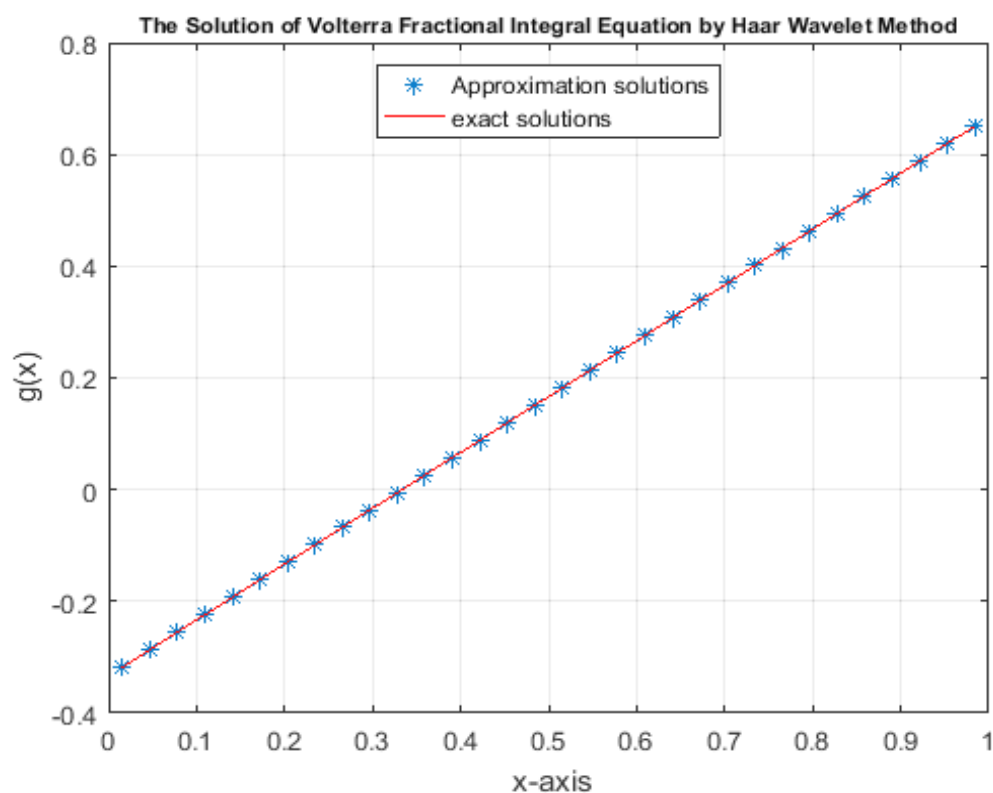


Fig. 3.5 (a) A comparison between the exact and numerical solutions in example 3.3 with $N = 32$.

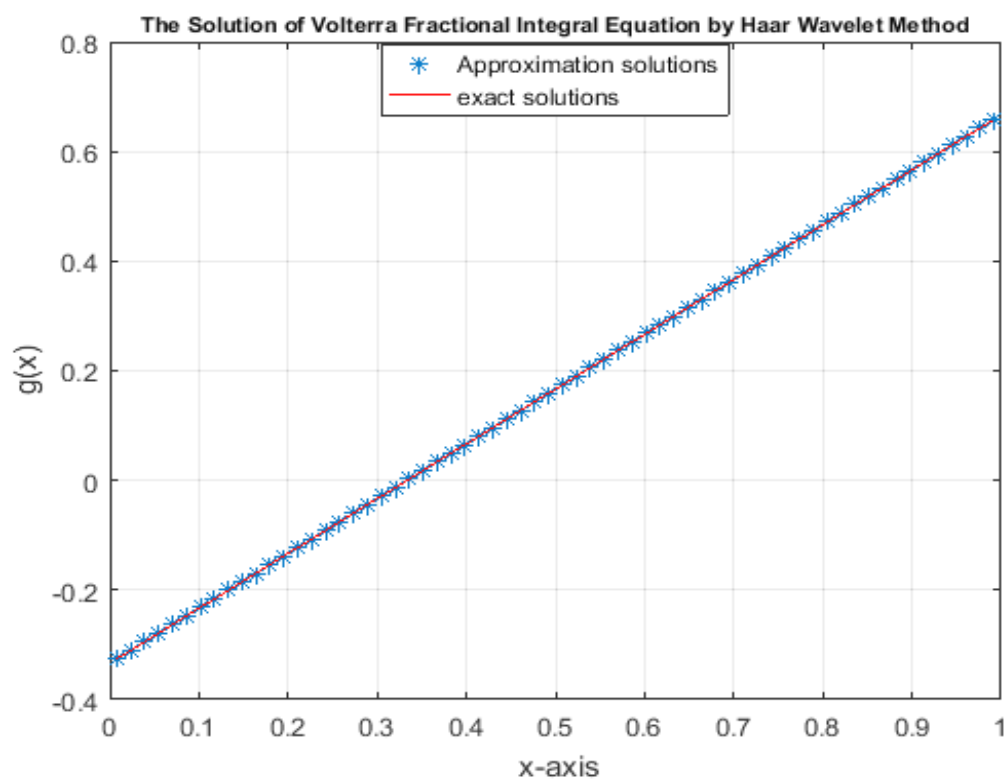


Fig. 3.5 (b) A comparison between the exact and numerical solutions in example 3.3 with $N = 64$.

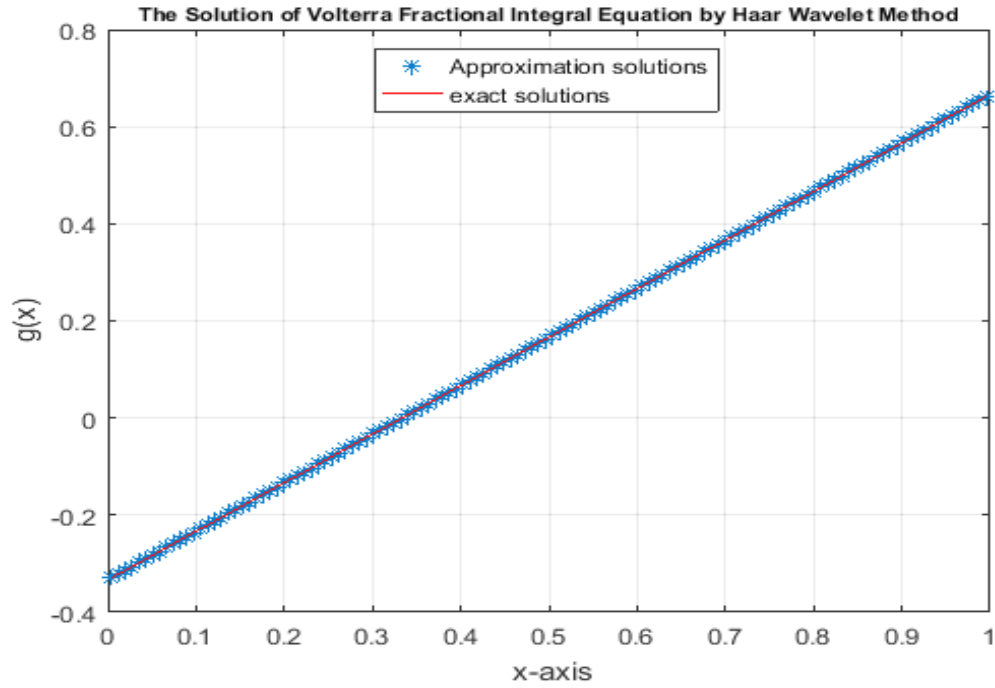


Fig. 3.5 (c) A comparison between the exact and numerical solutions in example 3.3 with $N = 128$.

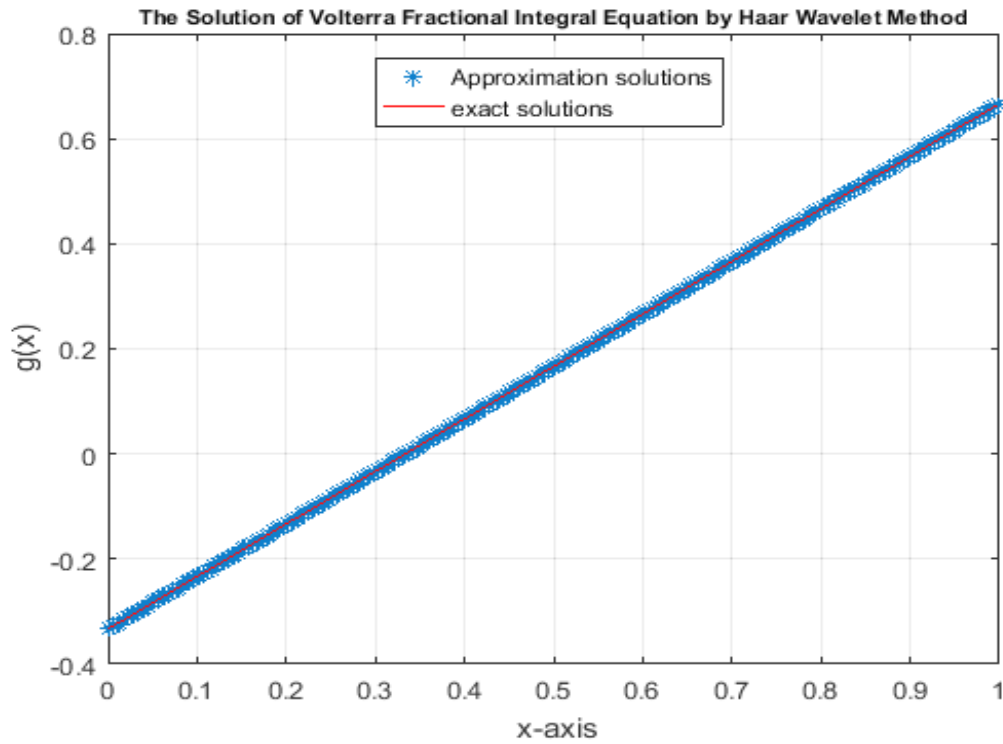


Fig. 3.5 (d) A comparison between the exact and numerical solutions in example 3.3 with $N = 256$.

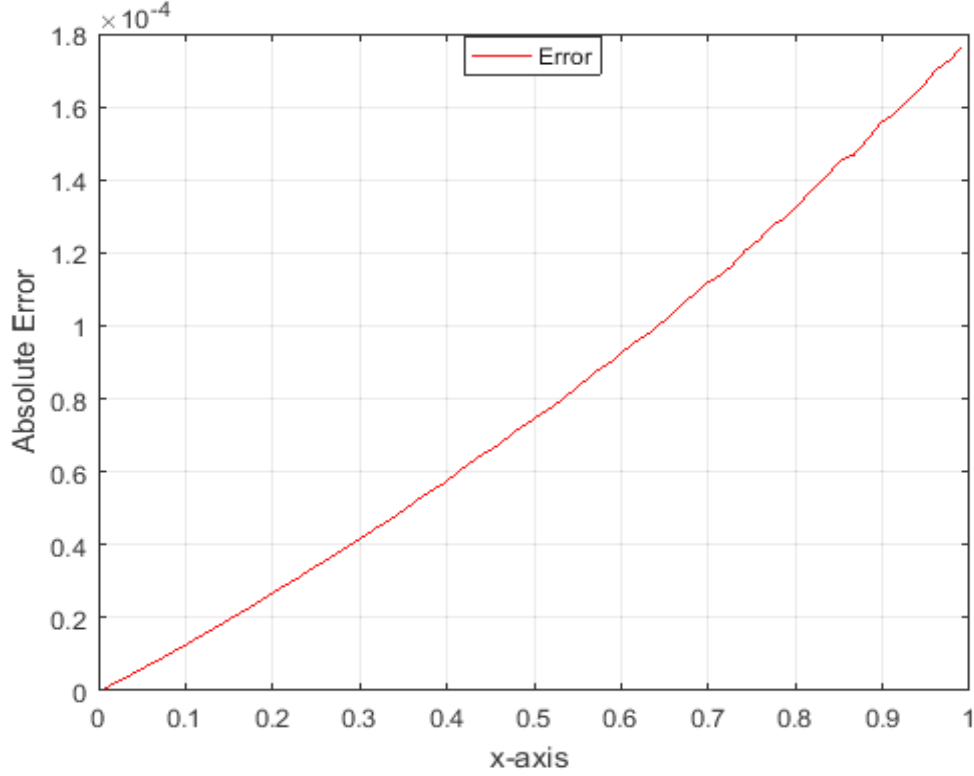


Fig. 3.5 (e) Absolute error between exact and numerical solutions in example 3.3 with $N = 64$.

3.9 The Numerical Realization of Equation (3.3) Using the Product Integration Method

We use algorithm (3.2) to solve equation (3.3). According to that, we get the following results:

W Function

If $p(x_i, t) = (x_i - t)^{-\frac{3}{4}}$, then the equations becomes:

$$w_{i0} = \frac{1}{h_0} \int_{t_0}^{t_1} p(x_i, t)(t_1 - t) dt, \quad \text{for } j = 0,$$

$$w_{i0} = \frac{1}{h} \int_0^h (x_i - t)^{-\frac{3}{4}} (h - t) dt,$$

$$w_{i0} = \frac{1}{h} \int_0^h (ih - t)^{-\frac{3}{4}} (h - t) dt,$$

$$w_{i0} = \frac{4}{5} h^{\frac{1}{4}} \left[5i^{\frac{1}{4}} + 4 \left[(i - 1)^{\frac{5}{4}} - (i)^{\frac{5}{4}} \right] \right].$$

$$w_{ij} = \int_{t_j}^{t_{j+1}} p(x_i, t) \frac{t_{j+1} - t}{h_j} dt + \int_{t_{j-1}}^{t_j} p(x_i, t) \frac{t - t_{j-1}}{h_{j-1}} dt, \text{ for } j$$

$$= 1, \dots, i - 1,$$

$$w_{ij} = \int_{jh}^{(j+1)h} (x_i - t)^{-\frac{3}{4}} \frac{(j+1)h - t}{h} dt$$

$$+ \int_{(j-1)h}^{jh} (x_i - t)^{-\frac{3}{4}} \frac{t - (j-1)h}{h} dt$$

$$w_{ij} = \int_{jh}^{(j+1)h} (ih - t)^{-\frac{3}{4}} \frac{(j+1)h - t}{h} dt$$

$$+ \int_{(j-1)h}^{jh} (ih - t)^{-\frac{3}{4}} \frac{t - (j-1)h}{h} dt$$

$$w_{ij} = \frac{16}{5} h^{\frac{1}{4}} \left[(i - j - 1)^{\frac{5}{4}} + (i - j + 1)^{\frac{5}{4}} - 2(i - j)^{\frac{5}{4}} \right].$$

$$w_{ii} = \frac{1}{h_{i-1}} \int_{t_{i-1}}^{t_i} p(x_i, t)(t - t_{i-1}) dt, \quad \text{for } i = j$$

$$w_{ii} = \frac{1}{h} \int_{(i-1)h}^{ih} (x_i - t)^{-\frac{3}{4}} (t - (i-1)h) dt,$$

$$w_{ii} = \frac{1}{h} \int_{(i-1)h}^{ih} (ih - t)^{-\frac{3}{4}} (t - (i-1)h) dt,$$

$$= \frac{16}{5} h^{\frac{1}{4}}.$$

Table (3.6) displays the exact and the numerical results using the product integration method for equation (3.3) with $h = 0.0156$.

Table (3.6): The exact and numerical solutions using the product integration method with $N = 64$.

x_i	Exact solution $g(x) = x - \frac{1}{3}$	Numerical solution $g_h(x)$	Error = $ g - g_h $
0	-0.3333333333	-0.3333333333	0
0.125	-0.2083333333	-0.2083242103	9.1230e-06
0.250	-0.0833333333	-0.0833182033	1.5130e-05
0.375	0.0416666666	0.04168859603	2.1929e-05
0.500	0.1666666666	0.16669655236	2.9886e-05
0.625	0.2916666666	0.29170591624	3.9250e-05
0.750	0.4166666666	0.41671693916	5.0273e-05
0.875	0.5416666666	0.54172990470	6.3238e-05
1	0.6666666666	0.6667451466	7.8480e-05

The maximum error with $N = 32$ is 1.2728e-04, the maximum error with $N = 64$ is 7.8480e-05, the maximum error with $N = 128$ is 6.5735e-05, and the maximum error with $N = 256$ is 6.2477e-05.

The exact and numerical results of $g(x)$ with $N = 32$, $N = 64$, $N = 128$ and $N = 256$ are shown in Fig. 3.6 (a), Fig. 3.6 (b), Fig. 3.6 (c), and Fig. 3.6 (d), respectively, and the resulted error with $N = 64$ is shown in Fig. 3.6 (e).

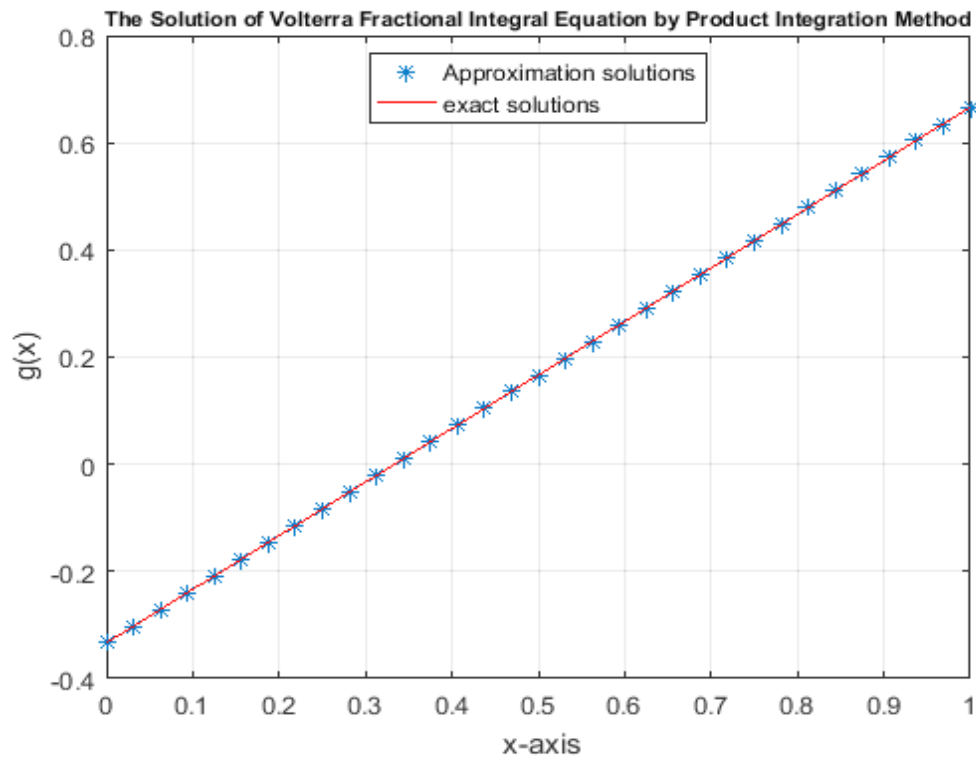


Fig. 3.6 (a) A comparison between the exact and numerical solutions in example 3.3 with $N = 32$.

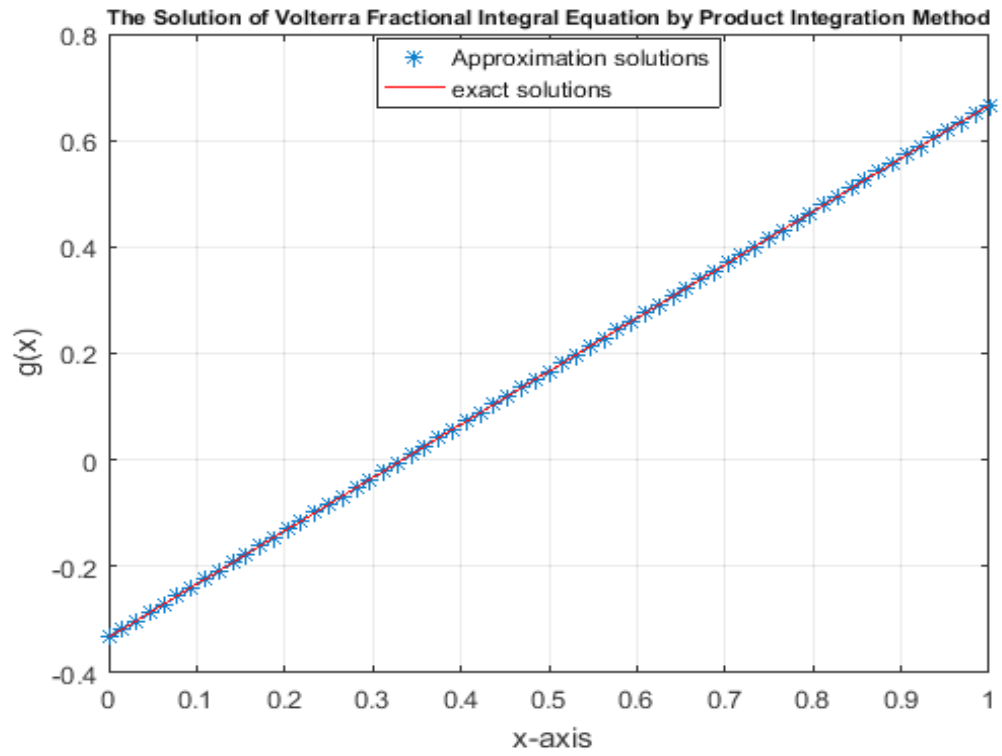


Fig. 3.6 (b) A comparison between the exact and numerical solutions in example 3.3 with $N = 64$.

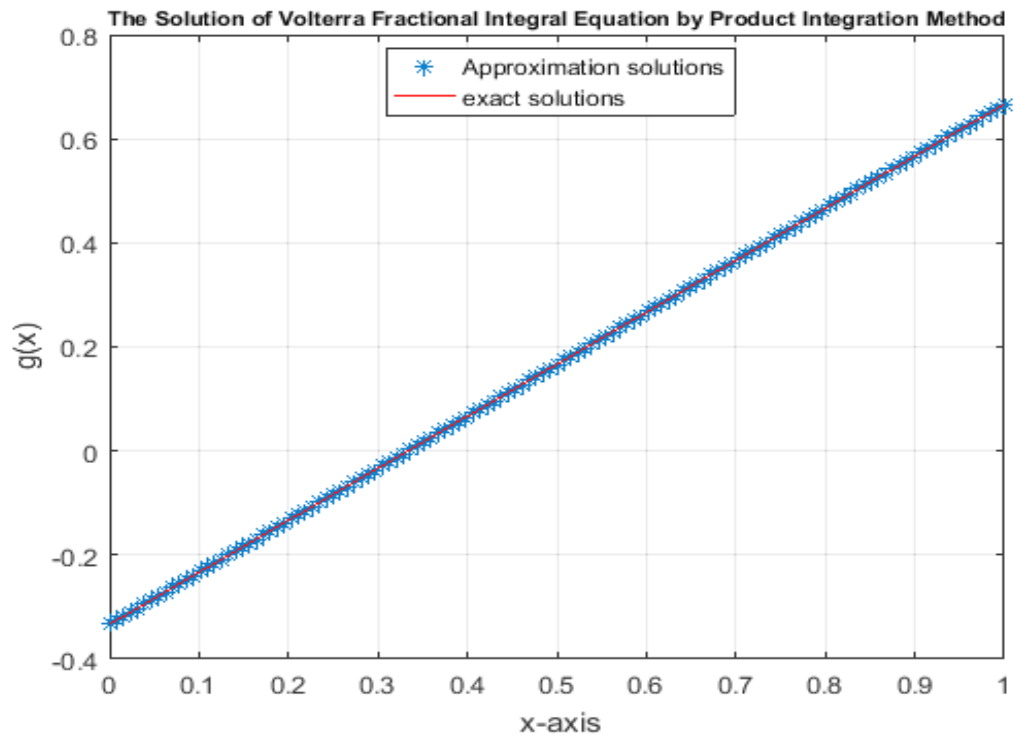


Fig. 3.6 (c) A comparison between the exact and numerical solutions in example 3.3 with $N = 128$.

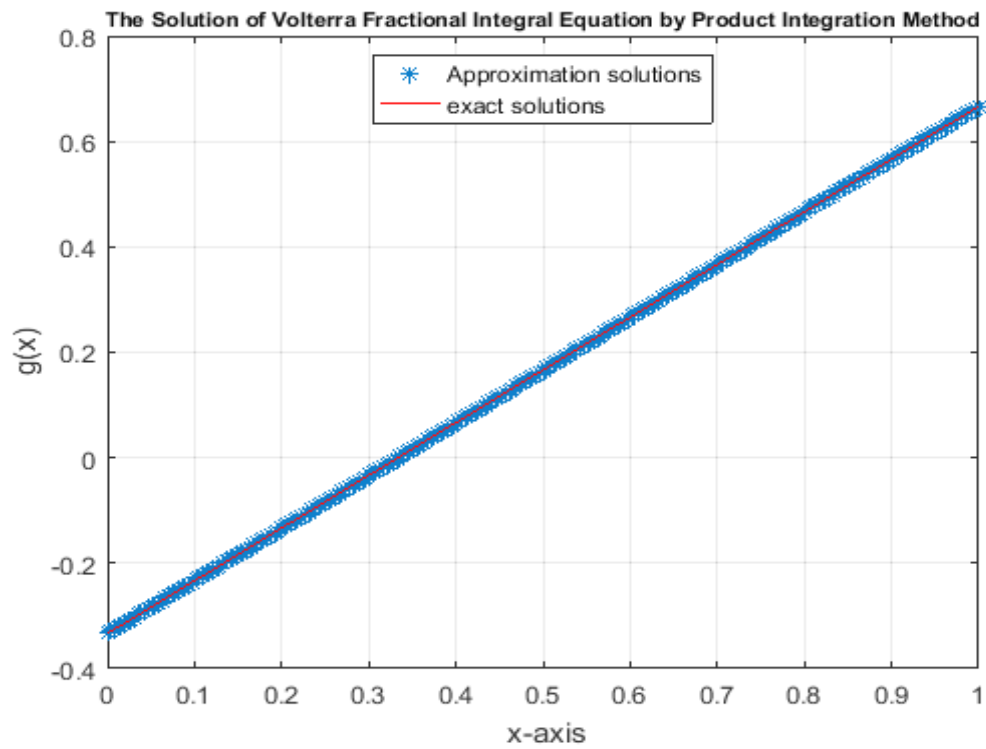


Fig. 3.6 (d) A comparison between the exact and numerical solutions in example 3.3 with $N = 256$.

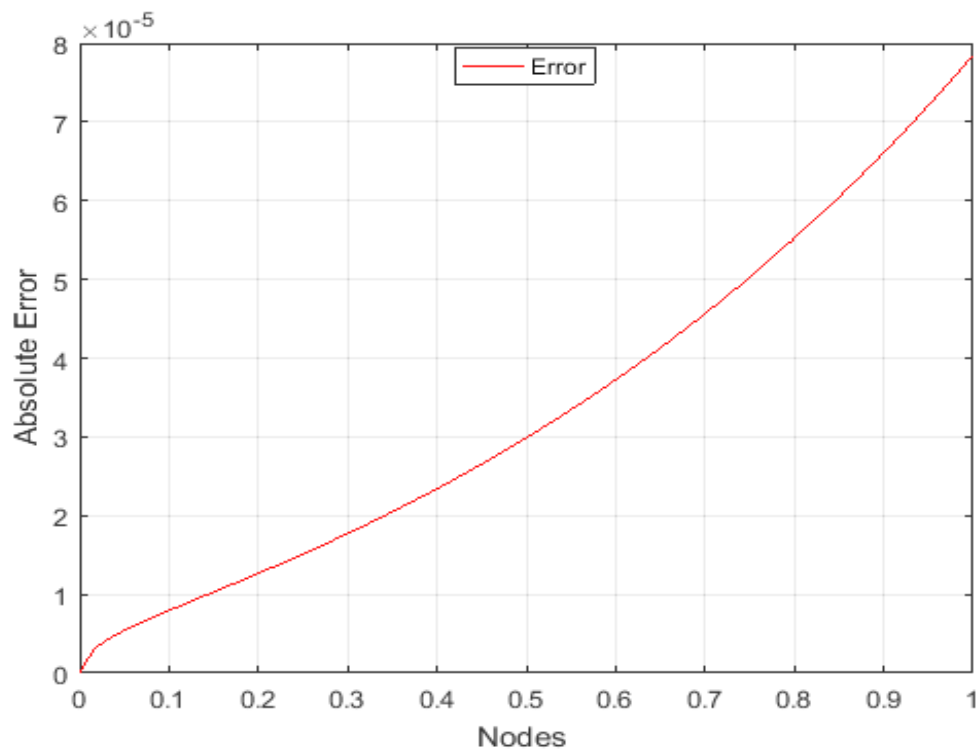


Fig. 3.6 (e) Absolute error between exact and numerical solutions in example 3.3 with $N = 64$.

Chapter Four

Applications and Results

Volterra fractional integral equation appears in many applications, for example, mathematical physics and chemical reactions including stereology [23], the radiation of heat from a semi-infinite solid [16], the heat conduction, crystal growth, electro-chemistry and superfluidity [22].

In this chapter we present numerical solutions to linear Volterra fractional integral equation of the first and the second kind appearing frequently in physics and engineering.

4.1 The Abel's Integral Equation

The linear Volterra fractional integral equation of the first kind has the form [32]:

$$f(x) = \frac{1}{\Gamma(\alpha)} \int_0^x (x-t)^{\alpha-1} k(x,t) g(t) dt. \quad (4.1)$$

Moreover, the linear Volterra fractional integral equation of the second kind has the form [17]:

$$g(x) = f(x) + \frac{1}{\Gamma(\alpha)} \int_0^x (x-t)^{\alpha-1} k(x,t) g(t) dt. \quad (4.2)$$

If $k(x,t) = 1$ and $0 < \alpha < 1$, then equations (4.1) and (4.2) become the so-called Abel's integral equation of the first and the second kind respectively,

$$f(x) = \lambda \int_0^x \frac{g(t)}{(x-t)^B} dt, \quad (4.3)$$

$$g(x) = f(x) + \lambda \int_0^x \frac{g(t)}{(x-t)^B} dt, \quad (4.4)$$

where $0 < B < 1$, $\Gamma(\alpha)$ is the gamma function, $B = 1 - \alpha$ and $\lambda = \frac{1}{\Gamma(\alpha)}$.

One of the most common examples of singular integral equation is the Abel's integral equation because the kernel in this equation becomes unbounded at the upper limit $t = x$.

Abel integral equation is one of the most famous equation that frequently appears in many physical and engineering problems, like semi-conductors, heat conduction, metallurgy and chemical reaction [11, 13]. In experimental physics, Abel's equation in the first finds applications in plasma diagnostics, physical electronics, nuclear physical, optics and astrophysics [18, 19].

Example 4.1

Consider the Abel integral equation of the second kind:

$$g(x) = \frac{x^2}{3} - x - 0.2399x^{\frac{7}{3}} + 0.8399x^{\frac{4}{3}} + 0.3733 \int_0^x (x-t)^{-\frac{2}{3}} g(t) dt \quad (4.5)$$

The exact solution of equation (4.5) [11] is:

$$g(x) = \frac{x^2}{3} - x.$$

Now, we apply all numerical methods mentioned in chapter two to solve (4.5).

4.2 The Numerical Realization of Equation (4.5) Using Adomian Decomposition Method

We notice that $f(x) = \frac{x^2}{3} - x - 0.2399x^{\frac{7}{3}} + 0.8399x^{\frac{4}{3}}$, and $\lambda = 0.3733$.

The solution $g(x)$ is supposed to have a series form given in (2.10).

Substituting the decomposition series (2.10) into both sides of equation (4.5) gives

$$\sum_{n=0}^{\infty} g_n(x) = \frac{x^2}{3} - x - 0.2399x^{\frac{7}{3}} + 0.8399x^{\frac{4}{3}} + \lambda \int_0^x (x-t)^{-\frac{2}{3}} \sum_{n=0}^{\infty} g_n(t) dt,$$

or equivalently

$$\begin{aligned} g_0(x) + g_1(x) + \dots \\ = \frac{x^2}{3} - x - 0.2399x^{\frac{7}{3}} + 0.8399x^{\frac{4}{3}} + \lambda \int_0^x (x-t)^{-\frac{2}{3}} [\\ g_0(t) + g_1(t) + \dots] dt. \end{aligned}$$

We identify the zeroth component $g_0(x)$ by all terms that are not included under the integral sign. There for, we obtain the following recurrence relation:

$$g_0(x) = \frac{x^2}{3} - x - 0.2399x^{\frac{7}{3}} + 0.8399x^{\frac{4}{3}},$$

$$g_{k+1}(x) = \lambda \int_0^x (x-t)^{-\frac{2}{3}} g_k(t) dt, \quad \forall k \geq 0,$$

thus, we obtain

$$g_0(x) = \frac{x^2}{3} - x - 0.2399x^{\frac{7}{3}} + 0.8399x^{\frac{4}{3}},$$

$$g_1(x) = \lambda \int_0^x (x-t)^{-\frac{2}{3}} g_0(t) dt,$$

$$g_1(x) = \lambda \int_0^x (x-t)^{-\frac{2}{3}} \left[\frac{t^2}{3} - t - 0.2399t^{\frac{7}{3}} + 0.8399t^{\frac{4}{3}} \right] dt,$$

$$g_1(x) = 0.2399x^{\frac{7}{3}} - 0.8399x^{\frac{4}{3}} - 0.1662x^{\frac{8}{3}} + 0.6646x^{\frac{5}{3}},$$

$$g_2(x) = \lambda \int_0^x (x-t)^{-\frac{2}{3}} g_1(t) dt,$$

$$g_2(x) = \lambda \int_0^x (x-t)^{-\frac{2}{3}} \left[0.2399t^{\frac{7}{3}} - 0.8399t^{\frac{4}{3}} - 0.1662t^{\frac{8}{3}} \right. \\ \left. + 0.6646t^{\frac{5}{3}} \right] dt,$$

$$g_2(x) = 0.1662x^{\frac{8}{3}} - 0.6646x^{\frac{5}{3}} - 0.1111x^3 + 0.4999x^2,$$

and so on. Using (2.11) gives the series solution:

$$g(x) = g_0(x) + g_1(x) + g_2(x) + \dots,$$

$$g(x) = \frac{x^2}{3} - x - 0.2399x^{\frac{7}{3}} + 0.8399x^{\frac{4}{3}} + 0.2399x^{\frac{7}{3}} - 0.8399x^{\frac{4}{3}} \\ - 0.1662x^{\frac{8}{3}} + 0.6646x^{\frac{5}{3}} + 0.1662x^{\frac{8}{3}} - 0.6646x^{\frac{5}{3}} \\ - 0.1111x^3 + 0.4999x^2 + \dots$$

We can easily notice the appearance of identical terms with opposite signs.

This phenomenon of such terms is called noise terms phenomenon.

Canceling the identical terms with opposite terms gives the exact solution:

$$g(x) = \frac{x^2}{3} - x.$$

4.3 The Numerical Realization of Equation (4.5) Using the Haar Wavelet Method

Using algorithm (3.1) for equation (4.5). Table (4.1) displays the exact and the numerical results using the Haar wavelet method for equation (4.5) with $\Delta z = 0.0156$.

Table (4.1): The exact and the numerical solutions using the Haar wavelet method with $N = 64$.

x_k	Exact solution $g(x) = \frac{x^2}{3} - x$	Numerical solution $g_h(x)$	Error = $ g - g_h $
0.0078	-0.0077921549	-0.0083481389	5.5598e-04
0.1172	-0.1126098632	-0.1131662257	5.5636e-04
0.2266	-0.2094523111	-0.2100916889	6.3938e-04
0.3359	-0.2983194986	-0.2990367942	7.1730e-04
0.4453	-0.3792114257	-0.3800030241	7.9160e-04
0.5547	-0.4521280924	-0.4529904969	8.6240e-04
0.6641	-0.5170694986	-0.5179996508	9.3015e-04
0.7734	-0.5740356445	-0.5750303556	9.9471e-04
0.8828	-0.6230265299	-0.6240817729	1.0552e-03
0.9922	-0.6640421549	-0.6651534675	1.1113e-03

The maximum error with $N = 32$ is $3.15785\text{e-}03$, the maximum error with $N = 64$ is $1.1113\text{e-}03$, and the maximum error with $N = 128$ is $3.4702\text{e-}04$.

The exact and numerical results of $g(x)$ with $N = 32$, $N = 64$, and $N = 128$, are shown in Fig. 4.1 (a), Fig. 4.1 (b), and Fig. 4.1 (c), respectively, and the resulted error with $N = 64$ is shown in Fig. 4.1 (d).

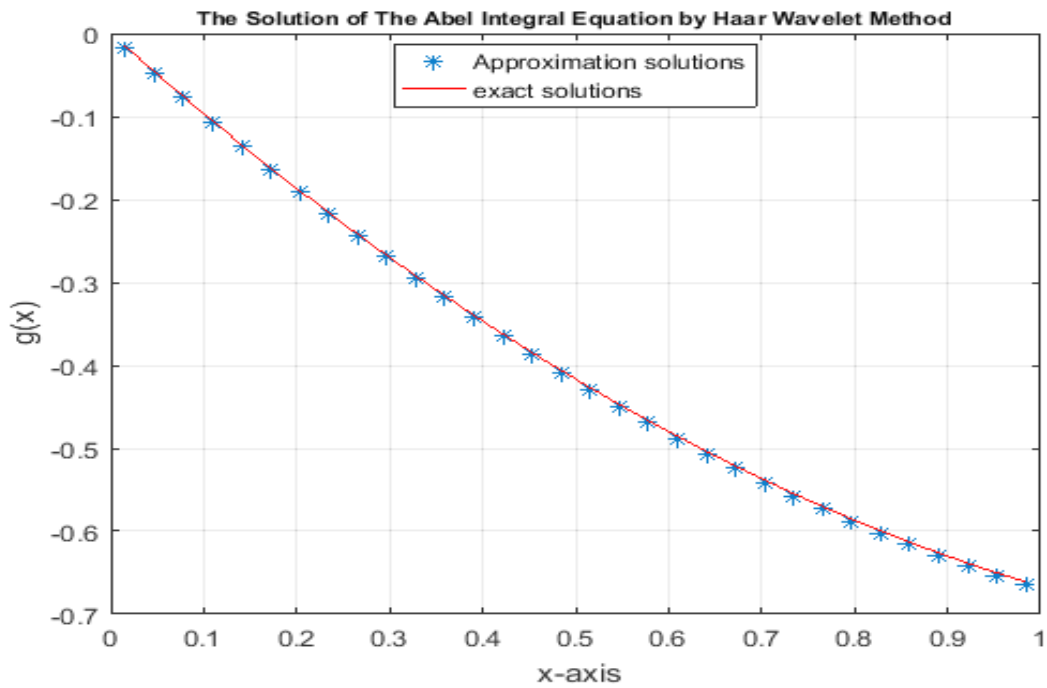


Fig. 4.1 (a) A comparison between the exact and numerical solutions in example 4.1 with $N = 32$.

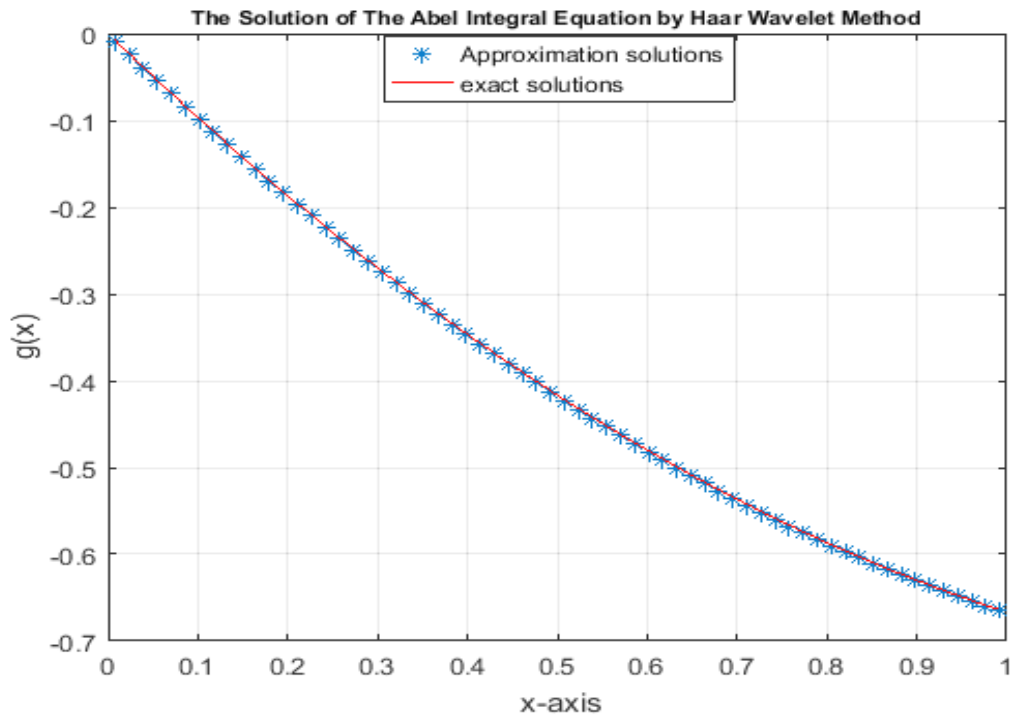


Fig. 4.1 (b) A comparison between the exact and numerical solutions in example 4.1
with $N = 64$.

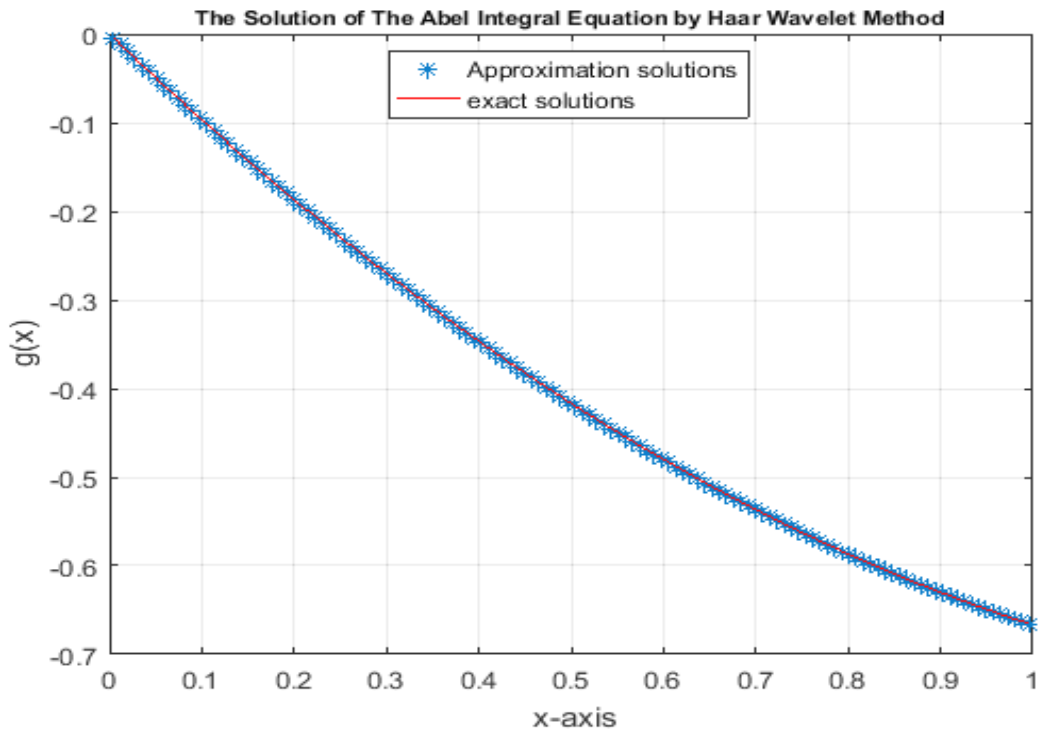


Fig. 4.1 (c) A comparison between the exact and numerical solutions in example 4.1
with $N = 128$.

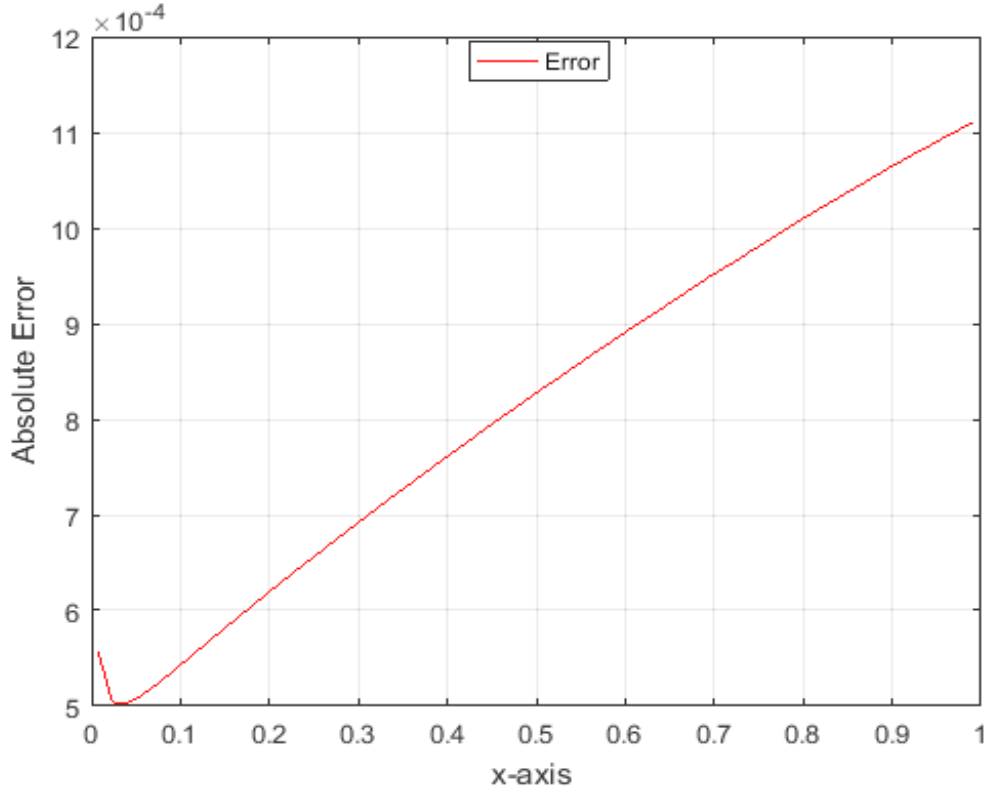


Fig. 4.1 (d) Absolute error between exact and numerical solutions in example 4.1 with $N = 64$.

4.4 The Numerical Realization of Equation (4.5) Using the Product Integration Method

We use algorithm (3.2) to solve equation (4.5). According to that, we get the following results:

W Function

If $p(x_i, t) = (x_i - t)^{-\frac{2}{3}}$, then the equations becomes:

$$w_{i0} = \frac{1}{h_0} \int_{t_0}^{t_1} p(x_i, t)(t_1 - t) dt, \quad \text{for } j = 0,$$

$$w_{i0} = \frac{1}{h} \int_0^h (x_i - t)^{-\frac{2}{3}} (h - t) dt,$$

$$w_{i0} = \frac{1}{h} \int_0^h (ih - t)^{-\frac{2}{3}} (h - t) dt,$$

$$w_{i0} = \frac{3}{4} h^{\frac{1}{3}} \left[4i^{\frac{1}{3}} + 3 \left[(i - 1)^{\frac{4}{3}} - (i)^{\frac{4}{3}} \right] \right].$$

$$w_{ij} = \int_{t_j}^{t_{j+1}} p(x_i, t) \frac{t_{j+1} - t}{h_j} dt + \int_{t_{j-1}}^{t_j} p(x_i, t) \frac{t - t_{j-1}}{h_{j-1}} dt, \text{ for } j$$

$$= 1, \dots, i - 1,$$

$$w_{ij} = \int_{jh}^{(j+1)h} (x_i - t)^{-\frac{2}{3}} \frac{(j+1)h - t}{h} dt$$

$$+ \int_{(j-1)h}^{jh} (x_i - t)^{-\frac{2}{3}} \frac{t - (j-1)h}{h} dt,$$

$$w_{ij} = \int_{jh}^{(j+1)h} (ih - t)^{-\frac{2}{3}} \frac{(j+1)h - t}{h} dt$$

$$+ \int_{(j-1)h}^{jh} (ih - t)^{-\frac{2}{3}} \frac{t - (j-1)h}{h} dt$$

$$w_{ij} = \frac{9}{4} h^{\frac{1}{3}} \left[(i - j - 1)^{\frac{4}{3}} + (i - j + 1)^{\frac{4}{3}} - 2(i - j)^{\frac{4}{3}} \right].$$

$$w_{ii} = \frac{1}{h_{i-1}} \int_{t_{i-1}}^{t_i} p(x_i, t) (t - t_{i-1}) dt, \quad \text{for } i = j$$

$$w_{ii} = \frac{1}{h} \int_{(i-1)h}^{ih} (x_i - t)^{-\frac{2}{3}} (t - (i-1)h) dt,$$

$$w_{ii} = \frac{1}{h} \int_{(i-1)h}^{ih} (ih - t)^{-\frac{2}{3}} (t - (i-1)h) dt,$$

$$w_{ii} = \frac{9}{4} h^{\frac{1}{3}}.$$

Table (4.2) displays the exact and the numerical results using the product integration method for equation (4.5) with $h = 0.0156$.

Table (4.2): The exact and numerical solutions using the product integration method with $N = 64$.

x_i	Exact solution $g(x) = \frac{x^2}{3} - x$	Numerical solution $g_h(x)$	Error = $ g - g_h $
0	0	0	0
0.125	-0.1197916666	-0.1197818969	9.7697e-06
0.250	-0.2291666666	-0.2291501145	1.6552e-05
0.375	-0.3281250000	-0.3280982056	2.6794e-05
0.500	-0.4166666666	-0.4166237294	4.2937e-05
0.625	-0.4947916666	-0.4947244207	6.7246e-05
0.750	-0.5625000000	-0.5623979179	1.0208e-04
0.875	-0.6197916666	-0.6196416593	1.5001e-04
1	-0.6666666666	-0.6664528164	2.1385e-04

The maximum error with $N = 32$ is 4.2922e-04, the maximum error with $N = 64$ is 2.1385e-04, and the maximum error with $N = 128$ is 1.5790e-04.

The exact and numerical results of $g(x)$ with $N = 32$, $N = 64$, and $N = 128$, are shown in Fig. 4.2 (a), Fig. 4.2 (b), and Fig. 4.2 (c), respectively, and the resulted error with $N = 64$ is shown in Fig. 4.2 (d).

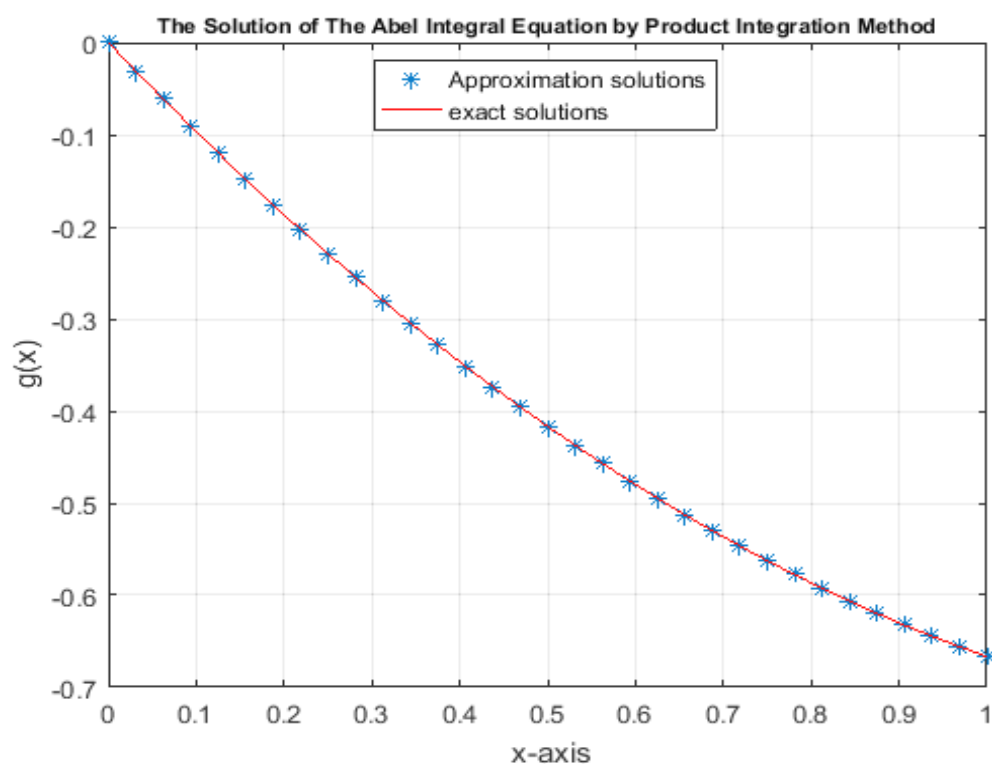


Fig. 4.2 (a) A comparison between the exact and numerical solutions in example 4.1 with $N = 32$.

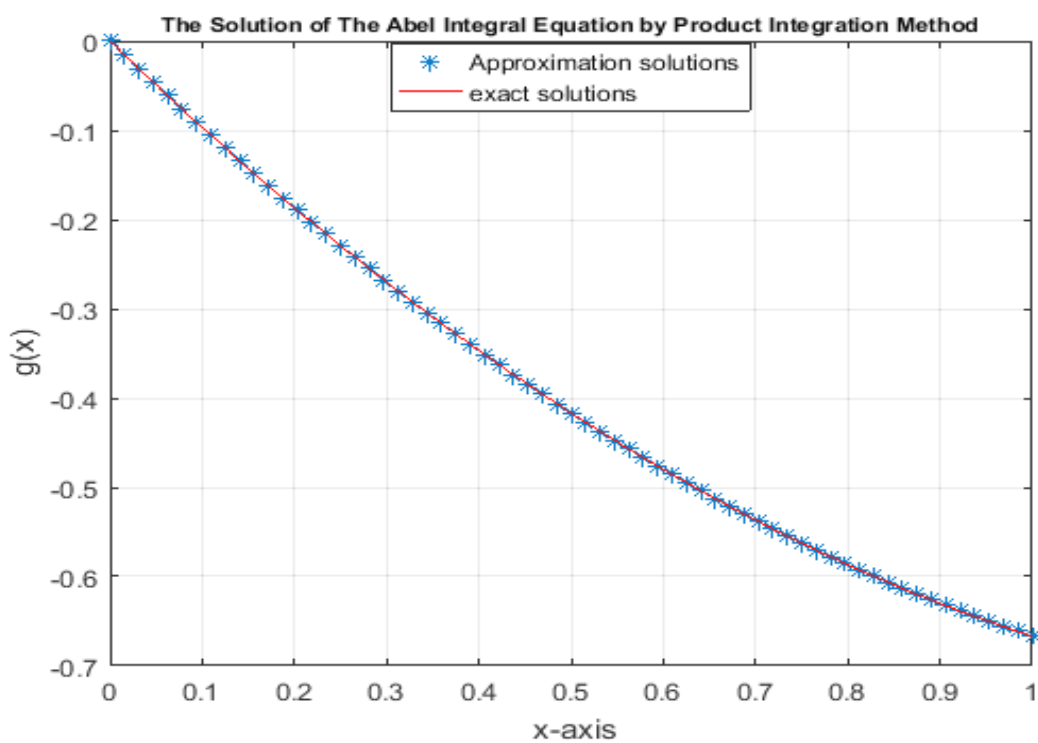


Fig. 4.2 (b) A comparison between the exact and numerical solutions in example 4.1 with $N = 64$.

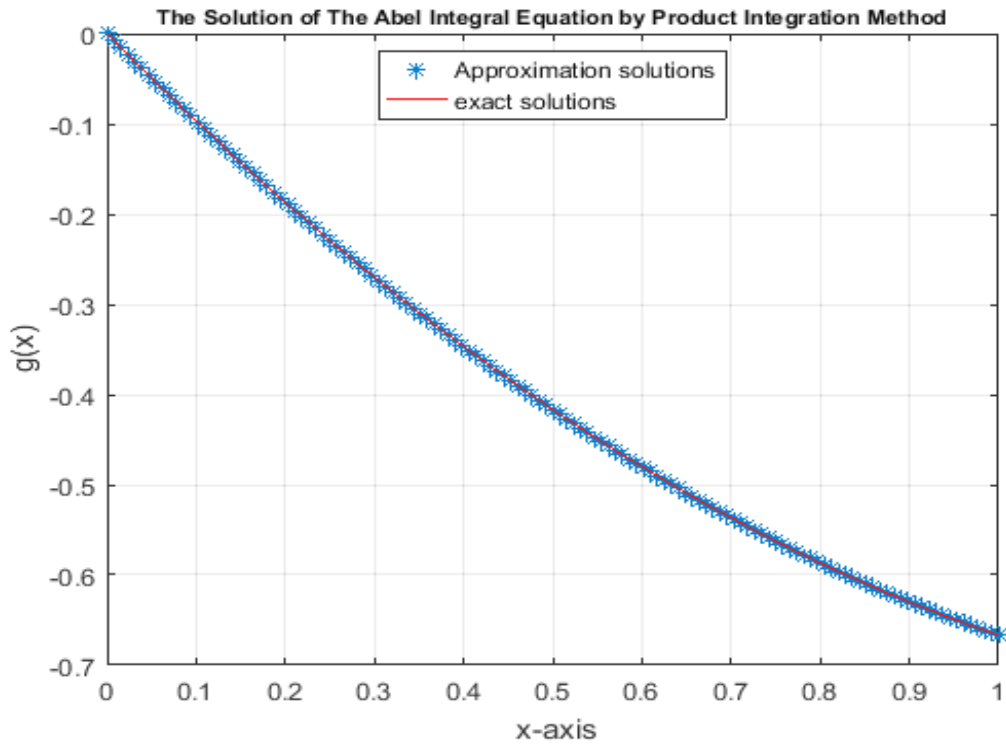


Fig. 4.2 (c) A comparison between the exact and numerical solutions in example 4.1 with $N = 128$.

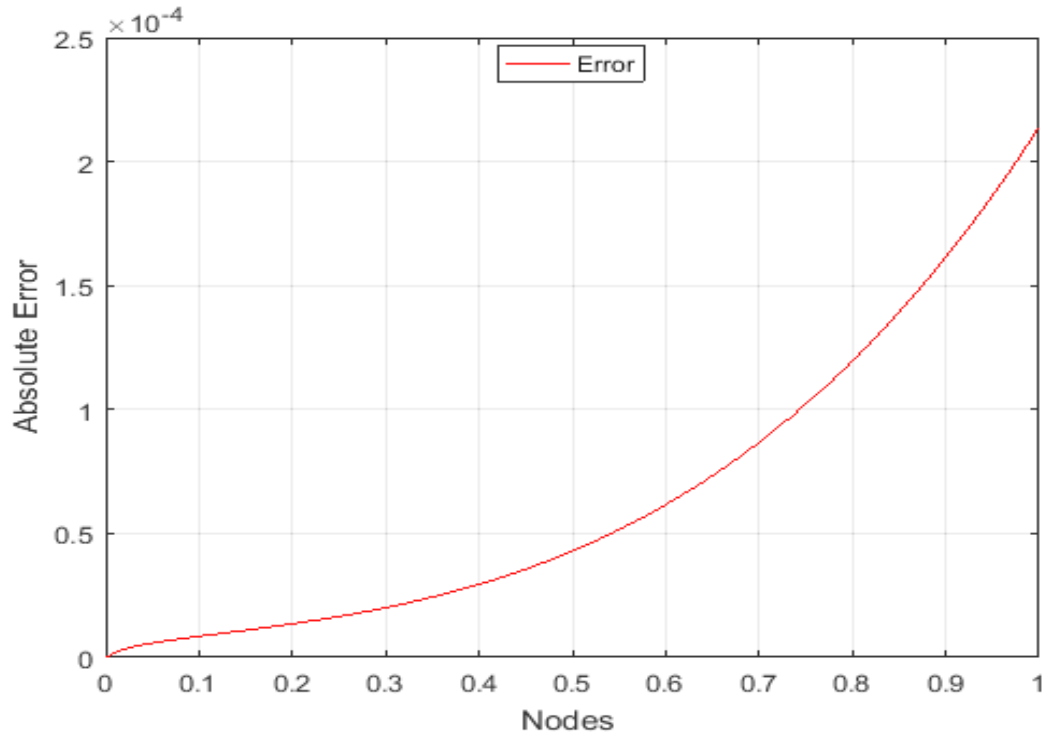


Fig. 4.2 (d) Absolute error between exact and numerical solutions in example 4.1 with $N = 64$.

4.5 Linear Volterra Integral Equation

The linear Volterra fractional integral equation of the first kind has the form [32]:

$$f(x) = \frac{1}{\Gamma(\alpha)} \int_0^x (x-t)^{\alpha-1} k(x,t) g(t) dt. \quad (4.6)$$

Moreover, the linear Volterra fractional integral equation of the second kind has the form [17]:

$$g(x) = f(x) + \frac{1}{\Gamma(\alpha)} \int_0^x (x-t)^{\alpha-1} k(x,t) g(t) dt. \quad (4.7)$$

If $\alpha = 1$, then equations (4.6) and (4.7) become the so-called linear Volterra integral equation of the first and the second kind respectively,

$$f(x) = \int_0^x k(x,t) g(t) dt, \quad (4.8)$$

$$g(x) = f(x) + \int_0^x k(x,t) g(t) dt. \quad (4.9)$$

Volterra integral equation of the second kind appears in many physical applications as Dirichlet problem, reactor theory, electrostatics, astrophysics, radiative heat transfer problems [34, 35, 37] and in insurance mathematics through the renewal equation.

Example 4.2

Consider the linear Volterra integral equation of the second kind:

$$g(x) = \frac{x^2}{2} - \frac{8}{15} x^{\frac{5}{2}} + \int_0^x (x-t)^{-\frac{1}{2}} g(t) dt. \quad (4.10)$$

The exact solution of equation (4.10) [15] is:

$$g(x) = \frac{x^2}{2}.$$

Now, we apply all numerical methods mentioned in chapter two to solve (4.10).

4.6 The Numerical Realization of Equation (4.10) Using Adomian Decomposition Method

We notice that $f(x) = \frac{x^2}{2} - \frac{8}{15}x^{\frac{5}{2}}$, $\lambda = 1$ and the kernel $k(x, t) = (x - t)^{-\frac{1}{2}}$. The solution $g(x)$ is supposed to have a series form given in (2.10). Substituting the decomposition series (2.10) into both sides of equation (4.10) gives

$$\sum_{n=0}^{\infty} g_n(x) = \frac{x^2}{2} - \frac{8}{15}x^{\frac{5}{2}} + \int_0^x (x - t)^{-\frac{1}{2}} \sum_{n=0}^{\infty} g_n(t) dt,$$

or equivalently

$$\begin{aligned} g_0(x) + g_1(x) + \dots \\ = \frac{x^2}{2} - \frac{8}{15}x^{\frac{5}{2}} + \int_0^x (x - t)^{-\frac{1}{2}} [g_0(t) + g_1(t) + \dots] dt. \end{aligned}$$

We identify the zeroth component $g_0(x)$ by all terms that are not included under the integral sign. There for, we obtain the following recurrence relation:

$$\begin{aligned} g_0(x) &= \frac{x^2}{2} - \frac{8}{15}x^{\frac{5}{2}}, \\ g_{k+1}(x) &= \int_0^x (x - t)^{-\frac{1}{2}} g_k(t) dt, \quad \forall k \geq 0, \end{aligned}$$

thus, we obtain

$$g_0(x) = \frac{x^2}{2} - \frac{8}{15}x^{\frac{5}{2}},$$

$$g_1(x) = \int_0^x (x-t)^{-\frac{1}{2}} g_0(t) dt,$$

$$g_1(x) = \int_0^x (x-t)^{-\frac{1}{2}} \left[\frac{t^2}{2} - \frac{8}{15}t^{\frac{5}{2}} \right] dt,$$

$$g_1(x) = \frac{8}{15}x^{\frac{5}{2}} - \frac{1}{6}\pi x^3,$$

$$g_2(x) = \int_0^x (x-t)^{-\frac{1}{2}} g_1(t) dt,$$

$$g_2(x) = \int_0^x (x-t)^{-\frac{1}{2}} \left[\frac{8}{15}t^{\frac{5}{2}} - \frac{1}{6}\pi t^3 \right] dt,$$

$$g_2(x) = \frac{1}{6}\pi x^3 - \frac{16}{105}\pi x^{\frac{7}{2}},$$

and so on. Using (2.11) gives the series solution:

$$g(x) = g_0(x) + g_1(x) + g_2(x) + \dots,$$

$$g(x) = \frac{x^2}{2} - \frac{8}{15}x^{\frac{5}{2}} + \frac{8}{15}x^{\frac{5}{2}} - \frac{1}{6}\pi x^3 + \frac{1}{6}\pi x^3 - \frac{16}{105}\pi x^{\frac{7}{2}} + \dots$$

We can easily notice the appearance of identical terms with opposite signs.

This phenomenon of such terms is called noise terms phenomenon.

Canceling the identical terms with opposite terms gives the exact solution:

$$g(x) = \frac{x^2}{2}.$$

4.7 The Numerical Realization of Equation (4.10) Using the Haar Wavelet Method

Using algorithm (3.1) for equation (4.10). Table (4.3) displays the exact and the numerical results using the Haar wavelet method for equation (4.10) with $\Delta z = 0.0156$.

Table (4.3): The exact and numerical solutions using the Haar wavelet method with $N = 64$.

x_k	Exact solution $g(x) = \frac{x^2}{2}$	Numerical solution $g_h(x)$	Error = $ g - g_h $
0.0078	3.0517578×10^{-5}	3.3575766×10^{-5}	3.0582e-06
0.1172	0.00686645507	0.00692649982	6.0045e-05
0.2266	0.02566528320	0.02581371854	1.4844e-04
0.3359	0.05642700195	0.05670677370	2.7977e-04
0.4453	0.09915161132	0.09962225863	4.7065e-04
0.5547	0.15383911132	0.15458396031	7.4485e-04
0.6641	0.22048950195	0.22162563521	1.1361e-03
0.7734	0.29910278320	0.30079502532	1.6922e-03
0.8828	0.38967895507	0.39215956311	2.4806e-03
0.9922	0.49221801757	0.49581443791	3.5964e-03

The maximum error with $N = 32$ is 1.043472e-02, the maximum error with $N = 64$ is 3.5964e-03, and the maximum error with $N = 128$ is 1.2437e-03.

The exact and numerical results of $g(x)$ with $N = 32$, $N = 64$, and

$N = 128$, are shown in Fig. 4.3 (a), Fig. 4.3 (b), and Fig. 4.3 (c), respectively, and the resulted error with $N = 64$ is shown in Fig. 4.3 (d).

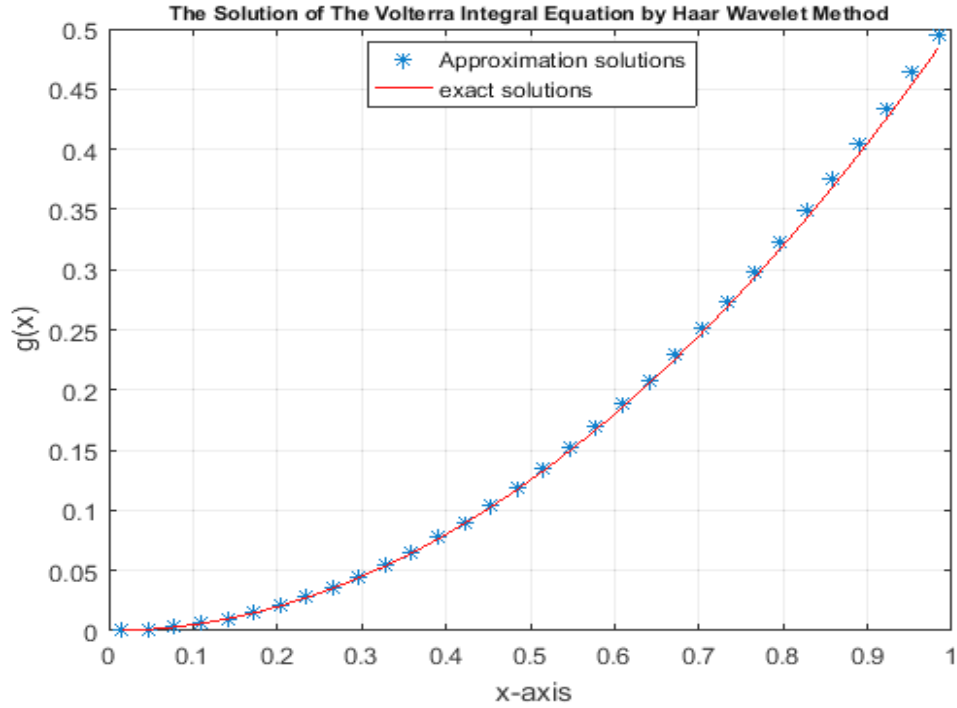


Fig. 4.3 (a) A comparison between the exact and numerical solutions in example 4.2 with $N = 32$.

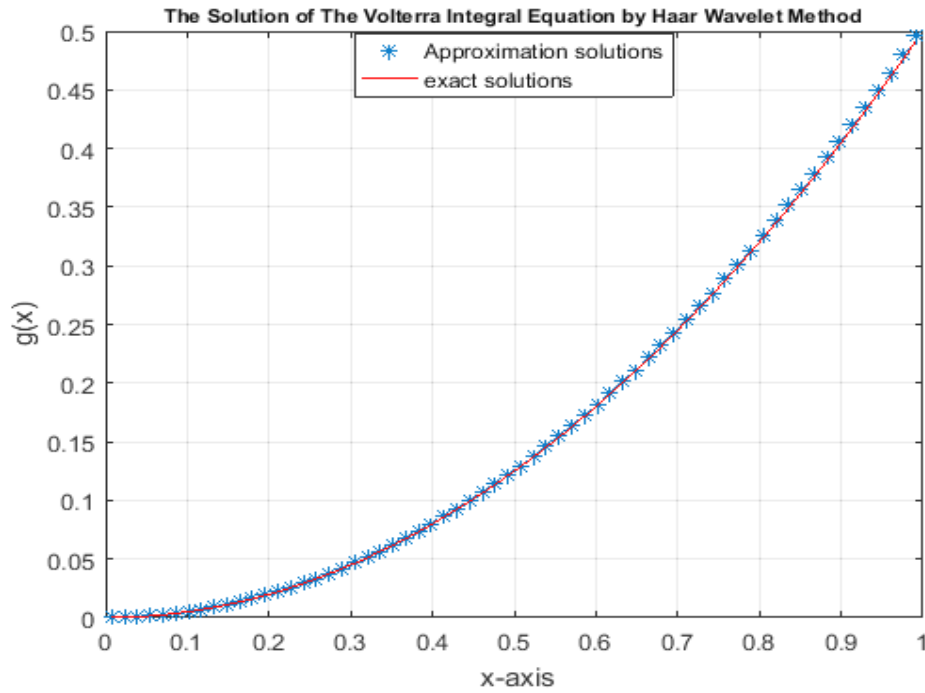


Fig. 4.3 (b) A comparison between the exact and numerical solutions in example 4.2 with $N = 64$.

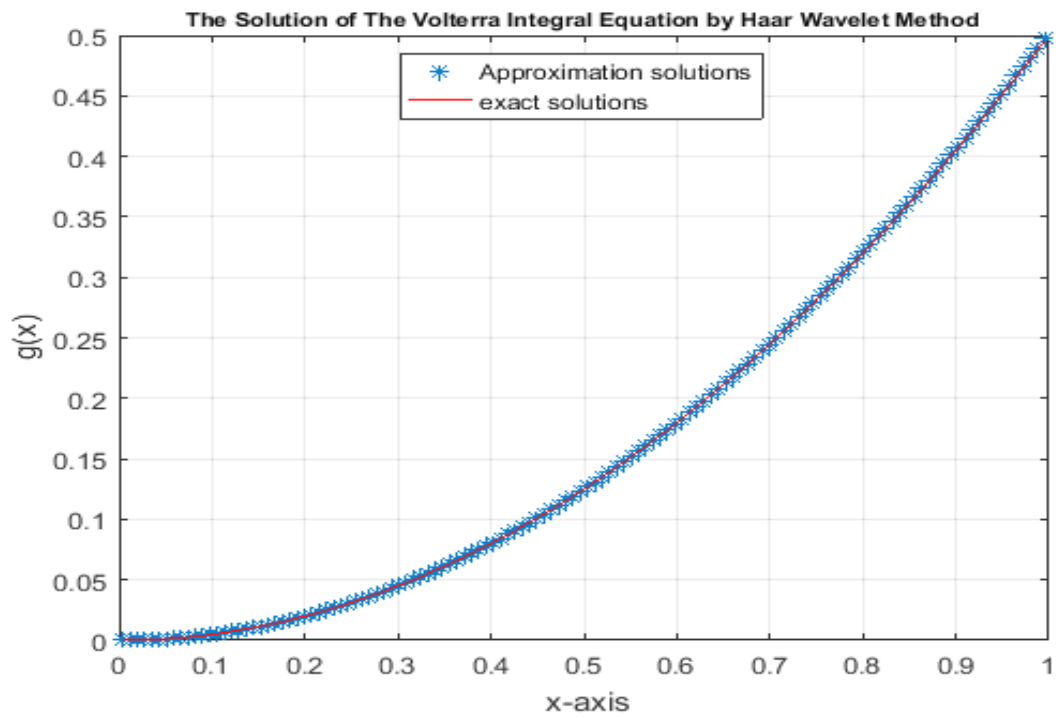


Fig. 4.3 (c) A comparison between the exact and numerical solutions in example 4.2 with $N = 128$.

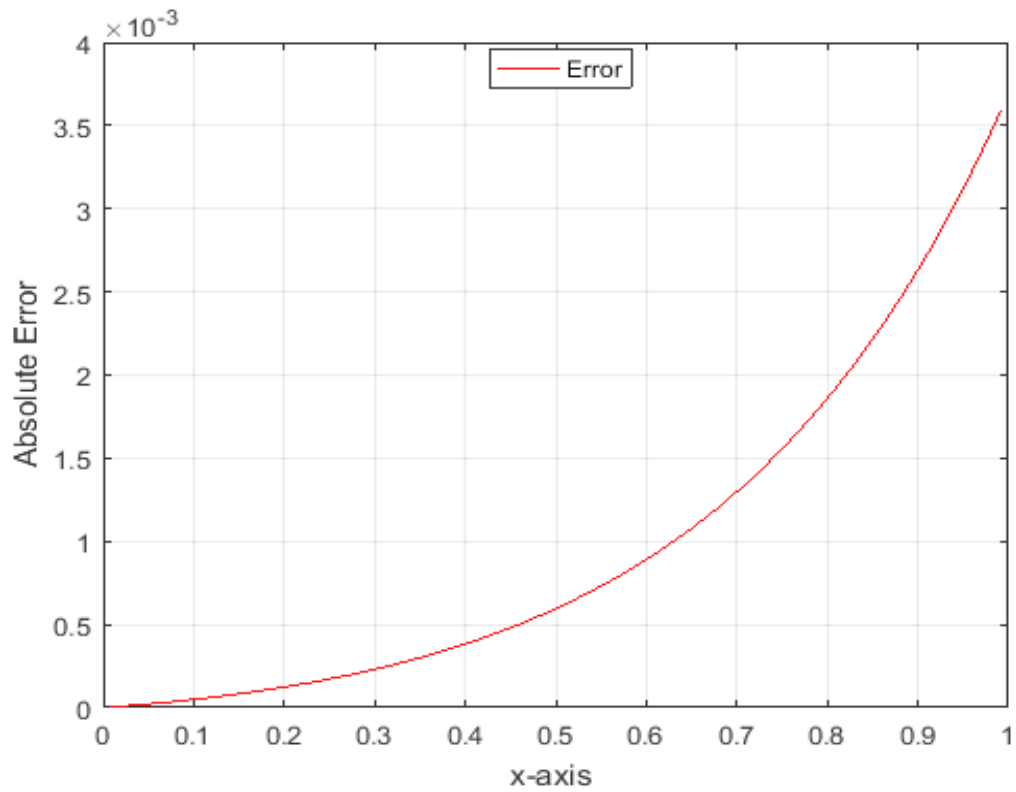


Fig. 4.3 (d) Absolute error between exact and numerical solutions in example 4.2 with $N = 64$.

4.8 The Numerical Realization of Equation (4.10) Using the Product Integration Method

Using algorithm (3.2) for equation (4.10). Table (4.4) displays the exact and the numerical results using the product integration method for equation (4.10) with $h = 0.0156$.

Table (4.4): The exact and numerical solutions using the product integration method with $N = 64$.

x_i	Exact solution $g(x) = \frac{x^2}{2}$	Numerical solution $g_h(x)$	Error = $ g - g_h $
0	0	0	0
0.125	0.00781250000	0.00783856885	2.6069e-05
0.250	0.03125000000	0.03130541526	5.5415e-05
0.375	0.07031250000	0.07040972535	9.7225e-05
0.500	0.12500000000	0.12515830464	1.5830e-04
0.625	0.19531250000	0.19556073450	2.4823e-04
0.750	0.28125000000	0.28163105523	3.8106e-04
0.875	0.38281250000	0.38338999896	5.7750e-04
1	0.50000000000	0.50086824131	8.6824e-04

The maximum error with $N = 32$ is 3.403082e-03, the maximum error with $N = 64$ is 8.6824e-04, and the maximum error with $N = 128$ is 2.2045e-04.

The exact and numerical results of $g(x)$ with $N = 32$, $N = 64$, and $N = 128$, are shown in Fig. 4.4 (a), Fig. 4.4 (b), and Fig. 4.4 (c), respectively, and the resulted error with $N = 64$ is shown in Fig. 4.4 (d).

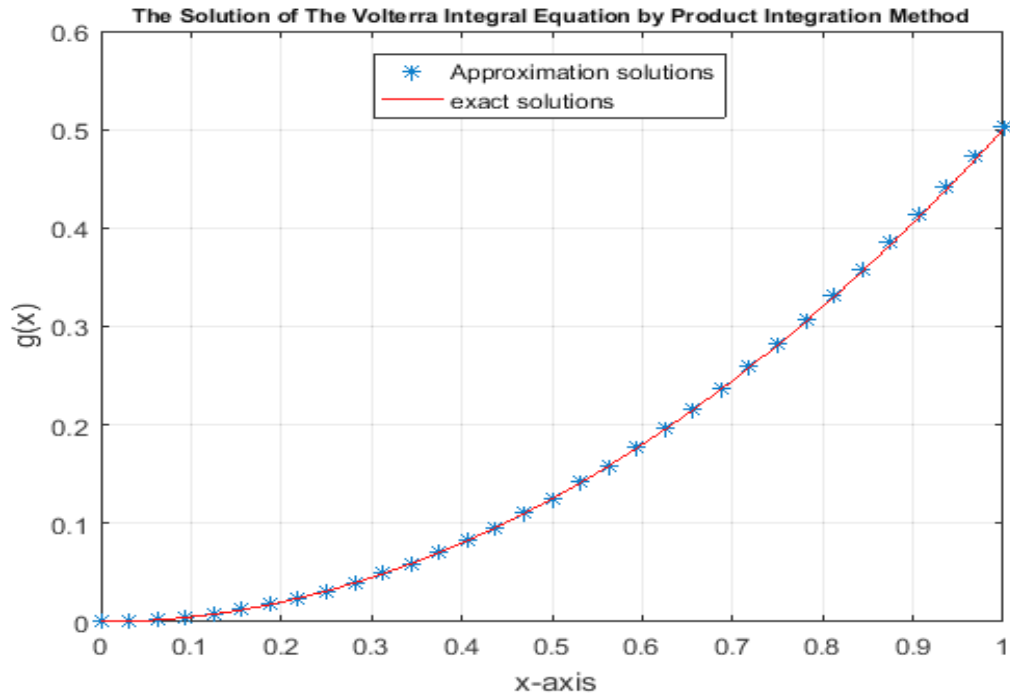


Fig. 4.4 (a) A comparison between the exact and numerical solutions in example 4.2

with $N = 32$

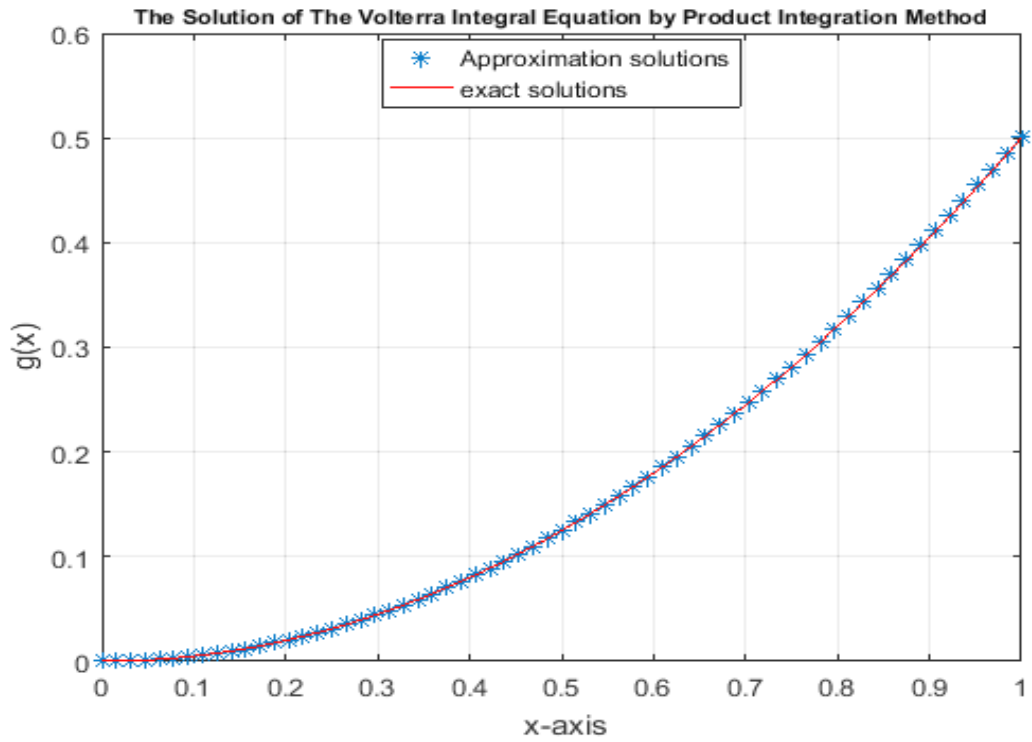


Fig. 4.4 (b) A comparison between the exact and numerical solutions in example 4.2

with $N = 64$

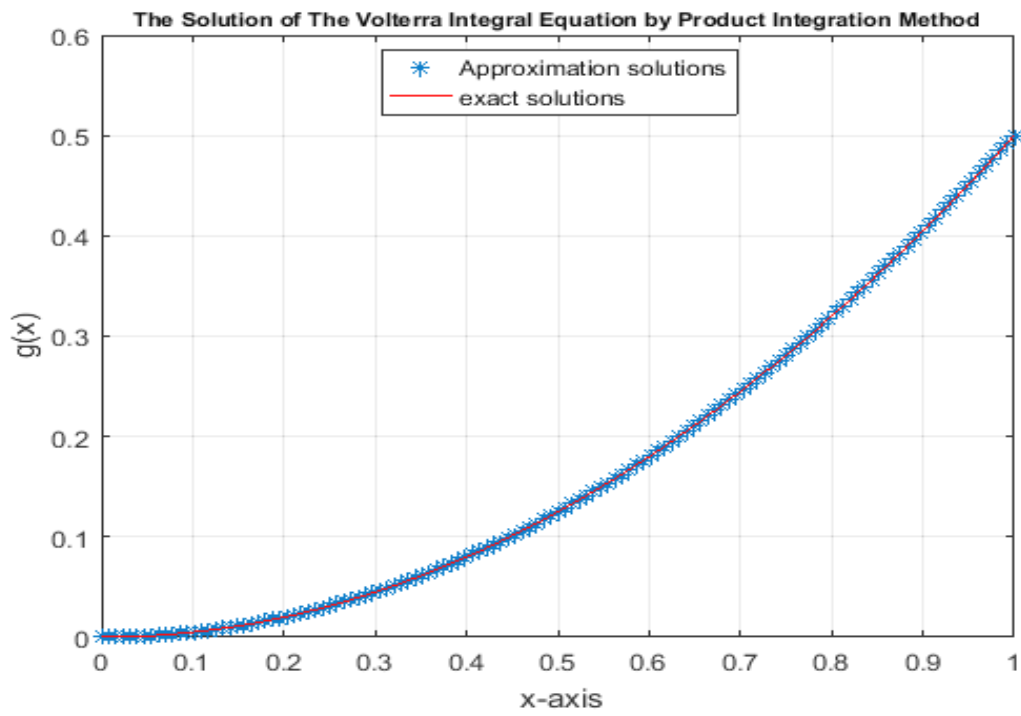


Fig. 4.4 (c) A comparison between the exact and numerical solutions in example 4.2 with $N = 128$.

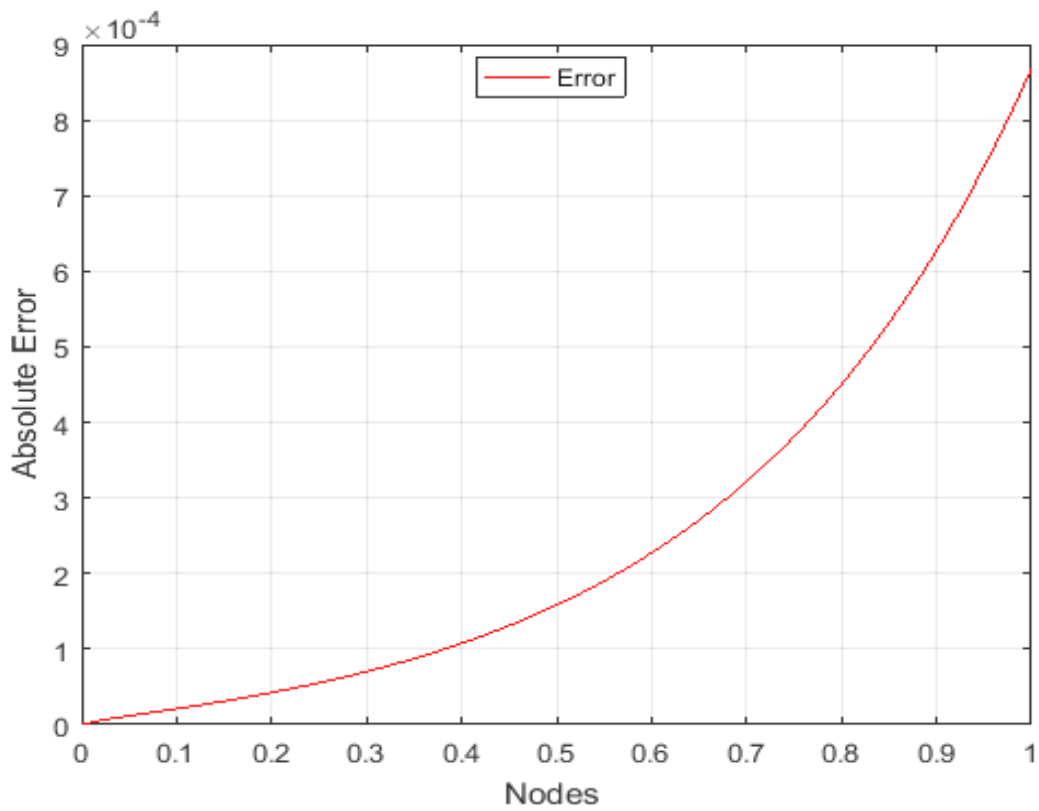


Fig. 4.4 (d) Absolute error between exact and numerical solutions in example 4.2 with $N = 64$.

Conclusions

Linear Volterra fractional integral equation is used frequently in various fields of physics and engineering.

In this thesis, we have solved the linear Volterra fractional integral equation of the second kind using various analytical and numerical techniques, namely; the Adomian decomposition method, the Haar wavelet method and the product integration method.

The numerical methods were implemented in a form of algorithms to solve some numerical test cases using Matlab software.

Numerical results have shown to be in a close agreement with the analytical ones. Moreover, the product integration method is one of the most powerful numerical technique for solving linear Volterra fractional integral equation of the second kind in comparison with other numerical techniques.

References

- [1] G. Adomian, **Solving Frontier Problems of Physics, The Decomposition Method**, Kluwer, Boston, (1994).
- [2] K. E. Atkinson, **The Numerical Solution of Integral Equation of Second Kind**, Cambridge Univ. Press. (1997).
- [3] K. Atkinson and W. Han, **Theoretical Numerical Analysis: A Functional Analysis Framework**, 2nd edition, Springer-Verlag, New York, (2005).
- [4] C. T. H. Baker, **The Numerical Treatment of Integral Equations**, Clarendon Press, Oxford, (1977).
- [5] H. Brunner, **Collocation Method for Volterra Integral and Related Functional Equations**, Cambridge University Press, Cambridge, (2004).
- [6] R. Burden and J. Faires, **Numerical Analysis**, 3rd Edition, 5th, PWS Publishing Company, Boston, USA, (1985).
- [7] M. Caputo, **Linear Models of Dissipation Whose Q is Almost Frequency Independent II**. Geophys. J. Royal astr. Soc., (1967).
- [8] W. Chena, H. Suna, X. Zhanga, D. Korosak, **Anomalous Diffusion Modeling by Fractal and Fractional Derivatives**, Comps. Math. Appl. (in press).
- [9] M. Colin Ramsay, A. Miguel Usabel, **Calculating Ruin Probabilities Via Product Integration**. Astin Bulletin: A Journal of the International Actuarial Association, (1997).

- [10] K. Diethelm, N. J Ford, A. D. Freed, and Yu. Luchko, **Algorithms for the Fractional Calculus: A selection of Numerical Methods**, Preprint
Submitted to Computer Methods in Applied Mechanics and Engineering, 17 March, (2003).
- [11] R. Gorenflo, **Abel Integral Equations with Special Emphasis on Applications**, Lectures in Mathematical Sciences, Vol. 13, The University of Tokyo, Graduate School of Mathematical Sciences, Tokyo, (1996).
- [12] R. Gorenflo and F. Mainardi, **Integral and Differential Equations of Fractional Order**, in A. Carpinteri and F. Mainardi (Eds), **Fractals and Fractional Calculus in Continuum Mechanics**, Springer-Verlag , New York, (1997) .
- [13] R. Gorenflo and S. Vessella, **Abel Integral Equations**, Lecture Notes in Mathematics, 1461, Springer, Berlin, (1991).
- [14] H. Guoqiang, K. Hayami, **Extrapolation Method of Iterated Collocation Solution of Two Dimensional Nonlinear Volterra Integral Equation**, J. Comput. Appl. Math. (1990).
- [15] P. Henrici, **Applied and Computational Complex Analysis**, Vol. 2, Wiley, New York, (1977).
- [16] J. B. Keller, W.E. Olmstead, **Temperature of A Nonlinearity Radiating Semi-Infinite Solid**, The Quarterly of Applied Mathematics, (1972).

- [17] A. A. Kilbas, H. M. Srivastava, J. J. Trujillo, **Theory and Applications of Fractional Differential Equations**, North-Holland Mathematic Studies, Vol. 204, Elsevier, (2006).
- [18] O. Knill, R. Dgani and M. Vogel, **A New Approach to Abel's Integral Operator and its Application to Stellar Winds**, Astronom. and Astrophys. 274, (1993).
- [19] E. L. Kosarev, **Applications of Integral Equations of the First Kind in Experiment Physics**, Comput. Phys. Commun. 20, (1980).
- [20] K. M. Kowankar, A.D Gangal, **Fractional Differentiability of Nowhere Differentiable Functions and Dimensions**, American Institute of Physics, (1996).
- [21] Ü. Lepik, **Solving Fractional Integral Equations by the Haar Wavelet Method**, Appl. Math. Comput. 214, (2009).
- [22] N. Levinson, **A Nonlinear Volterra Equation Arising in the Theory of Super fluidity**, Journal of Mathematical Analysis and Applications, (1960).
- [23] P. Linz, **Analytical and Numerical Methods for Volterra equations**, ch. 8, SIAM, Philadelphia, (1985).
- [24] Ch. Lubich, **Fractional Linear Multistep Methods for Able Volterra Integral Equations of the Second Kind**, Math. Comp. 45 (1985).
- [25] R. L. Magin, **Fractional Calculus Models of Complex Dynamics in Biological Tissues**, Comps. Math. Appl. (in press).

- [26] F. Mainardi, **Fractional Calculus: Some Basic Problems in Continuum and Statistical Mechanics**, in: **Fractals and Fractional Calculus in Continuum Mechanics** (Eds. A. Carpinteri and F. Mainardi), Springer Verlag, Wien, (1997).
- [27] F. C. Meral, T. J. Royston, R. Magin, **Fractional Calculus in Viscoelasticity: An Experimental Study**, Commun. Nonlinear Sci. Numer. Simulat. 15, (2010).
- [28] R. Metzler, T. F. Nonnenmacher, **Fractional Relaxation Processes and Fractional Rheological Models for the Description of A Class of Viscoelastic Materials**, Int. J. Plast. 19, (2003).
- [29] F. Metzler, W. Schick, H. G. Kilian and T. F. Nonnenmacher, Relaxation in filled polymers : **A Fractional Calculus Approach**, J. Chem. Phys (1995).
- [30] K. Miller, B. Ross, **An Introduction to the Fractional Calculus and Fractional Differential Equations**, John Wiley and Sons, (1993).
- [31] K. B. Oldham and J. Spanier, **The Fractional Calculus**, Academic Press, New York, London, (1974).
- [32] R. Plato, **Fractional Multistep Methods for Weakly Singular Volterra Integrals Equations of the First Kind with Perturbed Data**, Institute of Mathematics, October, (2003).
- [33] I. Podlubny, **Fractional Differential Equations**, New York: Academic Press, (1999).

- [34] C. Schneider, **Regularity of the Solution to A Class of Weakly Singular Fredholm Integral Equations of the Second Kind**, Integral Equations Oper. Theory, (1979).
- [35] R. Siegel, J. R. Howell, **Thermal Radiation Heat Transfer**, 3rd Edition, Hemisphere Publishing Co., Washington, DC, (1992).
- [36] S. G. Samko, A. A. Kilbas and O. I. Marichev: **Fractional Integrals and Derivatives, Theory and Applications**, Gordon and Breach, Amsterdam (1993). [Engl. Transl. from Russian, **Integrals and Derivatives of Fractional Order and some of Their Applications**, Nauka I Tekhnika, Minsk 1987].
- [37] E. M. Sparrow, R. D. Cess, **Radiation Heat Transfer**, Revised Edition, Wadsworth Publising Co., Inc, Belmont, CA, (1970).
- [38] R. Thomas and C. Fehmi , **An Immersed Finite Element Method with Integral Equation Correction**, Int. J. Numer. Meth. Engng. **86**, (2010).
- [39] A. M. Wazwaz, **Linear and Nonlinear Integral Equations Methods and Applications**, Springer, New York, (2011).

Appendix

Matlab code for the Haar wavelet method for solving Volterra fractional integral equation in the second kind

```
% The solution of the Volterra fractional integral
% equation by the Haar wavelet method

clc;
clear all;
syms x
F=@(x) x^0.5-
(3/4)*sqrt(pi)*x^2+(8/(3*sqrt(pi)))*x^(3/2)-1;
ExactSolution=@(x) x^0.5-1;
K=@(t,x) 2*t;
lambda=1/sqrt(pi);
A=0;
B=1;
I=5;
M=2^I;
dz=(B-A)/(2*M);
k=1:2*M;
x=(k-0.5)/(2*M);
for k=1:length(x);
for j=1;
if x(k)>=A && x(k)<=B;
H(j,k)=1;
U(j,k)=lambda*integral(@(t) (x(k)-t).^(-
0.5).*K(t),A,x(k));
end
end
for j=2;
if (x(k)<0.5)
H(2,k)=1;
U(2,k)=(lambda)*integral(@(t) (x(k)-t).^(-
0.5).*K(t),A,x(k));
elseif (x(k)>=0.5)
H(2,k)=-1;
U(2,k)=(lambda*(integral(@(t) (x(k)-t).^(-
0.5).*K(t),A,0.5)))-(lambda*(integral(@(t) (x(k)-
t).^(-0.5).*K(t),0.5,x(k))));
```

```

elseif (x(k)>=1)
    H(2,k)=0;
    U(2,k)=(lambda*(integral(@(t)(x(k)-t).^(-
0.5).*K(t),A,0.5)))-(lambda*(integral(@(t)(x(k)-
t).^(-0.5).*K(t),0.5,B)));
end;
end;
end
for i=1:I
    m=2^i;
    for c1=1:m
        c=c1-1;
        j=m+c1;
        csj1=c/m;
        csj2=(c+0.5)/m;
        csj3=(c+1)/m;
        if csj3==1
            h(j)=-1;
        else
            end;
        for k=1:2*M
            if x(k)<csj1
                H(j,k)=0;
                U(j,k)=0;
            else if x(k)<csj2
                H(j,k)=1;
                U(j,k)=(lambda)*integral(@(t)(x(k)-t).^(-
0.5).*K(t),csj1,x(k));
            else if x(k)<csj3
                H(j,k)=-1;
                U(j,k)=(lambda)*(integral(@(t)(x(k)-t).^(-
0.5).*K(t),csj1,csj2))-
(lambda)*(integral(@(t)(x(k)-t).^(-
0.5).*K(t),csj2,x(k)));
            else if x(k)>=csj3
                H(j,k)=0;
                U(j,k)=(lambda)*(integral(@(t)(x(k)-t).^(-
0.5).*K(t),csj1,csj2))-
(lambda)*(integral(@(t)(x(k)-t).^(-
0.5).*K(t),csj2,csj3)));
            else;end;end;
        end;end;
    end;
end;
end;

```

```

end;
end;
f=eval(subs(F,x));
b=f*inv((H-U));
g=b*H
e=eval(subs(ExactSolution,x))
error =g-e;
y=abs(g-e);
% Plot
m=[g',e',y'];
plot(x,g,'*',x,e,'r')

```

Matlab code for the product integration method for solving Volterra fractional integral equation in the second kind

```

% The solution of the Volterra fractional integral
% equation by the product integration method

```

```

clc;
clear all;
syms x t
F=@(x)x^0.5-
(3/4)*sqrt(pi)*x^2+(8/(3*sqrt(pi)))*x^(3/2)-1;
ExactSolution=@(x)x^0.5-1;
G=@(t,x)2*t;
lamda=1/sqrt(pi);
A=0;
b=1;
N=64;
h=(b-A)/N;
x=linspace(A,b,N+1);
t=linspace(A,b,N+1);
f=eval(subs(F,x))';
for i=1:N+1;
for j=1:N+1;
    W(i,i)=(4/3)*h^(1/2);
if (j==1);
    W(i,1)=(2/3)*h^(1/2)*((3*(i-j)^(1/2))+2*((i-
2)^(3/2)-(i-j)^(3/2)));
elseif(j>=2 && j<i);

```

```

W(i,j)=(4/3)*h^(1/2)*((i-j-1)^(3/2)+(i-
j+1)^(3/2)-2*(i-j)^(3/2));
end
end
end
for i=1:N+1;
for j=1:N+1;
    A(i,i)=1-(lamda*W(i,i)*G(t(i)));
if (j==1);
    A(i,1)=-(lamda*W(i,1)*G(t(1)));
elseif(j>=2 && j<i);
    A(i,j)=-(lamda*W(i,j)*G(t(j)));
elseif (i==1 && j==1);
    A(i,j)=1;
end
end
end
U=inv(A)*f;
E=eval(subs(ExactSolution,x))'
error =E-U;
y=abs(E-U);
plot(x,U,'r')
plot(x,E,'r')
m=[U',E',y'];
plot(x,U,'*',x,E,'r')

```

Matlab code for the Haar wavelet method for solving Abel integral equation in the second kind

```

% The solution of the Abel integral equation by Haar
% wavelet method

```

```

clc;
clear all;
syms x
F=@(x)((x^2)/3)-x-
(0.2399)*x^(7/3)+(0.8399)*x^(4/3);
ExactSolution=@(x)((x^2)/3)-x;
lambda=0.3733;
A=0;
B=1;

```



```

I=5;
M=2^I;
dz=(B-A)/(2*M);
k=1:2*M;
x=(k-0.5)/(2*M);
for k=1:length(x);
for j=1;
if x(k)>=A && x(k)<=B;
H(j,k)=1;
U(j,k)=lambda*integral(@(t)(x(k)-t).^(-(2/3)),A,x(k));
end
end
for j=2;
if (x(k)<0.5)
H(2,k)=1;
U(2,k)=(lambda)*integral(@(t)(x(k)-t).^(-(2/3)),A,x(k));
elseif (x(k)>=0.5)
H(2,k)=-1;
U(2,k)=(lambda*(integral(@(t)(x(k)-t).^(-(2/3)),A,0.5)))-(lambda*(integral(@(t)(x(k)-t).^(-(2/3)),0.5,x(k))));
elseif (x(k)>=1)
H(2,k)=0;
U(2,k)=(lambda*(integral(@(t)(x(k)-t).^(-(2/3)),A,0.5)))-(lambda*(integral(@(t)(x(k)-t).^(-(2/3)),0.5,B)));
end;
end;
end
for i=1:I
m=2^i;
for c1=1:m
c=c1-1;
j=m+c1;
csj1=c/m;
csj2=(c+0.5)/m;
csj3=(c+1)/m;
if csj3==1
h(j)=-1;
else end;
for k=1:2*M

```

```

    if x(k)<csj1
        H(j,k)=0;
        U(j,k)=0;
    else if x(k)<csj2
        H(j,k)=1;
        U(j,k)=(lambda)*integral(@(t) (x(k)-t).^(-
(2/3)),csj1,x(k));
    else if x(k)<csj3
        H(j,k)=-1;
        U(j,k)=(lambda)*(integral(@(t) (x(k)-t).^(-
(2/3)),csj1,csj2))-(lambda)*(integral(@(t) (x(k)-
t).^(-(2/3)),csj2,x(k)));
        else if x(k)>=csj3
            H(j,k)=0;
            U(j,k)=(lambda)*(integral(@(t) (x(k)-t).^(-
(2/3)),csj1,csj2))-(lambda)*(integral(@(t) (x(k)-
t).^(-(2/3)),csj2,csj3));
    else;end;end;
end;end;
end;
end;
end;
f=eval(subs(F,x));
b=f*inv((H-U));
g=b*H
e=eval(subs(ExactSolution,x))

error =e-g;
y=abs(e-g);
% Plot
plot(x,g,'r')
plot(x,e,'r')
m=[g',e',y'];
plot(x,g,'*',x,e,'r')

```

Matlab code for the product integration method for solving Abel integral equation in the second kind

```

% The solution of the Abel integral equation by
% product integration method

```

```

clc;
clear all;
syms x t
F=@(x) ((x^2)/3)-x-
(0.2399)*x^(7/3)+(0.8399)*x^(4/3);
ExactSolution=@(x) ((x^2)/3)-x;
G=@(t,x) 1;
lamda=0.3733;
A=0;
b=1;
N=64;
h=(b-A)/N;
x=linspace(A,b,N+1);
t=linspace(A,b,N+1);
f=eval(subs(F,x))';
for i=1:N+1;
for j=1:N+1;
    W(i,i)=(9/4)*h^(1/3);
if (j==1);
    W(i,1)=(3/4)*h^(1/3)*((4*(i-j)^(1/3))+2*((i-
2)^(4/3)-(i-j)^(4/3)));
elseif(j>=2 && j<i);
    W(i,j)=(9/4)*h^(1/3)*((i-j-1)^(4/3)+(i-
j+1)^(4/3)-2*(i-j)^(4/3));
end
end
end
    for i=1:N+1;
    for j=1:N+1;
        A(i,i)=1-(lamda*W(i,i)*G(t(i)));
if (j==1);
    A(i,1)=-(lamda*W(i,1)*G(t(1)));
elseif(j>=2 && j<i);
    A(i,j)=-(lamda*W(i,j)*G(t(j)));
elseif (i==1 && j==1);
    A(i,j)=1;
end
end
end
U=inv(A)*f;
E=eval(subs(ExactSolution,x))'

```

```

error =E-U;
y=abs(E-U);
m=[U',E',y'];
plot(x,U,'*',x,E,'r')

```

Matlab code for the Haar wavelet method for solving the Volterra integral equation in the second kind

```

% The solution of the Volterra integral equation by
% Haar wavelet method

```

```

clc;
clear all;
syms x
F=@(x)((x^2)/2)-((8/15)*x^(5/2));
ExactSolution=@(x)((x^2)/2);
K=@(t,x)1;
lambda=1;
A=0;
B=1;
I=5;
M=2^I;
dz=(B-A)/(2*M);
k=1:2*M;
x=(k-0.5)/(2*M);
for k=1:length(x);
for j=1;
if x(k)>=A && x(k)<=B;
H(j,k)=1;
U(j,k)=lambda*integral(@(t)(x(k)-t).^(-
0.5).*K(t),A,x(k));
end
end
for j=2;
if (x(k)<0.5)
H(2,k)=1;
U(2,k)=(lambda)*integral(@(t)(x(k)-t).^(-
0.5).*K(t),A,x(k));
elseif (x(k)>=0.5)
H(2,k)=-1;

```

```

    U(2,k)=(lambda*(integral(@(t) (x(k)-t).^(-
0.5).*K(t),A,0.5)))-(lambda*(integral(@(t) (x(k)-
t).^(-0.5).*K(t),0.5,x(k))));
elseif (x(k)>=1)
    H(2,k)=0;
    U(2,k)=(lambda*(integral(@(t) (x(k)-t).^(-
0.5).*K(t),A,0.5)))-(lambda*(integral(@(t) (x(k)-
t).^(-0.5).*K(t),0.5,B)));
end;
end;
end
for i=1:I
    m=2^i;
    for c1=1:m
        c=c1-1;
        j=m+c1;
        csj1=c/m;
        csj2=(c+0.5)/m;
        csj3=(c+1)/m;
        if csj3==1
            h(j)=-1;
        else end;
    for k=1:2*M
        if x(k)<csj1
            H(j,k)=0;
            U(j,k)=0;
        else if x(k)<csj2
            H(j,k)=1;
            U(j,k)=(lambda)*integral(@(t) (x(k)-t).^(-
0.5).*K(t),csj1,x(k));
        else if x(k)<csj3
            H(j,k)=-1;
            U(j,k)=(lambda)*(integral(@(t) (x(k)-t).^(-
0.5).*K(t),csj1,csj2))-
(lambda)*(integral(@(t) (x(k)-t).^(-
0.5).*K(t),csj2,x(k)));
        else if x(k)>=csj3
            H(j,k)=0;
            U(j,k)=(lambda)*(integral(@(t) (x(k)-t).^(-
0.5).*K(t),csj1,csj2))-
(lambda)*(integral(@(t) (x(k)-t).^(-
0.5).*K(t),csj2,csj3));
        else;end;end;
    end
end

```

```

end;end;
end;
end;
end;
f=eval(subs(F,x));
b=f*inv((H-U));
g=b*H
e=eval(subs(ExactSolution,x))
error =e-g;
y=abs(e-g);
% Plot
plot(x,g,'r')
plot(x,e,'r')
m=[g',e',y'];
plot(x,g,'*',x,e,'r')

```

Matlab code for the product integration method for solving Volterra integral equation in the second kind

```

% The solution of the Volterra integral equation by
% product integration method
clc;
clear all;
syms x t
F=@(x)((x^2)/2)-((8/15)*x^(5/2));
ExactSolution=@(x)((x^2)/2);
G=@(t,x)1;
lamda=1;
A=0;
b=1;
N=64;
h=(b-A)/N;
x=linspace(A,b,N+1);
t=linspace(A,b,N+1);
f=eval(subs(F,x))';
for i=1:N+1;
for j=1:N+1;
W(i,i)=(4/3)*h^(1/2);
if (j==1);
W(i,1)=(2/3)*h^(1/2)*((3*(i-j)^(1/2))+2*((i-
2)^(3/2)-(i-j)^(3/2)));
elseif(j>=2 && j<i);

```

```

    W(i,j)=(4/3)*h^(1/2)*((i-j-1)^(3/2)+(i-
j+1)^(3/2)-2*(i-j)^(3/2));
end
end
end
    for i=1:N+1;
    for j=1:N+1;
        A(i,i)=1-(lamda*W(i,i)*G(t(i)));
    if (j==1);
        A(i,1)=-(lamda*W(i,1)*G(t(1)));
    elseif(j>=2 && j<i);
        A(i,j)=-(lamda*W(i,j)*G(t(j)));
    elseif (i==1 && j==1);
        A(i,j)=1;
    end
    end
    end
U=inv(A)*f;
E=eval(subs(ExactSolution,x))'
error =E-U;
y=abs(E-U);
plot(x,U,'r')
plot(x,E,'r')
m=[U',E',y'];
plot(x,U,'*',x,E,'r')

```

الطرق العددية لحل معادلة فولتيرا الكسرية وتطبيقاتها

إعداد

صفاء عبد الحكيم محمد حمدان

إشراف

أ. د. ناجي قطناني

قدمت هذه الأطروحة استكمالاً لمتطلبات الحصول على درجة الماجستير في الرياضيات بكلية الدراسات العليا في جامعة النجاح الوطنية، نابلس-فلسطين.

2018

ب

الحلول العددية لحل معادلة فولتيرا التكاملية الكسرية

وتطبيقاتها

إعداد

صفاء عبد الحكيم محمد حمدان

إشراف

أ.د. ناجي قطناني

الملخص

في هذه الرسالة نحن نركز على الحلول التحليلية والعددية لمعادلة فولتيرا الكسرية من النوع الأول والثاني نظرا لمداهما الواسع في الفيزياء الرياضية والتفاعلات الكيميائية مثل التجسيم، التوصيل الحراري، نمو البلورات والكيمياء الكهربائية.

بعد أن تناولنا المفاهيم الأساسية في التكاملات الكسرية ومشتقات الكسور، قمنا بالتركيز على الطرق العددية والتحليلية لحل معادلة فولتيرا الكسرية من النوع الأول والثاني. هذه الطرق هي: طريقة أدوميان التحليلية، طريقة هار للموجه، طريقة تكامل المنتج وطريقة الكسور متعددة الخطوات.

وللتحقق من كفاءة الطرق العددية قمنا بحل بعض الأمثلة العددية ورسم المقارنات بين هذه الطرق، حيث أظهرت النتائج العددية دقتها وقربها من النتائج التحليلية، وكانت طريقة تكامل المنتج هي الأقوى والأدق في حل معادلة فولتيرا الكسرية من النوع الثاني بالمقارنة مع الطرق العددية الأخرى.